CRITICAL VARIETIES IN THE GRASSMANNIAN

PAVEL GALASHIN

Abstract. We introduce a family of spaces called *critical varieties*. Each critical variety is a subset of one of the positroid varieties in the Grassmannian. The combinatorics of positroid varieties is captured by the dimer model on a planar bipartite graph G, and the critical variety is obtained by restricting to Kenyon's critical dimer model associated to a family of isoradial embeddings of G. This model is invariant under square/spider moves on G, and we give an explicit boundary measurement formula for critical varieties which does not depend on the choice of G. This extends our recent results for the critical Ising model, and simultaneously also includes the case of critical electrical networks.

We systematically develop the basic properties of critical varieties. In particular, we study their real and totally positive parts, the combinatorics of the associated strand diagrams, and introduce a shift map motivated by the connection to zonotopal tilings and scattering amplitudes.

Contents

Introduction

The *totally nonnegative Grassmannian* $\mathrm{Gr}_{\geqslant 0}(k,n)$ is a remarkable space introduced by Lusztig [Lus94, Lus98] and Postnikov [Pos06], who described a stratification of $\mathrm{Gr}_{\geqslant 0}(k,n)$ into *positroid cells*. Building on Postnikov's work, Knutson–Lam–Speyer [KLS13] studied *positroid varieties* which are Zariski closures of positroid cells. These objects have been

Date: October 19, 2021.

2020 *Mathematics Subject Classification.* Primary: 14M15. Secondary: 15B48, 82B27, 05E99.

Key words and phrases. Critical varieties, totally nonnegative Grassmannian, positroids, critical dimer model, Ising model, electrical networks, zonotopal tilings.

P.G. was supported by an Alfred P. Sloan Research Fellowship and by the National Science Foundation under Grants No. DMS-1954121 and No. DMS-2046915.

studied extensively in the recent years, making surprising appearances in such fields as the physics of scattering amplitudes [AHT14, AHBC+16], knot theory [FPST17, STWZ19, GL20], and statistical mechanics [CW11, Lam18, GP20]. In fact, this paper is directly influenced by ideas from statistical mechanics: our goal is to apply them to introduce *critical parts* of positroid varieties and study their properties from the point of view of total positivity.

Postnikov gave a parametrization of each positroid cell using a weighted planar bipartite graph G in a disk. His construction was later recast in [Tal08, PSW09] in terms of the dimer model on G. Allowing arbitrary positive real edge weights of G parametrizes the whole positroid cell. To obtain a *critical cell* (which is the "totally positive part" of the corresponding critical variety), one restricts to the *critical dimer model* on G, introduced by Kenyon [Ken02]. Special cases of the critical dimer model yield Baxter's critical Z-invariant Ising model [Bax78, Bax86] and critical electrical resistor networks as discussed e.g. in [Ken02, Section 6]. Our construction is compatible with the recently discovered embeddings of the planar Ising model [GP20] and electrical networks [Lam18] into $\mathrm{Gr}_{\geqslant 0}(k,n)$.

Strictly speaking, Kenyon's critical dimer model is attached not just to a planar bipartite graph G, but to an isoradial embedding [Mer01] of G. An embedding is called *isoradial* if every interior face of G is inscribed in a circle of radius 1. The main observation that led to our below results was that the graphs appearing in Postnikov's parametrizations of positroid varieties admit natural isoradial embeddings known as *plabic tilings*, introduced by Oh–Postnikov–Speyer [OPS15]. While the critical dimer model and its connections to the Ising model and electrical networks are well known, the specialization to plabic tilings and the totally nonnegative Grassmannian appears to not have been studied before.

A given positroid cell can be parametrized by many different planar bipartite graphs, all of which are related by *square moves* (also known as spider moves or urban renewals) [KPW00, Pos06]. A crucial feature of the critical dimer model is that its *boundary measurements* are unchanged under square moves. An important consequence for our purposes is that *the critical variety depends only on the ambient positroid variety*, and not on a particular choice of the planar bipartite graph G. In fact, we give a simple explicit formula for the boundary measurement map that does not depend on the choice of G, generalizing our previous results [Gal20] for the critical Ising model.

We initiate a systematic study of critical varieties, which aims to be parallel to the well-developed theory of positroid varieties. We prove many results in different directions, some of which are highlighted below.

1. Main results

We explain our results and constructions, roughly following the order in which they appear in the main body of the paper.

1.1. Planar bipartite graphs.

We start by giving a brief background on the totally nonnegative Grassmannian. See Section 2 for further details.

Let G be a planar bipartite graph embedded in a disk. We assume that G has n black boundary vertices, each of degree 1, labeled $b_1, b_2, \ldots, b_n$ in clockwise order. A *strand* (or a *zig-zag path*) in G is a path that makes a sharp right turn at each black vertex and a sharp left turn at each white vertex. Thus G gives rise to a *strand permutation* $\bar{f}_G \in S_n$: for each $1 \leqslant p \leqslant n$, the strand that starts at b_p terminates at $b_{\bar{f}_G(p)}$. See Figure 1(b). We say that G is *reduced* [Pos06] if it has the minimal number of faces among all graphs with the same strand permutation. It is known that a reduced graph contains no closed strands, thus each

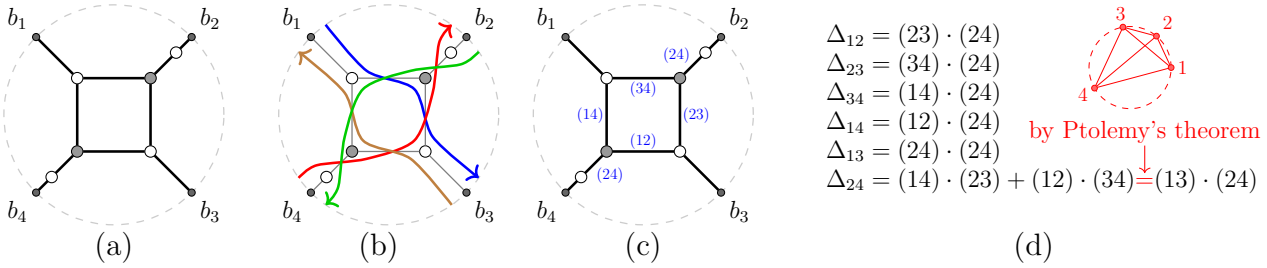

FIGURE 1. (a) A (reduced) planar bipartite graph G; (b) strands in G; (c) edge weights $\mathrm{wt}_{\boldsymbol{\theta}}$, where the unmarked edges have weight 1 and we abbreviate $(pq) := \sin(\theta_q - \theta_p)$; (d) the boundary measurements $\Delta_I(G, \mathrm{wt}_{\boldsymbol{\theta}})$.

strand starts and ends at the boundary of G. When p is a fixed point of $\bar{f}_G$ (i.e., $\bar{f}_G(p) = p$), we assume that b_p is incident to an interior white vertex of degree 1.

Remark 1.1. There is a bijection $\bar{f} \mapsto f$ between permutations $\bar{f} \in S_n$ and *loopless bounded affine permutations* f defined in Section 2.1. For a permutation $\bar{f} \in S_n$, the map $f : \mathbb{Z} \to \mathbb{Z}$ is uniquely determined by the conditions $f(p+n) = f(p) + n$ and $p < f(p) \leqslant p + n$ for all $p \in \mathbb{Z}$ together with $f(p) \equiv \bar{f}(p) \pmod{n}$ for all $1 \leqslant p \leqslant n$. We will use the permutation $\bar{f}$ to construct a critical variety, but we will label it by f in order to match the labeling of positroid varieties.

Given a reduced planar bipartite graph G, one can consider the dimer model on it. Let us assign a positive real weight $\mathrm{wt}(e)$ to each edge e of G. An *almost perfect matching* $\mathcal{A}$ of G is a collection of edges of G that uses each interior vertex exactly once, and uses some subset of boundary vertices. We denote by $\{b_p\}_{p \in I_{\mathcal{A}}}$ for $I_{\mathcal{A}} \subset [n] := \{1, 2, \ldots, n\}$ the set of boundary vertices used by $\mathcal{A}$. It is easy to check that there exists an integer $1 \leqslant k \leqslant n$ such that any almost perfect matching of G satisfies $|I_{\mathcal{A}}| = k$. The number k depends only on f_G.

Denote the set of k-element subsets of $[n]$ by $\binom{[n]}{k}$, and for $I \in \binom{[n]}{k}$, define

$$\Delta_I(G, \mathrm{wt}) := \sum_{\mathcal{A}:\, I_{\mathcal{A}} = I} \mathrm{wt}(\mathcal{A}), \quad \text{where} \quad \mathrm{wt}(\mathcal{A}) := \prod_{e \in \mathcal{A}} \mathrm{wt}(e). \tag{1.1}$$

Here the summation runs over almost perfect matchings of G. We consider the tuple $(\Delta_I(G, \mathrm{wt}))_{I \in \binom{[n]}{k}}$ to be defined up to multiplication by a common scalar. The *boundary measurements* $\mathrm{Meas}_G(\mathrm{wt}) := (\Delta_I(G, \mathrm{wt}))_{I \in \binom{[n]}{k}}$ give rise to a point in the *totally nonnegative Grassmannian* $\mathrm{Gr}_{\geqslant 0}(k, n)$. The *Grassmannian* $\mathrm{Gr}(k, n)$ is the set of all linear k-dimensional subspaces of $\mathbb{C}^n$. Each such subspace V is the row span of a full rank $k \times n$ matrix A, and the *Plücker coordinates* of V are by definition the maximal minors of A. Plücker coordinates are defined up to multiplication by a common nonzero scalar, and $\mathrm{Gr}_{\geqslant 0}(k, n)$ is the subset of $\mathrm{Gr}(k, n)$ where the ratio of any two nonzero Plücker coordinates is a positive real number. We have *positroid stratifications* [Pos06, KLS13]

$$\mathrm{Gr}_{\geqslant 0}(k, n) = \bigsqcup_{f \in \mathcal{B}(k,n)} \Pi_f^{>0} \quad \text{and} \quad \mathrm{Gr}(k, n) = \bigsqcup_{f \in \mathcal{B}(k,n)} \Pi_f^{\circ},$$

where $\mathcal{B}(k, n)$ is the set of (k, n)-*bounded affine permutations*; see Definition 2.1. The image of the map Meas_G is precisely the positroid cell $\Pi_{f_G}^{>0}$. The positroid stratification contains a unique open dense cell (called the *top cell*) labeled by $f_{k,n} \in \mathcal{B}(k, n)$. The map $f_{k,n} : \mathbb{Z} \to \mathbb{Z}$

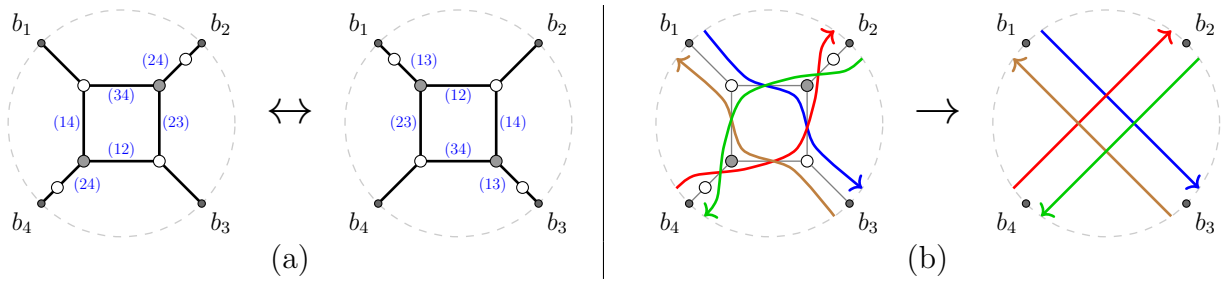

FIGURE 2. (a) A square move and its effect on $\mathrm{wt}_{\boldsymbol{\theta}}$; (b) converting a plabic graph G into a reduced strand diagram of f_G from Definition 1.5.

sends $p \mapsto p+k$ for all $p \in \mathbb{Z}$, and the permutation $\bar{f}_{k,n} \in S_n$ sends $p \mapsto p+k$ modulo n for all $p \in [n]$. An example for $k=2$, $n=4$ is shown in Figure 1(b).

Square moves are certain transformations of (G, wt) which preserve the boundary measurements; see Figure 2(a) for an example. The weights of the edges are changed appropriately (Figure 6), and the resulting weighted graph (G', wt') satisfies $\mathrm{Meas}_G(\mathrm{wt}) = \mathrm{Meas}_{G'}(\mathrm{wt}')$ and $f_G = f_{G'}$. Conversely, any two reduced planar bipartite graphs G and G' satisfying $f_G = f_{G'}$ can be related by a sequence of square moves.

1.2. **Critical dimer model.** Let G be a reduced planar bipartite graph with strand permutation $\bar{f}$. Choose a tuple $\boldsymbol{\theta} = (\theta_1, \theta_2, \ldots, \theta_n) \in \mathbb{R}^n$. For now, we assume that $\theta_1 < \theta_2 < \cdots < \theta_n < \theta_1 + \pi$; this condition will be weakened in Section 1.3. We define a weight function $\mathrm{wt}_{\boldsymbol{\theta}}$ on the edges of G as follows. Observe that every edge e of G belongs to exactly two strands. Suppose that one strand terminates at b_p and the other strand terminates at b_q for some $1 \leqslant p < q \leqslant n$. In this case, we say that e is *labeled by* $\{p, q\}$. We set

$$\mathrm{wt}_{\boldsymbol{\theta}}(e) := \begin{cases} \sin(\theta_q - \theta_p), & \text{if } e \text{ is not adjacent to a boundary vertex,} \\ 1, & \text{otherwise.} \end{cases} \tag{1.2}$$

Remark 1.2. Setting $v_r := \exp(2i\theta_r)$ for all $r \in [n]$, we find $\sin(\theta_q - \theta_p) = \frac{1}{2}|v_q - v_p|$. Thus the edge weights record distances between cyclically ordered points on a circle.

Remark 1.3. Setting $\mathrm{wt}_{\boldsymbol{\theta}}(e) := \sin(\theta_q - \theta_p)$ for *all* edges of G (including boundary edges) gives rise to *dual critical varieties* discussed in Section 3.2.

A crucial property of this choice of weights is that the resulting boundary measurement map is invariant under square moves: for any two reduced graphs G, G' with the same strand permutation $\bar{f}$, we have $\mathrm{Meas}_G(\mathrm{wt}_{\boldsymbol{\theta}}) = \mathrm{Meas}_{G'}(\mathrm{wt}'_{\boldsymbol{\theta}})$, where $\mathrm{wt}_{\boldsymbol{\theta}}$ and $\mathrm{wt}'_{\boldsymbol{\theta}}$ are defined by (1.2) on the edges of G and G', respectively. For instance, the two graphs in Figure 2(a) produce the same boundary measurements (up to a common scalar). Thus $\mathrm{Meas}_G(\mathrm{wt}_{\boldsymbol{\theta}})$ depends only on f and $\boldsymbol{\theta}$, therefore it makes sense to denote $\mathrm{Meas}_f(\boldsymbol{\theta}) := \mathrm{Meas}_G(\mathrm{wt}_{\boldsymbol{\theta}})$. In Section 1.5, we give an explicit simple formula for $\mathrm{Meas}_f(\boldsymbol{\theta})$ which depends only on f and $\boldsymbol{\theta}$ and does not involve choosing a reduced graph G.

Remark 1.4. As mentioned in the introduction, the formula (1.2) is obtained by combining the critical dimer model of [Ken02] with the plabic tilings of [OPS15], in which case the construction of [Ken02] simplifies considerably. It is not clear to us whether the complex edge weights in Section 1.4 below may also be obtained by specializing Kenyon's construction.

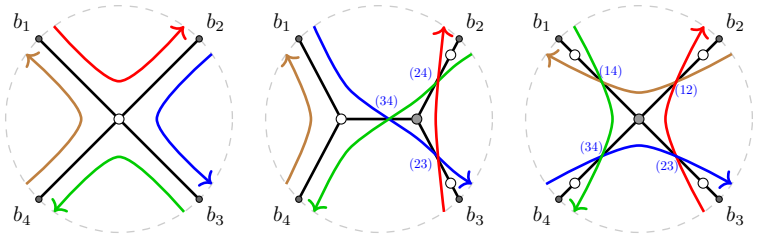

(a) $k = 1$ (b) $k = 2$ (c) $k = 3$

FIGURE 3. Examples of $\mathrm{wt}_{\boldsymbol{\theta}}$ for $n = 4$ and $f \in \mathcal{B}(k, n)$ for $k = 1, 2, 3$. Unmarked edges have weight 1.

We do not pursue this direction further since we will not rely on any known properties of isoradial embeddings in our approach.

1.3. **Critical cells.** Unexpectedly, the combinatorics of critical cells and varieties turns out to be described by the associated *reduced strand diagrams*. Let $\bar{f} \in S_n$ be a permutation and f be the corresponding loopless bounded affine permutation.

Definition 1.5. Place the points $b_1, b_2, \ldots, b_n$ on a circle in clockwise order, and for each $p \in [n]$, let b_p^- (resp., b_p^+) be a point slightly before (resp., after) b_p in clockwise order. The *reduced strand diagram* of f is obtained by drawing a straight arrow $b_s^+ \to b_p^-$ whenever $\bar{f}(s) = p$; see Figures 2(b) and 5. We say that $p \neq q \in [n]$ *form an f-crossing* if the arrows $b_s^+ \to b_p^-$ and $b_t^+ \to b_q^-$ cross.

Definition 1.6. A tuple $\boldsymbol{\theta} = (\theta_1, \theta_2, \ldots, \theta_n) \in \mathbb{R}^n$ is called *f-admissible* if for all $1 \leqslant p < q \leqslant n$ such that p and q form an f-crossing, we have

$$\theta_p < \theta_q < \theta_p + \pi. \tag{1.3}$$

Remark 1.7. We show in Proposition 4.2 that if $\boldsymbol{\theta}$ is f-admissible then all edge weights $\mathrm{wt}_{\boldsymbol{\theta}}(e)$ are strictly positive. This is a surprising property since in general, G contains edges of weight $\sin(\theta_q - \theta_p)$ where p, q need not form an f-crossing. For example, the two graphs in Figure 2(a) contain edges of weight (24) and (13), respectively.

Definition 1.8. The *critical cell* $\mathrm{Crit}_f^{>0} \subset \Pi_f^{>0}$ is defined by

$$\mathrm{Crit}_f^{>0} := \{\mathrm{Meas}_f(\boldsymbol{\theta}) \mid \boldsymbol{\theta} \in \mathbb{R}^n \text{ is } f\text{-admissible}\}.$$

Example 1.9. We give several examples in Figure 3. In the first example, we see that $\mathrm{Crit}_{f_{1,4}}^{>0}$ is a single point. In the second example, we see that $\mathrm{Meas}_f(\boldsymbol{\theta})$ does not depend on θ_1. In the third example, (the ratios of) the Plücker coordinates of $\mathrm{Meas}_f(\boldsymbol{\theta}) \in \mathrm{Gr}_{\geqslant 0}(3, 4)$ record (the ratios of) the side lengths of a convex inscribed quadrilateral with vertices v_1, v_2, v_3, v_4 (cf. Remark 1.2).

We show in Section 4 that the dimension of $\mathrm{Crit}_f^{>0}$ is at most (and conjecturally equal to) $n - c_f$, where c_f is the number of connected components of the reduced strand diagram of f. For the top cell ($f = f_{k,n}$), we establish the equality in Theorem 4.4.

Theorem 1.10. *Let $1 < k < n$ and $f = f_{k,n}$. Then*

$$\mathrm{Crit}_{f_{k,n}}^{>0} \cong \mathbb{R}_{>0}^{n-1}.$$

For $k = 1$ or $k = n$, $\mathrm{Crit}^{>0}_{f_{k,n}}$ is a single point.

Remark 1.11. We caution that our notion of connectedness is different from the one studied in e.g. [OPS15, ARW16]. For example, the permutation $f_{1,n}$ is usually considered connected in the literature, while in our case, the reduced strand diagram of $f_{1,n}$ has n connected components (which is why $\mathrm{Crit}^{>0}_{f_{1,n}}$ has dimension 0). We compare the two notions in Proposition 4.11.

1.4. **Critical varieties.** The *critical variety* Crit_f is the Zariski closure of $\mathrm{Crit}^{>0}_f$ inside the complex Grassmannian $\mathrm{Gr}(k,n)$. Our goal is to describe a certain subset $\mathrm{Crit}^{\circ}_f \subset \mathrm{Crit}_f$ called an *open critical variety*.

Definition 1.12. A tuple $\mathbf{t} = (t_1, t_2, \ldots, t_n) \in (\mathbb{C}^*)^n$ is *f-admissible* if $t_p \neq \pm t_q$ whenever p, q form an f-crossing.

Given a reduced planar bipartite graph G with strand permutation $\bar{f}$ and a tuple $\mathbf{t} \in (\mathbb{C}^*)^n$, we introduce a weight function $\mathrm{wt}_{\mathbf{t}} : E(G) \to \mathbb{C}$ defined by

$$\mathrm{wt}_{\mathbf{t}}(e) := \begin{cases} [\![t_q, t_p]\!], & \text{if } e \text{ is not adjacent to a boundary vertex,} \\ 1, & \text{otherwise,} \end{cases} \tag{1.4}$$

where $e \in E(G)$ is labeled by $\{p, q\}$ with $1 \leqslant p < q \leqslant n$ and $[\![x, y]\!] := \frac{x}{y} - \frac{y}{x}$ for $x, y \in \mathbb{C}^*$. Setting $t_p := \exp(i\theta_p)$ for all $p \in [n]$, $\mathrm{wt}_{\mathbf{t}}$ specializes[1] to $\mathrm{wt}_{\boldsymbol{\theta}}$ and the corresponding notions of f-admissibility coincide.

Example 1.13. Abbreviating $[\![t_q, t_p]\!]$ as (pq), the edge weights $\mathrm{wt}_{\mathbf{t}}(e)$ in the case $f = f_{2,4}$ are given in Figure 1(c) and the corresponding boundary measurements are computed in Figure 1(d). Observe that any tuple $\mathbf{t} = (t_1, t_2, t_3, t_4) \in (\mathbb{C}^*)^4$ satisfying $t_1 = t_3$, $t_2 = t_4$, and $t_1 \neq \pm t_2$ is f-admissible. On the other hand, for any reduced graph G with strand permutation $\bar{f}$ (both of which are shown in Figure 2(a)), such a tuple $\mathbf{t}$ gives $\mathrm{wt}_{\mathbf{t}}(e) = 0$ for some interior edge e of G. Moreover, the dimer partition functions $\Delta_I(G, \mathrm{wt}_{\mathbf{t}})$ in (1.1) will be zero for *all* $I \in \binom{[4]}{2}$.

Nevertheless, it turns out that for *any* f-admissible $\mathbf{t} \in (\mathbb{C}^*)^n$, there is a well-defined element $\mathrm{Meas}_f(\mathbf{t}) \in \Pi^{\circ}_f$ which coincides with the dimer partition functions $(\Delta_I(G, \mathrm{wt}_{\mathbf{t}}))_{I \in \binom{[n]}{k}}$ up to multiplication by a common scalar whenever the latter are not all zero. This is a consequence of a remarkable property of critical varieties which we call *the Laurent phenomenon* (Theorem 5.6). Just as in the case of cluster algebras [FZ02], it involves a certain amount of non-trivial cancellation, which in the case of Figure 1(d) manifests itself in that all minors are divisible by (24). In fact, we conjecture that after writing $\mathrm{Meas}_f(\mathbf{t})$ in a certain canonical form, all *cluster variables* in the cluster algebra structure [GL19] on Π°_f are Laurent polynomials in the $\mathbf{t}$-variables (Conjecture 5.8).

Definition 1.14. The *open critical variety* $\mathrm{Crit}^{\circ}_f \subset \Pi^{\circ}_f$ is defined as

$$\mathrm{Crit}^{\circ}_f := \{\mathrm{Meas}_f(\mathbf{t}) \mid \mathbf{t} \in (\mathbb{C}^*)^n \text{ is } f\text{-admissible}\}.$$

[1]Strictly speaking, we have $\mathrm{wt}_{\boldsymbol{\theta}}(e) = \frac{1}{2i}\,\mathrm{wt}_{\mathbf{t}}(e)$ for all non-boundary $e \in E(G)$, but this rescaling does not affect the boundary measurements since $\mathrm{wt}_{\mathbf{t}}$ and $\mathrm{wt}_{\boldsymbol{\theta}}$ are *gauge-equivalent*; see the proof of Lemma 5.9.

The question of whether Crit_f° is actually an open subvariety of Crit_f remains unanswered (Problem 5.2). In Section 5.3, we give a conjectural description of its set $\mathrm{Crit}_f^\circ(\mathbb{R})$ of real points (assuming $\mathbf{t}$ is *generic* as in Definition 1.16 below) and prove it in Section 9 in the case $f = f_{k,n}$ for $1 \leqslant k \leqslant n-2$.

1.5. **Boundary measurement formula.** Currently, in order to compute $\mathrm{Meas}_f(\boldsymbol{\theta})$, one needs to choose a reduced planar bipartite graph G, and then the result does not depend on this choice. It is therefore natural to look for an expression for $\mathrm{Meas}_f(\boldsymbol{\theta})$ purely in terms of f and $\boldsymbol{\theta}$. The answer turns out to be an explicitly defined point of $\mathrm{Gr}_{\geqslant 0}(k,n)$ as we now explain. The results of this section give a natural extension of our previous results [Gal20] obtained in the case of the Ising model.

Take the reduced strand diagram of f as in Figure 2(b). For each $r \in [n]$, let

$$J_r := \{p \in [n] \mid b_r \text{ is to the left of the arrow } b_s^+ \to b_p^-\}. \tag{1.5}$$

Here we set $s := \bar{f}^{-1}(p)$. The integer k from Section 1.1 satisfies $|J_r| = k-1$. We have $r \notin J_r$, and the collection $(J_r \sqcup \{r\})_{r\in[n]}$ is known as the *Grassmann necklace* [Pos06] of f.

For an index $r \in [n]$, let $\epsilon_r \in \{\pm 1\}$ be given by

$$\epsilon_r := (-1)^{\#\{p\in[n] \mid \bar{f}(p) \leqslant p < r\}}.$$

Definition 1.15. Let $\boldsymbol{\theta} = (\theta_1, \theta_2, \ldots, \theta_n)$ be a tuple of angles. Define a curve $\boldsymbol{\gamma}_{f,\boldsymbol{\theta}} : \mathbb{R} \to \mathbb{R}^n$ whose coordinates $\boldsymbol{\gamma}_{f,\boldsymbol{\theta}}(t) = (\gamma_1(t), \gamma_2(t), \ldots, \gamma_n(t))$ are given by

$$\gamma_r(t) := \epsilon_r \prod_{p\in J_r} \sin(t-\theta_p) \qquad \text{for } r \in [n]. \tag{1.6}$$

In Section 6.3, we give a boundary measurement formula for an arbitrary f-admissible tuple $\boldsymbol{\theta}$. For simplicity, here we restrict to the case when $\boldsymbol{\theta}$ satisfies a certain genericity assumption.

Definition 1.16. A tuple $\boldsymbol{\theta} \in \mathbb{R}^n$ is called *generic* if all angles in $\boldsymbol{\theta}$ are pairwise non-congruent modulo π. Similarly, $\mathbf{t} \in (\mathbb{C}^*)^n$ is *generic* if $t_p \neq \pm t_q$ for all $p \neq q \in [n]$.

Theorem 1.17. *Suppose that $\boldsymbol{\theta}$ is a generic f-admissible tuple. Then the linear span $\mathrm{Span}(\boldsymbol{\gamma}_{f,\boldsymbol{\theta}}) \subset \mathbb{R}^n$ has dimension k and we have*

$$\mathrm{Meas}_f(\boldsymbol{\theta}) = \mathrm{Span}(\boldsymbol{\gamma}_{f,\boldsymbol{\theta}}) \quad \textit{inside } \mathrm{Gr}_{\geqslant 0}(k,n). \tag{1.7}$$

Replacing $\sin(t-\theta_p)$ with $[\![t, t_p]\!]$ in (1.6), one obtains a formula for $\mathrm{Meas}_f(\mathbf{t})$ for all generic $\mathbf{t} \in (\mathbb{C}^*)^n$; cf. Theorem 6.2.

Example 1.18. Let $k=2$, $n=4$, and $\bar{f} = \bar{f}_{k,n}$ be the permutation sending $p \mapsto p+2$ modulo 4. The boundary measurement map $\mathrm{Meas}_f(\boldsymbol{\theta})$ was computed in Figure 1(d). Since the Plücker coordinates are defined up to a common scalar, the term (24) cancels out. The sets J_r are given by $J_1 = \{2\}$, $J_2 = \{3\}$, $J_3 = \{4\}$, and $J_4 = \{1\}$, so $\boldsymbol{\gamma}_{f,\boldsymbol{\theta}}$ has coordinates

$$\boldsymbol{\gamma}_{f,\boldsymbol{\theta}}(t) = (\sin(t-\theta_2), \sin(t-\theta_3), \sin(t-\theta_4), -\sin(t-\theta_1)).$$

We can choose a basis of $\mathrm{Span}(\boldsymbol{\gamma}_{f,\boldsymbol{\theta}})$ consisting of e.g. $\boldsymbol{\gamma}_{f,\boldsymbol{\theta}}(0)$ and $\boldsymbol{\gamma}_{f,\boldsymbol{\theta}}(\pi/2)$, which we can write in the rows of the following matrix:

$$A = \begin{pmatrix} -\sin(\theta_2) & -\sin(\theta_3) & -\sin(\theta_4) & \sin(\theta_1) \\ \cos(\theta_2) & \cos(\theta_3) & \cos(\theta_4) & -\cos(\theta_1) \end{pmatrix}.$$

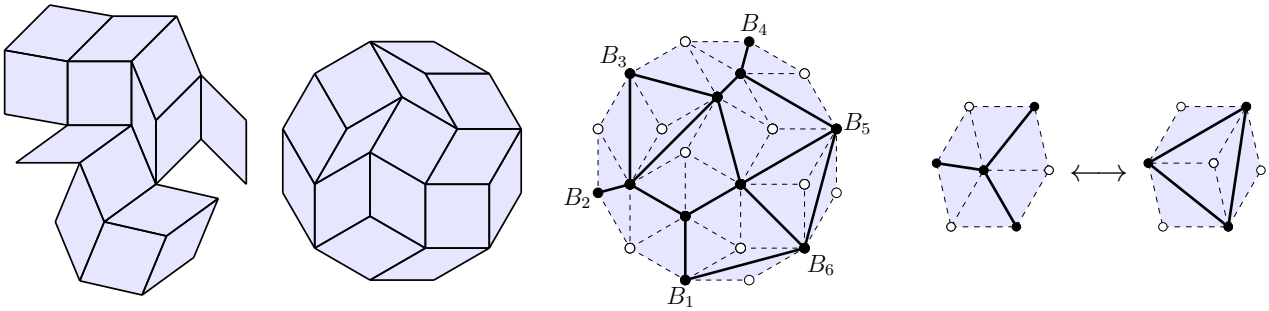

(a) arbitrary polygon R (b) regular polygon R_N (c) isoradial graph $G_{\mathbb{T}}$ (d) star-triangle move

FIGURE 4. (a) A rhombus tiling of an arbitrary polygon R; (b) a rhombus tiling of a regular polygon R_N for $N = 6$; (c) the associated isoradial graph $G_{\mathbb{T}}$ consists of black vertices and black solid edges; (d) a flip of a rhombus tiling resulting in a star-triangle move on $G_{\mathbb{T}}$. Figure reproduced from [Gal20].

We see that the maximal minors of A coincide with the values computed in Figure 1(d).

Remark 1.19. For a generic $\boldsymbol{\theta}$, an explicit basis of $\mathrm{Span}(\boldsymbol{\gamma}_{f,\boldsymbol{\theta}})$ can be chosen by taking any k distinct points on the curve $\boldsymbol{\gamma}_{f,\boldsymbol{\theta}}$ (Proposition 6.7). A more canonical way to produce a basis of $\mathrm{Span}(\boldsymbol{\gamma}_{f,\boldsymbol{\theta}})$ is to observe that each coordinate $\gamma_r(t)$ is a trigonometric polynomial of degree $k-1$. Therefore it has precisely k non-trivial Fourier coefficients. The rows of the resulting $k \times n$ matrix of Fourier coefficients form a basis of $\mathrm{Span}(\boldsymbol{\gamma}_{f,\boldsymbol{\theta}})$ which does not depend on anything besides f and the angles $\theta_1, \theta_2, \ldots, \theta_n$; see Proposition 6.8.

1.6. **Applications.** Our boundary measurement formula can be specialized to the cases of the Ising model and electrical resistor networks. For the Ising model, this was done in [Gal20]; here we focus on the case of electrical networks.

Critical electrical networks are defined on isoradial graphs. To produce an isoradial graph, take a rhombus tiling $\mathbb{T}$ of a polygonal region R, such as the one in Figure 4(a,b), color its vertices black and white in a bipartite way, and let $G_{\mathbb{T}}$ be the graph consisting of all diagonals of rhombi that connect their black vertices; see Figure 4(c). The graph $G_{\mathbb{T}}$ is isoradial, with white vertices of $\mathbb{T}$ being the centers of the corresponding unit circles.

We consider $G_{\mathbb{T}}$ as an electrical resistor network, replacing every edge by a resistor. Given a rhombus $ABCD$ of $\mathbb{T}$ with black vertices A and C, the edge AC of $G_{\mathbb{T}}$ is treated as a resistor whose resistance equals the ratio $\frac{|AC|}{|BD|}$ of the lengths of the rhombus diagonals.

Denote by $B_1, B_2, \ldots, B_N$ the vertices of $G_{\mathbb{T}}$ that belong to the boundary of R, listed in clockwise order. Fix $p \in [N]$. Let us apply the voltage of 1 to B_p and the voltage of 0 to all other boundary vertices. Then the voltages at all interior vertices, as well as the currents through all edges, can be computed from Ohm's and Kirchhoff's laws. For each $q \in [N]$, denote by $\Lambda^{\mathbb{T}}_{p,q}$ the current that flows into B_q.[2] (Thus $\Lambda^{\mathbb{T}}_{p,q} \geqslant 0$ for $p \neq q$.) The matrix $\Lambda^{\mathbb{T}}_{\mathrm{elec}} = (\Lambda^{\mathbb{T}}_{p,q})$ is known as the *response matrix* of the electrical network associated with $G_{\mathbb{T}}$.

[2]By linearity of Ohm's and Kirchhoff's laws, knowing $\Lambda^{\mathbb{T}}_{p,q}$ for all $1 \leqslant p, q \leqslant N$ allows one to solve the more general problem: for any known voltages that are applied to the boundary vertices, one finds the resulting currents flowing through each boundary vertex.

It is known [Ken93] that any two rhombus tilings of the same region can be related by a sequence of *flips* as in Figure 4(d). Applying a flip to a rhombus tiling results in applying a *star-triangle move* to the electrical network $G_{\mathbb{T}}$. A well-known property of the electrical response matrix $\Lambda^{\mathbb{T}}_{\text{elec}}$ is that it is preserved by such moves. Therefore $\Lambda^{\mathbb{T}}_{\text{elec}}$ depends only on the region R itself, and not on the particular choice of a rhombus tiling $\mathbb{T}$. It is thus natural to denote $\Lambda^{R}_{\text{elec}} := \Lambda^{\mathbb{T}}_{\text{elec}}$. A consequence of our boundary measurement formula is a formula for $\Lambda^{R}_{\text{elec}}$ that depends manifestly only on the region R.

Lam [Lam18] has constructed an embedding ϕ^{elec} of the space of $N \times N$ electrical response matrices into $\text{Gr}_{\geqslant 0}(N+1, 2N)$.[3] The image of the map ϕ^{elec} is contained inside the positroid cell labeled by a bounded affine permutation $f^{\text{elec}}_R \in \mathcal{B}(N+1, 2N)$. One can also choose a (essentially unique) f^{elec}_R-admissible tuple $\boldsymbol{\theta}_R := (\theta_1, \theta_2, \ldots, \theta_n)$ such that the directions of the sides of R are given by $\exp(-2i\theta_1), \exp(-2i\theta_2), \ldots, \exp(-2i\theta_n)$ in clockwise order. The following result reflects the well-known connection [Ken02, Section 6] between the critical dimer model and critical electrical networks.

Theorem 1.20. *For any region R, we have*

$$\phi^{\text{elec}}(\Lambda^{R}_{\text{elec}}) = \text{Meas}_{f^{\text{elec}}_R}(\boldsymbol{\theta}_R) \quad \textit{inside } \text{Gr}_{\geqslant 0}(N+1, 2N). \tag{1.8}$$

For generic regions, the right hand side of (1.8) is described by Theorem 1.17. The matrix $\Lambda^{R}_{\text{elec}}$ can be easily recovered from its image under ϕ^{elec}; see Section 7 for details.

Remark 1.21. An analogous result

$$\phi^{\text{Ising}}(M^{R}_{\text{Ising}}) = \text{Meas}_{f^{\text{Ising}}_R}(\boldsymbol{\theta}_R) \quad \text{inside } \text{Gr}_{\geqslant 0}(N, 2N)$$

holds for the critical Ising model; see Theorem 7.3 and [KLRR18, Section 7]. Curiously, in both cases, the tuple $\boldsymbol{\theta}_R$ is the same. In addition to being f^{Ising}_R-admissible (equivalently, f^{elec}_R-admissible), the tuple $\boldsymbol{\theta}_R$ is required to satisfy an additional *isotropic condition* (7.2) which is also identical in the Ising and electrical cases.

1.7. **Cyclically symmetric case.** Let $\boldsymbol{\theta}^{\text{reg}} = (\theta_1, \theta_2, \ldots, \theta_n)$ be given by $\theta_r := \frac{r\pi}{n}$ for all $r \in [n]$. In this case, $\text{Meas}_{f_{k,n}}(\boldsymbol{\theta}^{\text{reg}})$ is easily seen to coincide with the unique cyclically symmetric point[4] $X_0^{(k,n)} \in \text{Gr}_{\geqslant 0}(k, n)$, studied in [GKL17, Kar19]. This result is already of independent interest: previously, the Plücker coordinates of $X_0^{(k,n)}$ were known, but the corresponding explicit weighted planar bipartite graphs have not been constructed.

We describe the consequences of this observation for electrical networks. Having $\boldsymbol{\theta} = \boldsymbol{\theta}^{\text{reg}}$ corresponds to the case where the region R is a regular $2N$-gon, denoted R_N.

Theorem 1.22. *For $1 \leqslant p, q \leqslant N$ and $d := |p - q|$, we have*

$$\Lambda^{R_N}_{p,q} = \frac{\sin(\pi/N)}{N \cdot \sin((2d-1)\pi/2N) \cdot \sin((2d+1)\pi/2N)}. \tag{1.9}$$

Example 1.23. Consider the star electrical network as in Figure 4(d) inside a regular hexagon R_3. Then the resistance of each edge equals $\frac{1}{\sqrt{3}}$. Applying the voltage of 1 to B_1 and the voltage of 0 to B_2 and B_3, we calculate that the resulting voltage at the unique

[3] More precisely, Lam's embedding lands in $\text{Gr}_{\geqslant 0}(N-1, 2N)$. To get an element of $\text{Gr}_{\geqslant 0}(N+1, 2N)$, one needs to apply the duality discussed in Section 3.2.

[4] The point $X_0^{(k,n)}$ is the unique element of $\text{Gr}_{\geqslant 0}(k, n)$ satisfying $S(X_0^{(k,n)}) = X_0^{(k,n)}$, where $S : \text{Gr}_{\geqslant 0}(k, n) \to \text{Gr}_{\geqslant 0}(k, n)$ is the cyclic shift automorphism discussed in Section 3.1.

interior vertex is $\frac{1}{3}$, and thus the currents through B_2 and B_3 are both equal to $\frac{1}{\sqrt{3}}$. This agrees with (1.9) for $N = 3$ and $d = 1, 2$. For $d = 0$, we also obtain the correct value $-\frac{2}{\sqrt{3}}$ for the current through B_1, the negative sign representing the fact that the current flows *into* the network.

Remark 1.24. Despite the simplicity of Theorem 1.22 (and its Ising model analog [Gal20, Theorem 1.1]), both results are apparently new. In the Ising model case, this leads to new asymptotic consequences (including a convergence result to a conformally invariant limit [Gal20]).

1.8. **Shift by 1.** For $f \in \mathcal{B}(k, n)$, its *shift* $f^{\downarrow} \in \mathcal{B}(k-1, n)$ is defined by $f^{\downarrow}(p) := f(p-1)$ for all $p \in \mathbb{Z}$ (this operation is well defined when f is loopless). Taking p and $p-1$ modulo n, we obtain a shift map $\bar{f} \to \bar{f}^{\downarrow}$ on permutations.

The first appearance of this combinatorial shift map for bounded affine permutations occurred in the construction of the *BCFW triangulation* [BCFW05] of the *amplituhedron* [AHT14]. More precisely, that construction involved a "shift by 2," corresponding to passing between the momentum space and the momentum-twistor space. A linear-algebraic map from a subset of $\Pi_f^{>0}$ to a subset of $\Pi_{f^{\downarrow}}^{>0}$ can be found on [AHBC+16, Section 8.3]; see also [LPW20, Section 5.2]. The combinatorial shift map $f \mapsto f^{\downarrow}$ played a major role also in the study of the *parity duality* [GL18] and *T-duality* [LPW20] operations for amplituhedra.

The second appearance of the shift map arises when one compares the results of [GP20] for the Ising model with the results of [Lam18] for electrical networks. Specifically, [GP20, Question 9.2] and the discussion below it provides evidence for a stratification-preserving homeomorphism between a subset $\mathcal{X}^{\text{elec}} \subset \text{Gr}_{\geqslant 0}(N+1, 2N)$ and a subset $\mathcal{X}^{\text{Ising}} \subset \text{Gr}_{\geqslant 0}(N, 2N)$ sending $\mathcal{X}^{\text{elec}} \cap \Pi_f^{>0} \xrightarrow{\sim} \mathcal{X}^{\text{Ising}} \cap \Pi_{f^{\downarrow}}^{>0}$ homeomorphically for all f for which the intersection is nonempty. One easily checks that the above linear-algebraic map from [AHBC+16] does not provide such a homeomorphism. In view of our current approach, it is natural to additionally require such a map to restrict to a homeomorphism between the critical parts of $\mathcal{X}^{\text{elec}}$ and $\mathcal{X}^{\text{Ising}}$.

In Section 8, we give a new construction that provides partial progress towards this goal. Namely, building on our previous results [Gal18] connecting planar bipartite graphs to zonotopal tilings and on the results of [GPW19], we describe a simple map on the level of weighted planar bipartite graphs that gives the desired result for critical varieties. We discuss the relationship of this map with the boundary measurement map and square moves of planar bipartite graphs, and prove some of its surprising properties. The problem of constructing a stratification-preserving homeomorphism $\mathcal{X}^{\text{elec}} \xrightarrow{\sim} \mathcal{X}^{\text{Ising}}$ however remains open.

Acknowledgments. I am indebted to Pasha Pylyavskyy for his numerous contributions at various stages of the development of [Gal20], where the boundary measurement formula was first discovered in the context of the Ising model. The generalization to the Grassmannian level was inspired by the results of [CLR20, KLRR18], presented by Marianna Russkikh at the "Dimers in Combinatorics and Cluster Algebras" conference at the University of Michigan. I thank Marianna for bringing these results to my attention, and also thank the organizers of the conference (Sebastian Franco, Gregg Musiker, Richard Kenyon, David Speyer, and Lauren Williams) for making such an interaction possible. Finally, I am grateful to Lauren Williams and to the anonymous referee for their valuable comments on the first version of the text.

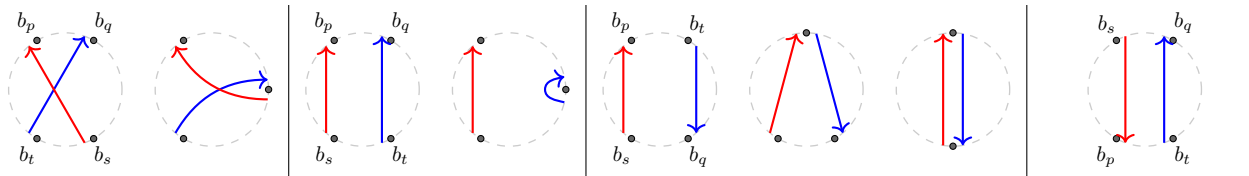

(a) crossing (b) alignment (c) $\{p,q\} \in \mathrm{Mis}_f^{\uparrow\downarrow}$ (d) $\{p,q\} \in \mathrm{Mis}_f^{\downarrow\uparrow}$

FIGURE 5. Crossings, alignments, and two types of misalignments for loopless bounded affine permutations.

2. Background on the totally nonnegative Grassmannian

The below constructions are well known in total positivity; see [Pos06, Lam16] for further details.

2.1. **Bounded affine permutations.** Positroid varieties are labeled by many families of combinatorial objects. We choose to work with bounded affine permutations introduced in [KLS13].

Definition 2.1. A (k,n)-*bounded affine permutation* is a bijection $f : \mathbb{Z} \to \mathbb{Z}$ such that

- $f(j+n) = f(j) + n$ for all $j \in \mathbb{Z}$,
- $\sum_{j=1}^{n}(f(j) - j) = kn$, and
- $j \leqslant f(j) \leqslant j+n$ for all $j \in \mathbb{Z}$.

We let $\mathcal{B}(k,n)$ denote the (finite) set of (k,n)-bounded affine permutations. For $f \in \mathcal{B}(k,n)$, we let $\bar{f} \in S_n$ be the permutation defined by the condition that $\bar{f}(p) \equiv f(p) \pmod{n}$. We let $f_{k,n} \in \mathcal{B}(k,n)$ be the "top cell" bounded affine permutation given by $f_{k,n}(p) := p + k$ for all $p \in \mathbb{Z}$.

Notation 2.2. Whenever we have a family X_f of objects labeled by $f \in \mathcal{B}(k,n)$, we denote $X_{f_{k,n}}$ by $X_{k,n}$.

We say that $f \in \mathcal{B}(k,n)$ is *loopless* if it satisfies $f(p) > p$ for all $p \in \mathbb{Z}$. Similarly, $f \in \mathcal{B}(k,n)$ is called *coloopless* if it satisfies $f(p) < p+n$ for all $p \in \mathbb{Z}$. The procedure in Remark 1.1 describes a bijection between the symmetric group S_n and the set of loopless (k,n)-bounded affine permutations for $1 \leqslant k \leqslant n$.

The *length* $\ell(f)$ of $f \in \mathcal{B}(k,n)$ is the number of pairs $s,t \in \mathbb{Z}$ such that $s \in [n]$, $s < t$, and $f(s) > f(t)$. Given such a pair and assuming f is loopless, the reductions of $p := f(s)$ and $q := f(t)$ modulo n are said to form an *alignment*; see Figure 5(b).

2.2. **Planar bipartite graphs.** Let G be a planar bipartite graph embedded in a disk as in Section 1.1. First, let us drop the assumption that the boundary vertices of G are colored black. For an almost perfect matching $\mathcal{A}$ of G, let $I_{\mathcal{A}} \in \binom{[n]}{k}$ be the set of black boundary vertices used by $\mathcal{A}$ together with the set of white boundary vertices *not* used by $\mathcal{A}$.

Recall that the boundary vertices of G are labeled by $b_1, b_2, \ldots, b_n$. We extend this labeling to all $p \in \mathbb{Z}$ by setting $b_p := b_{\bar{p}}$ where $p \in [n]$ is the reduction of $p \in \mathbb{Z}$ modulo n.

An *interior leaf* is an interior vertex of degree 1. We always assume that G admits an almost perfect matching, that every connected component of G contains a boundary vertex, and that each interior leaf of G is adjacent to the boundary. It follows [Pos06] that if G is reduced and $\bar{f}_G(p) = p$ then either

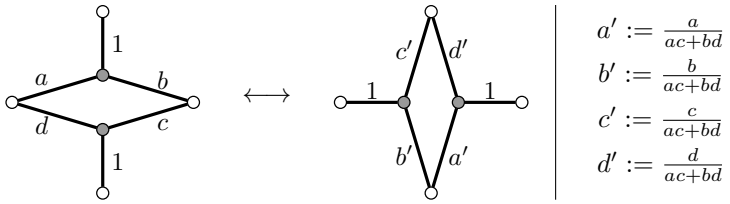

FIGURE 6. A square move.

- b_p is white and is adjacent to a black interior leaf, or
- b_p is black and is adjacent to a white interior leaf.

In the former case, we set $f_G(p) := p$ and say that p is a *loop*, and in the latter case, we set $f_G(p) := p + n$ and say that p is a *coloop*. All other values of f_G are uniquely determined by the values of $\bar{f}_G$ since we require $f_G(p) \equiv \bar{f}_G(p) \pmod{n}$ for all $p \in [n]$. From now on, we refer to f_G (as opposed to $\bar{f}_G$) as *the strand permutation* of G. Thus the reduced property may be restated as follows: a graph G satisfying the above assumptions is *reduced* if and only if it has $k(n-k) + 1 - \ell(f_G)$ faces. We refer to reduced planar bipartite graphs simply as *reduced graphs* and denote by $\mathcal{G}_{\mathrm{red}}(f)$ the set of reduced graphs with strand permutation $f \in \mathcal{B}(k, n)$.

We say that G has *black boundary* if all of its boundary vertices are black. The notion of having *white boundary* is defined analogously. Unless stated otherwise, we assume that G has black boundary, and the only other case we consider is when G has white boundary.

For an edge $e \in E(G)$, we say that e is *labeled* by $\{p, q\}$ if the strands passing through e terminate at b_p and b_q. It is known [Pos06] that if p, q form an alignment (Figure 5(b)) then for any $G \in \mathcal{G}_{\mathrm{red}}(f)$, no edge in G is labeled by $\{p, q\}$.

We also label the faces of G by k-element subsets of $[n]$. For a face F of G, let $\lambda(F) \in \binom{[n]}{k}$ be the set of all $p \in [n]$ such that f is to the left of the strand ending at b_p. This convention is known as *target-labeling* of the faces.

It was shown in [Pos06] that any two graphs $G, G' \in \mathcal{G}_{\mathrm{red}}(f)$ may be related by a sequence of *square moves* (Figure 6) and *contraction-uncontraction moves* (Figure 23). Specifically, given a square face F of G, one first uncontracts some edges so that all vertices of F become trivalent, adding degree 2 vertices as midpoints of uncontracted edges to preserve the bipartite property.[5] Next, one applies *gauge transformations* at the black vertices (see Section 2.4 below) to fix the weights of the vertical edges in Figure 6(left) to 1. Finally, one performs the local transformation as in Figure 6. These moves change the edge weights while preserving the boundary measurements (up to a common scalar).

2.3. **Bridge removal.** Let $f \in \mathcal{B}(k, n)$ and $r \in [n]$. Following [Lam16, Section 7.4], we say that f *has a bridge at* r if f satisfies $r < r+1 \leqslant f(r) < f(r+1) \leqslant r+n$. In this case, there exists a graph $G \in \mathcal{G}_{\mathrm{red}}(f)$ such that the neighborhood of the points b_r, b_{r+1} contains a *bridge configuration* shown in Figure 7(left). Removing the bridge edge yields a configuration in Figure 7(right), and the corresponding graph is also reduced and has strand permutation denoted $s_r f \in \mathcal{B}(k, n)$ which sends $r \mapsto f(r+1)$, $r+1 \mapsto f(r)$, and $q \mapsto f(q)$ for all $q \in \mathbb{Z}$ not congruent to r or $r+1$ modulo n. Any $f \in \mathcal{B}(k, n)$ without loops and coloops has a

[5]When (un)contracting a degree 2 interior vertex, we always assume that both edges incident to it have weight 1; this is always achievable by applying gauge transformations.

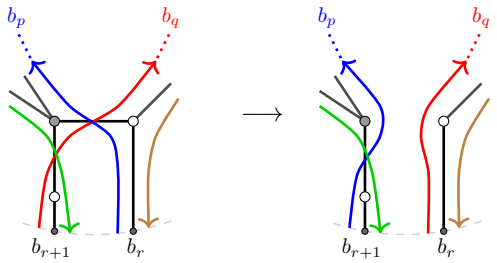

FIGURE 7. Removing a bridge (Section 2.3).

bridge at some $r \in [n]$. Thus, starting with any $f \in \mathcal{B}(k,n)$ and removing bridges, loops, and coloops, we can always reach a permutation in either $\mathcal{B}(0,1)$ or $\mathcal{B}(1,1)$.

2.4. **Positroid varieties.** Recall that the Grassmannian $\mathrm{Gr}(k,n)$ is identified with the space of full rank complex $k \times n$ matrices modulo row operations. Given a $k \times n$ matrix A, we let $\mathrm{RowSpan}(A) \in \mathrm{Gr}(k,n)$ denote its row span and $A_1, A_2, \ldots, A_n$ be its columns. We extend this to a sequence $(A_q)_{q \in \mathbb{Z}}$ by requiring

$$A_{q+n} = (-1)^{k-1} A_q \quad \text{for all } q \in \mathbb{Z}. \tag{2.1}$$

The sign twist is related to the cyclic shift automorphism of $\mathrm{Gr}_{\geqslant 0}(k,n)$ discussed in Section 3.1. For a full rank $k \times n$ matrix A, we let $f_A : \mathbb{Z} \to \mathbb{Z}$ be given by

$$f_A(p) = \min\{q \geqslant p \mid A_p \in \mathrm{Span}\,(A_{p+1}, A_{p+2}, \ldots, A_q)\} \quad \text{for } p \in \mathbb{Z}. \tag{2.2}$$

For example, if A_p is a zero column (i.e., a *loop*) then $f_A(p) = p$, and if A_p is not in the span of other columns (i.e., a *coloop*) then $f_A(p) = p + n$. It is known [KLS13] that f_A is a (k,n)-bounded affine permutation which depends only on the row span of A. The *positroid stratification* of $\mathrm{Gr}(k,n)$ is given by

$$\mathrm{Gr}(k,n) = \bigsqcup_{f \in \mathcal{B}(k,n)} \Pi_f^\circ, \quad \text{where} \quad \Pi_f^\circ := \{\mathrm{RowSpan}(A) \in \mathrm{Gr}(k,n) \mid f_A = f\}.$$

We let $\Pi_f^{>0} := \Pi_f^\circ \cap \mathrm{Gr}_{\geqslant 0}(k,n)$ denote the corresponding *positroid cell*. We also have the *positroid variety* Π_f which is the Zariski closure of $\Pi_f^{>0}$ (equivalently, of Π_f°). In fact, Π_f° is an explicit open subvariety of Π_f. Namely, for each $q \in \mathbb{Z}$, let

$$\tilde{I}_q := \{f(p) \mid p \in \mathbb{Z} \text{ is such that } p < q \leqslant f(p)\}. \tag{2.3}$$

For $q \in [n]$, let $I_q \in \binom{[n]}{k}$ be obtained from $\tilde{I}_q$ by reducing all elements modulo n. The sequence $\mathcal{I}_f := (I_1, I_2, \ldots, I_n)$ is called the *Grassmann necklace* of f. Alternatively, for loopless f, we have $I_q = J_q \sqcup \{q\}$ for all $q \in [n]$, where J_q was defined in (1.5). We have

$$\Pi_f^\circ := \{X \in \Pi_f \mid \Delta_{I_q}(X) \neq 0 \text{ for all } q \in [n]\}. \tag{2.4}$$

Grassmann necklaces also allow one to describe Π_f as an explicit subvariety of $\mathrm{Gr}(k,n)$. Namely, each $f \in \mathcal{B}(k,n)$ gives rise to a *positroid* $\mathcal{M}_f \subset \binom{[n]}{k}$ defined as follows. For each $q \in [n]$, introduce a total order $\preceq_q$ on $[n]$ given by

$$q \preceq_q q+1 \preceq_q \cdots \preceq_q q-1,$$

where the indices are taken modulo n. For two k-element sets $I = \{i_1 \prec_q i_2 \prec_q \cdots \prec_q i_k\}$ and $J = \{j_1 \prec_q j_2 \prec_q \cdots \prec_q j_k\}$, we write $I \preceq_q J$ if $i_r \preceq_q j_r$ for all $r \in [k]$. Then the

positroid $\mathcal{M}_f$ consists of all sets $J \in \binom{[n]}{k}$ such that $I_q \preceq_q J$ for all $q \in [n]$. (Thus a positroid is an intersection of n cyclically shifted Schubert matroids.) The variety Π_f is described by

$$\Pi_f = \{X \in \mathrm{Gr}(k,n) \mid \Delta_J(X) = 0 \text{ for all } J \notin \mathcal{M}_f\}. \tag{2.5}$$

Finally, we have

$$\Pi_f^{>0} = \{X \in \mathrm{Gr}(k,n) \mid \Delta_J(X) > 0 \text{ for } J \in \mathcal{M}_f \text{ and } \Delta_J(X) = 0 \text{ otherwise}\}. \tag{2.6}$$

The dimension of $\Pi_f^{>0}$ (as well as Π_f°, and Π_f) is given by $k(n-k) - \ell(f)$, where $\ell(f)$ is the length of f introduced in Section 2.1.

Positroid cells $\Pi_f^{>0}$ and Grassmann necklaces were first studied by Postnikov [Pos06] while positroid varieties Π_f and their open subvarieties Π_f° were introduced by Knutson–Lam–Speyer [KLS13].

Let $E = E(G)$ be the edge set of a reduced graph G. The map $\mathrm{Meas}_G : \mathbb{R}_{>0}^E \to \mathrm{Gr}_{\geqslant 0}(k,n)$ restricts to a homeomorphism $\mathrm{Meas}_G : \mathbb{R}_{>0}^E/\,\mathrm{Gauge} \xrightarrow{\sim} \Pi_{f_G}^{>0}$, where $\mathbb{R}_{>0}^E/\,\mathrm{Gauge}$ denotes the space of positive edge weights of G considered modulo *gauge transformations*, that is, rescalings of the weights of all edges incident to a given interior vertex. For each (interior or boundary) face F of G, let $e_1, e_2, \ldots, e_{2m}$ be the edges on the boundary of F in clockwise order. The number of edges is even since we are assuming that G has either black boundary or white boundary. For any weight function $\mathrm{wt} \in \mathbb{R}_{>0}^E$, we may consider an alternating product

$$\frac{\mathrm{wt}(e_1)\,\mathrm{wt}(e_3)\cdots\mathrm{wt}(e_{2m-1})}{\mathrm{wt}(e_2)\,\mathrm{wt}(e_4)\cdots\mathrm{wt}(e_{2m})}. \tag{2.7}$$

It is clearly invariant under gauge transformations, and in fact may be recovered from $\mathrm{Meas}_G(\mathrm{wt})$ using the *left twist map* (see [MuSp17, Corollary 5.11]) of Muller–Speyer discussed in Section 5.4.

3. Cyclic symmetry and duality

In this section, we discuss how critical varieties are affected by some natural operations on the totally nonnegative Grassmannian, namely, cyclically shifting the columns and taking orthogonal complements.

3.1. **Cyclic symmetry.** The totally nonnegative Grassmannian $\mathrm{Gr}_{\geqslant 0}(k,n)$ admits a nontrivial shift homeomorphism $S : \mathrm{Gr}_{\geqslant 0}(k,n) \to \mathrm{Gr}_{\geqslant 0}(k,n)$. It sends (the row span of) a matrix A with columns $A_1, A_2, \ldots, A_n$ to (the row span of) the matrix $S(A)$ with columns $A_2, \ldots A_n, (-1)^{k-1}A_1$. The sign $(-1)^{k-1}$ ensures that the nonnegativity of maximal minors is preserved. The map S restricts to a homeomorphism $S : \Pi_f^{>0} \xrightarrow{\sim} \Pi_{\sigma^{-1}f\sigma}^{>0}$, where $\sigma : \mathbb{Z} \to \mathbb{Z}$ sends $p \mapsto p+1$ for all $p \in \mathbb{Z}$. Thus $\sigma^{-1}f\sigma \in \mathcal{B}(k,n)$ is defined by $(\sigma^{-1}f\sigma)(p) = f(p+1) - 1$ for $p \in \mathbb{Z}$.

Note that the definition of the critical cell $\mathrm{Crit}_f^{>0}$ in Section 1.3 does not appear to respect this cyclic symmetry, since we choose the edge weights to be $\sin(\theta_q - \theta_p)$ for $1 \leqslant p < q \leqslant n$. Nevertheless, we have the following result.

Proposition 3.1. *For a loopless $f \in \mathcal{B}(k,n)$, the map S restricts to a homeomorphism*

$$S : \mathrm{Crit}_f^{>0} \xrightarrow{\sim} \mathrm{Crit}_{\sigma^{-1}f\sigma}^{>0}.$$

While this result is not hard to see directly, we prefer to use this opportunity to introduce *affine notation* that reflects the cyclic symmetry of critical cells. First, we always extend a tuple $\boldsymbol{\theta} = (\theta_1, \theta_2, \ldots, \theta_n) \in \mathbb{R}^n$ to an infinite sequence $\tilde{\boldsymbol{\theta}} : \mathbb{Z} \to \mathbb{R}$ uniquely determined by the conditions $\tilde{\theta}_p = \theta_p$ for $p \in [n]$ and

$$\tilde{\theta}_{p+n} = \tilde{\theta}_p + \pi \quad \text{for all } p \in \mathbb{Z}. \tag{3.1}$$

Since $\boldsymbol{\theta}$ and $\tilde{\boldsymbol{\theta}}$ determine each other, we use them interchangeably and write e.g. $\mathrm{Meas}_f(\tilde{\boldsymbol{\theta}})$ for $\mathrm{Meas}_f(\boldsymbol{\theta})$.

Let us describe f-admissibility in the affine language. For $p, q \in \mathbb{Z}$, we say that (p, q) form an *affine f-crossing* if we have $s < t < p < q \leqslant s + n$, where $s := f^{-1}(p)$ and $t := f^{-1}(p)$.

It is easy to check that if $1 \leqslant p < q \leqslant n$ form an f-crossing then either (p, q) or $(q, p + n)$ form an affine f-crossing. Conversely, if (p, q) form an affine f-crossing then their reductions $\bar{p}, \bar{q} \in [n]$ modulo n form an f-crossing. It follows that a tuple $\boldsymbol{\theta} = (\theta_1, \theta_2, \ldots, \theta_n)$ is f-admissible if and only if the corresponding sequence $\tilde{\boldsymbol{\theta}} : \mathbb{Z} \to \mathbb{R}$ satisfies

$$\tilde{\theta}_p < \tilde{\theta}_q < \tilde{\theta}_{p+n} \tag{3.2}$$

whenever (p, q) form an affine f-crossing. In this case, we say that $\tilde{\boldsymbol{\theta}}$ is *f-admissible*.

For a sequence $\tilde{\boldsymbol{\theta}} : \mathbb{Z} \to \mathbb{R}$, let $\tilde{\boldsymbol{\theta}} \circ \sigma : \mathbb{Z} \to \mathbb{R}$ be given by $(\tilde{\boldsymbol{\theta}} \circ \sigma)_p := \tilde{\theta}_{p+1}$. Proposition 3.1 follows from the following observation.

Lemma 3.2. *For a loopless $f \in \mathcal{B}(k, n)$, a sequence $\tilde{\boldsymbol{\theta}} : \mathbb{Z} \to \mathbb{R}$ is f-admissible if and only if $\tilde{\boldsymbol{\theta}} \circ \sigma$ is $(\sigma^{-1} f \sigma)$-admissible. In this case, we have*

$$\mathrm{Meas}_f(\tilde{\boldsymbol{\theta}}) = \mathrm{Meas}_{\sigma^{-1} f \sigma}(\tilde{\boldsymbol{\theta}} \circ \sigma). \tag{3.3}$$

Proof. The f-admissibility part is clear from (3.2). To prove (3.3), consider a graph $G \in \mathcal{G}_{\mathrm{red}}(f)$. Relabeling its boundary vertices as $(b_n, b_1, \ldots, b_{n-1})$, we obtain a graph $G' \in \mathcal{G}_{\mathrm{red}}(\sigma^{-1} f \sigma)$. Let $e \in E(G) = E(G')$ be an edge not adjacent to the boundary, and suppose that it is labeled in G by $\{p, q\}$ with $1 \leqslant p < q \leqslant n$. The weights $\mathrm{wt}_{\tilde{\boldsymbol{\theta}}}(e)$ and $\mathrm{wt}'_{\tilde{\boldsymbol{\theta}} \circ \sigma}(e)$ coincide unless $p = 1$. If $p = 1$ then $\mathrm{wt}_{\tilde{\boldsymbol{\theta}}}(e) = \sin(\theta_q - \theta_1)$ while $\mathrm{wt}'_{\tilde{\boldsymbol{\theta}} \circ \sigma}(e) = \sin(\theta'_n - \theta'_{q-1})$, where $\tilde{\boldsymbol{\theta}}' := \tilde{\boldsymbol{\theta}} \circ \sigma$. It remains to note that $\theta'_n = \theta_{n+1} = \theta_1 + \pi$ and $\theta'_{q-1} = \theta_q$, thus $\mathrm{wt}'_{\tilde{\boldsymbol{\theta}} \circ \sigma}(e) = \sin(\theta_q - \theta_1) = \mathrm{wt}_{\tilde{\boldsymbol{\theta}}}(e)$ in this case as well. □

3.2. **Duality.** For $V \in \mathrm{Gr}(k, n)$, denote by $V^\perp \in \mathrm{Gr}(n - k, n)$ its orthogonal complement. We let $\mathrm{alt}(V) \in \mathrm{Gr}(k, n)$ be obtained from V by changing the sign of every second column of the matrix representing V. We set

$$\mathrm{alt}^\perp(V) := \mathrm{alt}(V^\perp) = (\mathrm{alt}(V))^\perp.$$

We discuss several well-known properties of the map $\mathrm{alt}^\perp$; see e.g. [Kar17, Lemma 1.11] and references therein. The map $\mathrm{alt}^\perp$ restricts to an involutive homeomorphism $\mathrm{Gr}_{\geqslant 0}(k, n) \xrightarrow{\sim} \mathrm{Gr}_{\geqslant 0}(n - k, n)$. For $f \in \mathcal{B}(k, n)$, let $\widehat{f} \in \mathcal{B}(n - k, n)$ be given by

$$\widehat{f}(p) = f^{-1}(p) + n \quad \text{for all } p \in \mathbb{Z}. \tag{3.4}$$

The map $f \mapsto \widehat{f}$ is an involution. The map $\mathrm{alt}^\perp$ restricts to a homeomorphism $\Pi_f^{\geqslant 0} \xrightarrow{\sim} \Pi_{\widehat{f}}^{\geqslant 0}$. It satisfies

$$\Delta_I(X) = \Delta_{[n] \setminus I}(\mathrm{alt}^\perp(X)) \quad \text{for all } I \in \binom{[n]}{k}. \tag{3.5}$$

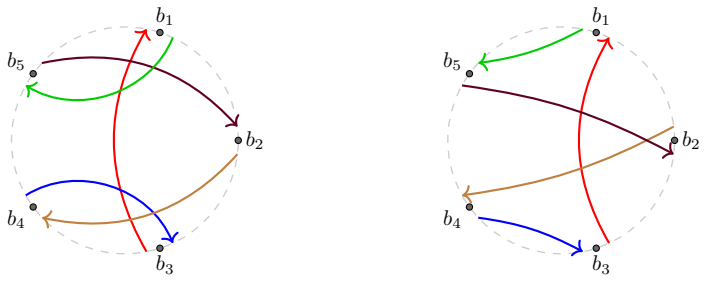

(a) reduced strand diagram of f (b) dual reduced strand diagram of f

FIGURE 8. A (dual) reduced strand diagram.

Recall from Section 1.3 that any loopless $f \in \mathcal{B}(k,n)$ gives rise to a critical cell $\mathrm{Crit}_f^{>0}$. We are interested in the effect of the map $\mathrm{alt}^\perp$ on critical cells. Note that in general $\widehat{f} \in \mathcal{B}(n-k,n)$ need not be loopless, but it is coloopless. What we will show below is that the map $\mathrm{alt}^\perp$ sends critical cells to *dual critical cells*.

Recall that we have placed points b_p^-, b_p, b_p^+ on the circle for each $p \in [n]$.

Definition 3.3. Let $f \in \mathcal{B}(k,n)$ be coloopless. The *dual reduced strand diagram* of f is obtained by drawing a straight arrow $b_s^- \to b_p^+$ whenever $\bar{f}(s) = p$. We say that $p \neq q$ form a *dual f-crossing* if the arrows $b_s^- \to b_p^+$ and $b_t^- \to b_q^+$ cross. We say that $\boldsymbol{\theta} = (\theta_1, \theta_2, \ldots, \theta_n)$ is *dual f-admissible* if whenever $1 \leqslant p < q \leqslant n$ form a dual f-crossing, (1.3) is satisfied.

In general, the reduced strand diagram of f and the dual reduced strand diagram of the same f behave quite differently; see Figure 8 for an example.

Let $f \in \mathcal{B}(k,n)$ be coloopless and let $G \in \mathcal{G}_{\mathrm{red}}(f)$ be a graph with black boundary. For the purposes of this section, if $f(p) = p$ for some p then by convention we treat b_p as a black boundary vertex of degree zero, or, equivalently, as a white boundary vertex adjacent to a black interior leaf.

For an edge $e \in E(G)$ labeled by $\{p,q\}$, set

$$\widehat{\mathrm{wt}}_{\boldsymbol{\theta}}(e) := \sin(\theta_q - \theta_p). \tag{3.6}$$

This is different from (1.2) in that the boundary edges no longer have weight 1. Let

$$\widehat{\mathrm{Meas}}_f(\boldsymbol{\theta}) := \mathrm{Meas}_G(\widehat{\mathrm{wt}}_{\boldsymbol{\theta}}).$$

Finally, define the *dual critical cell*

$$\widehat{\mathrm{Crit}}_f^{>0} := \{\widehat{\mathrm{Meas}}_f(\boldsymbol{\theta}) \mid \boldsymbol{\theta} = (\theta_1, \theta_2, \ldots, \theta_n) \text{ is a dual } f\text{-admissible tuple}\}.$$

Proposition 3.4. *Let $f \in \mathcal{B}(k,n)$ and $\tilde{\boldsymbol{\theta}} : \mathbb{Z} \to \mathbb{R}$.*

(i) *$\tilde{\boldsymbol{\theta}}$ is f-admissible $\iff$ $\tilde{\boldsymbol{\theta}} \circ f$ is dual $\widehat{f}$-admissible.*

(ii) $\mathrm{Meas}_f(\tilde{\boldsymbol{\theta}}) = \mathrm{alt}^\perp(\widehat{\mathrm{Meas}}_{\widehat{f}}(\tilde{\boldsymbol{\theta}} \circ f))$.

(iii) *The map $\mathrm{alt}^\perp$ yields an involutive homeomorphism*

$$\mathrm{Crit}_f^{>0} \cong \widehat{\mathrm{Crit}}_{\widehat{f}}^{>0}.$$

Remark 3.5. Our constructions are invariant with respect to adding the same constant to all values of $\tilde{\boldsymbol{\theta}}$. Modulo such transformations, the map $(f, \tilde{\boldsymbol{\theta}}) \mapsto (\widehat{f}, \tilde{\boldsymbol{\theta}} \circ f)$ is an involution.

Proof. Suppose that $\tilde{\boldsymbol{\theta}}$ is f-admissible and let $\tilde{\boldsymbol{\theta}}' := \tilde{\boldsymbol{\theta}} \circ f$. Let us say that $p < q \in \mathbb{Z}$ form a *dual affine $\widehat{f}$-crossing* if we have $s < t \leqslant p < q < s + n$, where $\widehat{f}(s) = p$ and $\widehat{f}(t) = q$. As in Section 3.1, we see that $\tilde{\boldsymbol{\theta}}'$ is dual $\widehat{f}$-admissible if and only if for all $p < q$ forming a dual affine $\widehat{f}$-crossing, we have $\tilde{\theta}'_p < \tilde{\theta}'_q < \tilde{\theta}'_{p+n}$. We claim that this is equivalent to $\tilde{\theta}_s < \tilde{\theta}_t < \tilde{\theta}_{s+n}$. Indeed, by definition, we have $p = \widehat{f}(s) = f^{-1}(s) + n$ and $q = \widehat{f}(t) = f^{-1}(t) + n$, thus $f(p) = s + n$ and $f(q) = t + n$. The inequalities $s < t \leqslant p < q < s + n$ may be rewritten as $p < q < s + n < t + n \leqslant p + n$, and since $f(p) = s + n$ and $f(q) = t + n$, we see that $s < t$ form an affine f-crossing. Since $\tilde{\boldsymbol{\theta}}$ is f-admissible, we find $\tilde{\theta}_s < \tilde{\theta}_t < \tilde{\theta}_{s+n}$, so $\tilde{\boldsymbol{\theta}}'$ is dual $\widehat{f}$-admissible, proving the forward direction of (i). The converse direction is handled similarly.

To show (ii), choose $G \in \mathcal{G}_{\mathrm{red}}(f)$. Let $\widehat{G}$ be obtained by changing the colors of all vertices of G. Thus $\widehat{G}$ has white boundary and strand permutation $\widehat{f}$. Let $\widehat{G}'$ be obtained from $\widehat{G}$ by putting a white degree 2 vertex on each boundary edge of $\widehat{G}$ and then changing the color of all boundary vertices to black.

By (3.5), it follows that $\mathrm{alt}^{\perp} \circ \mathrm{Meas}_G = \mathrm{Meas}_{\widehat{G}}$ as maps $\mathbb{R}^E_{>0} \to \mathrm{Gr}_{\geqslant 0}(n-k, n)$. Here we identify the sets of edges of G and $\widehat{G}$ and denote them by E. Let $e \in E$ be an edge whose weight in G is $\mathrm{wt}_{\boldsymbol{\theta}}(e) = \sin(\theta_q - \theta_p)$. Suppose that $\bar{f}(s) = p$ and $\bar{f}(t) = q$ for some $s, t, p, q \in [n]$ such that $p < q$. Then the weight $\widehat{\mathrm{wt}}_{\boldsymbol{\theta}'}(e)$ in $\widehat{G}'$ is given by $\sin(\theta'_s - \theta'_t)$ if $s > t$ and by $\sin(\theta'_t - \theta'_s)$ if $s < t$, where $\tilde{\boldsymbol{\theta}}' = \tilde{\boldsymbol{\theta}} \circ f$ as above. Note also that $\theta'_s = \theta_p$ if $s < p$ and $\theta'_s = \theta_p + \pi$ if $s > p$, and similarly for θ'_q. As explained in Section 2.2, since e is labeled by $\{p, q\}$, the strands $s \to p$ and $t \to q$ cannot form an alignment. Using this condition, one checks directly that we have $\widehat{\mathrm{wt}}_{\boldsymbol{\theta}'}(e) = \sin(\theta_q - \theta_p)$ in all cases. Thus we have $\mathrm{wt}_{\boldsymbol{\theta}}(e) = \widehat{\mathrm{wt}}_{\boldsymbol{\theta}'}(e)$ for each interior edge $e \in E$. If e is a boundary edge of G then $\mathrm{wt}_{\boldsymbol{\theta}}(e) = 1$ and e corresponds to two edges e', e'' in $\widehat{G}'$ sharing a white degree 2 vertex and satisfying $\widehat{\mathrm{wt}}_{\boldsymbol{\theta}'}(e') = \widehat{\mathrm{wt}}_{\boldsymbol{\theta}'}(e'')$. Thus applying a gauge transformation at these white degree 2 vertices, we find $\mathrm{alt}^{\perp} \circ \mathrm{Meas}_G(\mathrm{wt}_{\boldsymbol{\theta}}) = \mathrm{Meas}_{\widehat{G}}(\widehat{\mathrm{wt}}_{\boldsymbol{\theta}'})$. This completes the proof of (ii), and (iii) follows from (ii) as a direct corollary. □

4. Connected components and strand diagrams

Recall that we have defined in Section 1.3 a critical cell $\mathrm{Crit}^{>0}_f$ for any loopless $f \in \mathcal{B}(k, n)$. We mentioned that the edge weights in $\mathrm{wt}_{\boldsymbol{\theta}}$ are positive when $\boldsymbol{\theta}$ is f-admissible and discussed the relationship between the dimension of $\mathrm{Crit}^{>0}_f$ and connected components of the reduced strand diagram of f. In this section, we justify these claims, studying the combinatorics of reduced strand diagrams along the way.

4.1. **Connected components.** We start by stating several results concerning connected components of the reduced strand diagram of f. Their proofs turn out to be quite involved, and are deferred to later sections.

Fix a loopless $f \in \mathcal{B}(k, n)$. Let $G^{\times}_f$ be the undirected graph with vertex set $[n]$ and edge set

$$E(G^{\times}_f) := \{\{p, q\} \mid p, q \text{ form an } f\text{-crossing}\}. \tag{4.1}$$

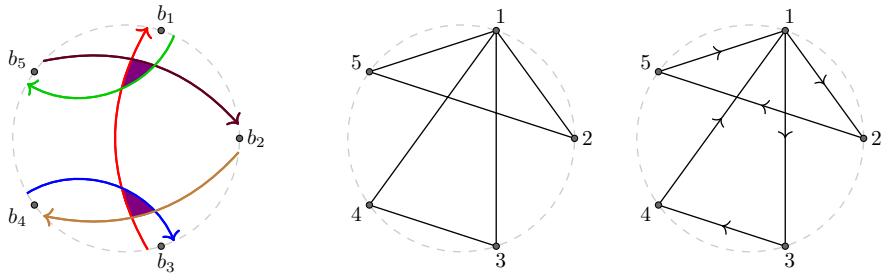

(a) reduced strand diagram D (b) graph $G_D^\times$ (c) directed graph $\vec{G}_D^\times$

FIGURE 9. The graphs $G_D^\times$ and $\vec{G}_D^\times$ defined in (4.1) and (5.7). The shaded regions on the left represent convex regions from Definition 4.9.

See Figure 9(b) for an example. Let c_f be the number of connected components of $G_f^\times$. (Thus c_f is the number of connected components of the reduced strand diagram of f, viewed as a topological union of strands in a disk.) We set $d_f := n - c_f$.

Definition 4.1. We say that a reduced graph G is *contracted* if it has no degree 2 vertices that are not adjacent to the boundary.

The following result will be proved in Section 4.3.

Proposition 4.2. *Suppose a non-boundary edge e of a graph $G \in \mathcal{G}_{\mathrm{red}}(f)$ is labeled by $\{p, q\}$ with $1 \leqslant p < q \leqslant n$. Then for any f-admissible tuple $\boldsymbol{\theta}$, we have*

$$\theta_p < \theta_q < \theta_p + \pi. \tag{4.2}$$

In particular, p and q belong to the same connected component of $G_f^\times$ and we have $\mathrm{wt}_{\boldsymbol{\theta}}(e) > 0$.

Let $C \subset [n]$ be a connected component of $G_f^\times$. By Proposition 4.2, adding a constant to θ_p for all $p \in C$ preserves $\mathrm{Meas}_f(\boldsymbol{\theta})$. Choose some representatives $p_1, p_2, \ldots, p_{c_f} \in [n]$, one from each connected component of $G_f^\times$. Let

$$\Theta_f^{>0} := \{\boldsymbol{\theta} = (\theta_1, \theta_2, \ldots, \theta_n) \in \mathbb{R}^n \mid \boldsymbol{\theta} \text{ is } f\text{-admissible and } \theta_{p_1} = \theta_{p_2} = \cdots = \theta_{p_{c_f}} = 0\}. \tag{4.3}$$

Thus the map $\mathrm{Meas}_f : \Theta_f^{>0} \to \mathrm{Crit}_f^{>0}$ is surjective. Note that $\Theta_f^{>0}$ is easily seen to be homeomorphic to $\mathbb{R}_{>0}^{d_f}$ since it may be identified with the interior of a d_f-dimensional polytope.

Conjecture 4.3 (The injectivity conjecture)**.** The map $\mathrm{Meas}_f : \Theta_f^{>0} \to \mathrm{Crit}_f^{>0}$ is a homeomorphism.

The special case of Conjecture 4.3 for the top cell is proved in Section 9.

Theorem 4.4. *The injectivity conjecture holds for $f = f_{k,n}$ for $1 \leqslant k \leqslant n$. In particular,*

$$\dim_{\mathbb{C}}(\mathrm{Crit}_{k,n}) = n - 1 \quad \text{and} \quad \mathrm{Crit}_{k,n}^{>0} \cong \mathbb{R}_{>0}^{n-1} \quad \text{for } 2 \leqslant k \leqslant n-1.$$

4.2. **Reduced strand diagrams.** As in Section 1.3, let us consider a disk with $2n$ boundary points $b_1^-, b_1^+, b_2^-, b_2^+, \ldots, b_n^-, b_n^+$ ordered clockwise.

Definition 4.5. A *strand diagram* D is a collection of n smooth oriented paths (*strands*) $S_1, S_2, \ldots, S_n$ in a disk such that

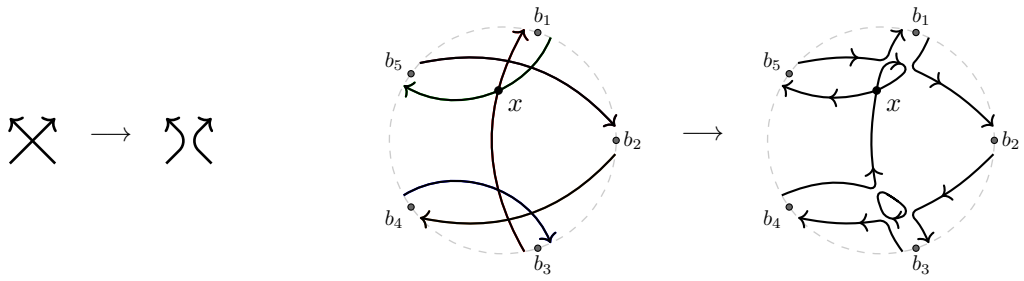

(a) resolving a crossing (b) resolving all crossings except one

FIGURE 10. Resolving crossings in reduced strand diagrams. For the picture on the right, the point x belongs to two strands denoted S'_p and S'_q in the proof of Proposition 4.8.

(1) no three strands intersect at one point and no strand intersects itself,
(2) all intersections are transversal and lie in the interior of the disk,
(3) each strand S_p starts at b_s^+ (for some $s \in [n]$) and ends at b_p^-.

Thus the directions of the strands alternate around the boundary of the disk.

As a special case, this definition contains Postnikov's *alternating strand diagrams* [Pos06], which are essentially the diagrams that arise by drawing the strands associated to a given reduced graph G. Alternating strand diagrams usually contain pairs of strands that intersect multiple times. We will focus on the opposite special case.

Definition 4.6. A *reduced strand diagram* is a strand diagram in which any two strands intersect at most once.

For example, Figure 2(b) contains an alternating strand diagram on the left and a reduced strand diagram on the right. Definition 4.6 includes Definition 1.5 as a special case: given $f \in \mathcal{B}(k,n)$, we denote by D_f its reduced strand diagram where all strands are straight.

Let D be a reduced strand diagram. We introduce two graphs, $G_D^\times$ and $\vec{G}_D^\times$ with vertex set $[n]$. As before, $G_D^\times$ is an undirected graph containing an edge $\{p,q\}$ whenever S_p and S_q form a crossing. Note that $G_D^\times$ admits a natural orientation. Let us say that two strands S_p and S_q form a *positive crossing* if the points $b_s^+, b_t^+, b_p^-, b_q^-$ are cyclically ordered clockwise, where S_p connects $b_s^+ \to b_p^-$ and S_q connects $b_t^+ \to b_q^-$; see Figure 5(a). We then let $\vec{G}_D^\times$ be the directed graph containing an edge $(p \to q)$ whenever S_p and S_q form a positive crossing. See Figure 9(c).

Definition 4.7. An *increasing cycle* is a directed cycle $(a_1 \to a_2 \to \cdots \to a_m \to a_1)$ in $\vec{G}_D^\times$ such that $1 \leqslant a_1 < a_2 < \cdots < a_m \leqslant n$.

In the special case where each strand is straight, if the strands $S_{a_1}, S_{a_2}, \ldots, S_{a_m}$ bound a convex region R in the disk such that the boundary of R is oriented either clockwise or counterclockwise then the corresponding edges of $\vec{G}_D^\times$ form an increasing cycle (after cyclically shifting the indices). We will define convex regions for arbitrary reduced strand diagrams below in Definition 4.9. A fundamental tool that we will use to study critical cells is the following result which states that every crossing of D is a vertex of such a convex region.

Proposition 4.8. *Every edge of $\vec{G}_D^\times$ belongs to an increasing cycle.*

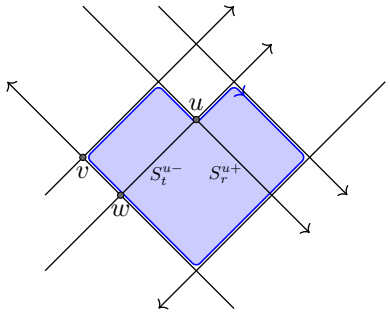

FIGURE 11. A (clockwise) cycle C which turns right at v, goes straight at w, and turns left at u.

For instance, the diagram in Figure 9(a) contains six crossings, and they form two convex regions (shaded triangles). This corresponds to having increasing cycles $(1 \to 2 \to 5 \to 1)$ and $(1 \to 3 \to 4 \to 1)$ in $\vec{G}_D^{\times}$ shown in Figure 9(c).

Proof. Let $e = (p \to q)$ be an edge of $\vec{G}_D^{\times}$, thus S_p and S_q form a positive crossing. Let x be the intersection point of S_p and S_q. Let D_x be obtained from D by "resolving" all crossings except for x; see Figure 10(b) for an example. Here *resolving* a crossing x' is a local transformation that replaces a neighborhood of a crossing point x' as shown in Figure 10(a). Thus D_x contains a single crossing point x. Some of the strands of D_x are closed curves in the interior of the disk, however, it is still true that for each $r \in [n]$, one strand of D_x starts at b_r^+ and one strand of D_x ends at b_r^-. Consider the two strands S'_p and S'_q of D_x emanating from x. Assume that they both terminate at the boundary of the disk, say, at points $b_{p'}^-$ and $b_{q'}^-$ for some $p', q' \in [n]$. Then the arc between $b_{p'}^-$ and $b_{q'}^-$ contains more starting strands than ending strands. None of such strands can intersect either S'_p or S'_q. We arrive at a contradiction. Thus at least one of the strands S'_p or S'_q does not terminate at the boundary, and therefore it terminates at x. Thus it forms a closed directed path C' starting and ending at x; see Figure 10(b).

Let us introduce another directed graph, the *topological graph* $\vec{G}_D^{\text{top}}$ of D. The vertices of $\vec{G}_D^{\text{top}}$ are the crossing points and the boundary vertices of the strands of D. Thus each strand of D passes through the vertices $u_0, u_1, \ldots, u_r$ of $\vec{G}_D^{\text{top}}$, where u_0 and u_r lie on the boundary of the disk. The edge set of $\vec{G}_D^{\text{top}}$ consists of these directed line segments $(u_0 \to u_1)$, $\ldots$, $(u_{r-1} \to u_r)$ for all strands of D. Thus each interior vertex of $\vec{G}_D^{\text{top}}$ has two incoming and two outgoing edges.

Definition 4.9. Consider a simple directed cycle C in $\vec{G}_D^{\text{top}}$ passing through a vertex u. Then C either *turns right*, *turns left*, or *goes straight* at u, depending on which incoming and which outgoing edge of u it uses; see Figure 11. We say that C is *clockwise convex* if it either turns right or goes straight at each of its vertices. Similarly, C is *counterclockwise convex* if it either turns left or goes straight at each of its vertices. Each (counter)clockwise convex cycle is a Jordan curve, and we say that it bounds a *(counter)clockwise convex region*.

Recall that we have constructed a directed cycle C' in $\vec{G}_D^{\text{top}}$ passing through x. It is straightforward to check that this cycle is simple, i.e., passes through each vertex at most once. By construction, C' does not go straight at x. Without loss of generality, let us assume that it turns right at x. Therefore C' is oriented clockwise around the boundary of a (not

necessarily convex) region R'. Our goal is to find a clockwise convex region $R \subset R'$ that contains x. Let C be a cycle that turns right at x and bounds a region $R \subset R'$ of minimal possible area. Then we claim that C is clockwise convex. Indeed, suppose otherwise that it turns left at some vertex u of $\vec{G}_D^{\mathrm{top}}$; see e.g. Figure 11. Consider the strand S_r passing through the unique outgoing edge of u that is not used by C. Let us consider the part S_r^{u+} of S_r between u and the endpoint of S_r. The path S_r^{u+} must intersect C at some other vertex. Let $u' \neq u$ be the first vertex on S_r^{u+} that belongs to C. We see that C either turns left or goes straight at u'. In particular, neither u nor u' is equal to x, since C turns right at x. Let $C^{(r)}$ be obtained by replacing the arc of C connecting u to u' with the corresponding part of S_r.

Consider also the strand S_t passing through the unique incoming edge of u not used by C. We let S_t^{u-} denote the part of S_t before u, and let $u'' \neq u$ be the last vertex belonging to both S_t^{u-} and C. Replacing the arc of C connecting u'' to u with the corresponding part of S_t^{u-}, we get another cycle $C^{(t)}$. It is clear that x must belong to either $C^{(r)}$ or $C^{(t)}$ (or both), since the strands S_r and S_t intersect only at u. Thus we have found a cycle satisfying the above conditions that bounds a region of area smaller than R. This is a contradiction, and thus C is clockwise convex. It is then easy to check that a clockwise (or counterclockwise) convex cycle in $\vec{G}_D^{\mathrm{top}}$ yields an increasing cycle in $\vec{G}_f^{\times}$ in the sense of Definition 4.7. □

4.3. **Proof of Proposition 4.2.** Let e be a non-boundary edge of G labeled by $\{p, q\}$ with $1 \leqslant p < q \leqslant n$. First, observe that if (4.2) holds for any f-admissible tuple $\boldsymbol{\theta}$ then p and q belong to the same connected component of $G_f^{\times}$. Indeed, suppose otherwise that they belong to different connected components. The notion of f-admissibility is invariant under adding a constant to all $\theta_{q'}$ for q' in the same connected component as q. We can choose the constant so that θ_p becomes equal to θ_q, contradicting (4.2). It is also clear that (4.2) implies $\mathrm{wt}_{\boldsymbol{\theta}}(e) > 0$. It thus remains to prove (4.2) for all f-admissible tuples $\boldsymbol{\theta}$.

Recall that G is assumed to be contracted. More generally, each (not necessarily contracted) graph G' may be transformed into a contracted graph G by removing interior degree 2 vertices. Clearly, showing (4.2) for some graph G' whose contracted version is G implies that (4.2) also holds for G. In addition, observe that if two graphs G and G' are connected by a square move then (4.2) holds for G if and only if it holds for G'. To see that, notice that whenever one performs a square move (Figure 6) on a contracted reduced graph G, this graph G contains four edges labeled by $\{a, b\}$, $\{b, c\}$, $\{c, d\}$, and $\{a, d\}$ for $1 \leqslant a < b < c < d \leqslant n$. Assuming (4.2) holds for G, we must have $\theta_a < \theta_b < \theta_c < \theta_d < \theta_a + \pi$ for all f-admissible $\boldsymbol{\theta}$. It is then easy to see that after performing the square move, (4.2) still holds for all non-boundary edges of G'. Since all (contracted) graphs $G \in \mathcal{G}_{\mathrm{red}}(f)$ are related by square moves, it suffices to prove the statement for just one of them.

We shall proceed by induction on f using the bridge removal procedure from Section 2.3. For the base case, observe that when $k = 1$ and f is loopless, all edges of G are adjacent to the boundary and therefore have weight 1. Let us now assume that $f \in \mathcal{B}(k, n)$ is loopless and $k > 1$. Choose $r \in [n]$ such that f has a bridge at r. Thus we have $r < r + 1 \leqslant f(r) < f(r + 1) \leqslant r + n$. Let $G \in \mathcal{G}_{\mathrm{red}}(f)$ be such that G has a bridge configuration at b_r, b_{r+1} as in Figure 7(left).

Let us first consider the case $r + 1 = f(r)$. Then the interior black vertex in Figure 7(left) has degree 2 and therefore G is not contracted. Contracting the two edges incident to that vertex, we see that both b_r and b_{r+1} become connected to the same interior white vertex.

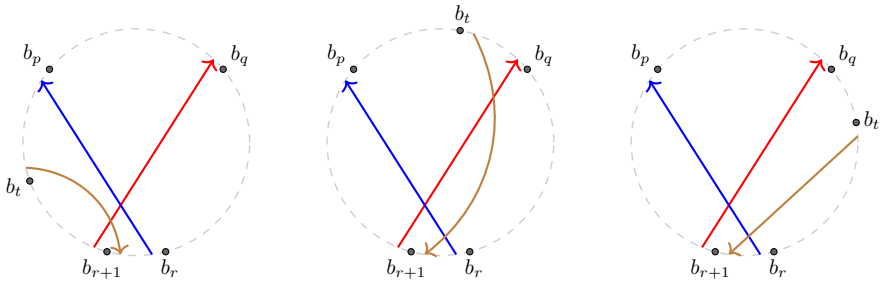

FIGURE 12. The strand S_{r+1} has to cross either S_p or S_q.

Therefore $r+1$ does not appear in the label of any non-boundary edge of G. We may therefore remove the vertex b_{r+1} from G and deduce the result by induction.

Assume now that $r+1 < f(r)$, thus $r < r+1 < f(r) < f(r+1) \leqslant r+n$. By definition, $p := f(r)$ and $q := f(r+1)$ form an affine f-crossing (cf. Section 3.1), and thus by (3.2), we have $\tilde{\theta}_p < \tilde{\theta}_q < \tilde{\theta}_{p+n}$ for any f-admissible sequence $\tilde{\boldsymbol{\theta}}$. Let $t := f^{-1}(r+1)$. Since p and q form an affine f-crossing, the strands $S_q = (b^+_{(r+1)} \to b^-_q)$ and $S_p = (b^+_r \to b^-_p)$ form an f-crossing. The strand $S_{r+1} = (b^+_t \to b^-_{(r+1)})$ therefore must cross either one or both of these strands; cf. Figure 12. Assume for example that it crosses S_q as in Figure 12(left). Choose a reduced strand diagram D of f such that both crossings are closer to $b^+_{(r+1)}$ than all other crossings. Denote the crossing point of the strands S_q and S_{r+1} by x and let C be a convex cycle from the proof of Proposition 4.8 that passes through x. We see that C must turn left at x and therefore it is a counterclockwise convex cycle. Moreover, denoting by u the crossing point of S_q and S_p, the construction in the proof of Proposition 4.8 implies that C must turn left at u as well. We have therefore found an increasing cycle passing through the edges $p \to q \to r+1$ in $\vec{G}^\times_D$, where the indices again are taken modulo n. Label the vertices of this cycle by $(a_1 \to a_2 \to \cdots \to a_m \to a_1)$ as in Definition 4.7. Then we see that $\theta_{a_1} < \theta_{a_2} < \cdots < \theta_{a_m} < \theta_{a_1} + \pi$ for any f-admissible $\boldsymbol{\theta}$. Since $r+1 < p < q < r+1+n$, it follows that $\tilde{\theta}_{r+1} < \tilde{\theta}_p < \tilde{\theta}_q < \tilde{\theta}_{r+1} + \pi$.

Let G' be the graph obtained from G by removing the bridge at p. Thus G' is reduced and has strand permutation $s_r f$. Even though G' may not be contracted, the only edges that may need to get contracted are labeled by $\{p, r+1\}$. Let $\boldsymbol{\theta}$ be an f-admissible tuple. Since $\tilde{\theta}_{r+1} < \tilde{\theta}_p < \tilde{\theta}_q < \tilde{\theta}_{r+1} + \pi$, it follows that $\boldsymbol{\theta}$ is also $s_r f$-admissible. By the induction hypothesis, we may assume that (4.2) holds for all non-boundary edges of (the contracted version of) G'. Again using $\tilde{\theta}_{r+1} < \tilde{\theta}_p < \tilde{\theta}_q < \tilde{\theta}_{r+1} + \pi$, we see that (4.2) holds for all non-boundary edges of G. This completes the induction step. □

4.4. **Factorization.** Let $f \in \mathcal{B}(k,n)$ be loopless and consider the connected components $[n] = C^{(1)} \sqcup C^{(2)} \sqcup \cdots \sqcup C^{(c_f)}$ of $G^\times_f$. Our goal is to define "restrictions" of f to each connected component and argue that Meas_f "factors" as an independent product of the boundary measurement maps for the restrictions. This is not completely straightforward: for $p \in [n]$, it may happen that the vertices b^-_p and b^+_p belong to different connected components of the strand diagram D_f, thus the vertex b_p of the corresponding reduced graph G appears to belong to both components simultaneously.

Consider a connected component $C \subset [n]$ of $G^\times_f$ and consider the strands $\{S_p \mid p \in C\}$ of D_f that belong to C. Let $D_f|_C$ be obtained from D_f by erasing all other strands. Then

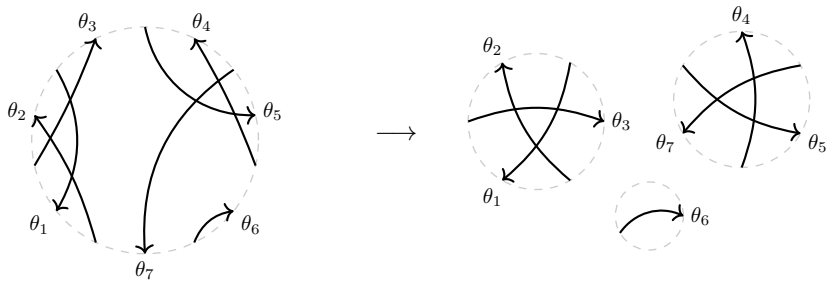

FIGURE 13. Splitting a strand diagram into connected components.

the directions of the strands of $D_f|_C$ still alternate around the boundary of the disk. Thus after relabeling the strands and boundary vertices by integers in $[n']$ where $n' := |C|$, $D_f|_C$ becomes a strand diagram in the sense of Definition 4.5. We denote by $f|_C \in \mathcal{B}(k', n')$ the corresponding loopless bounded affine permutation. Finally, given any f-admissible tuple $\boldsymbol{\theta}$, the restriction $\boldsymbol{\theta}|_C$ is defined in an obvious way: for $p \in C$, if the strand S_p in D_f is labeled as $S_{p'}$ in $D_f|_C$ for some $p' \in [n']$ then we set $(\boldsymbol{\theta}|_C)_{p'} := \theta_p$. In other words, θ_p is viewed as a real parameter attached to the *endpoint* of the strand S_p. See Figure 13 for an example.

For $r \in [c_f]$, we denote by $f^{(r)} := f|_{C^{(r)}}$ the restriction of f to the connected component $C^{(r)}$ of $G_f^{\times}$. We are ready to state our factorization result.

Proposition 4.10. *We have a homeomorphism*

$$\mathrm{Crit}_f^{>0} \xrightarrow{\sim} \mathrm{Crit}_{f^{(1)}}^{>0} \times \mathrm{Crit}_{f^{(2)}}^{>0} \times \cdots \times \mathrm{Crit}_{f^{(c_f)}}^{>0}.$$

Proof. Let $[n]_\varepsilon := \{b_1^+, b_1^-, b_2^+, b_2^-, \ldots, b_n^+, b_n^-\}$. For $C \subset [n]$, let $C_\varepsilon \subset [n]_\varepsilon$ denote the set containing b_s^+ and b_p^- for each $p \in C$, where $s := \bar{f}^{-1}(p)$. We have a non-crossing partition $[n]_\varepsilon = C_\varepsilon^{(1)} \sqcup C_\varepsilon^{(2)} \sqcup \cdots \sqcup C_\varepsilon^{(c_f)}$ into parts of even sizes.

Consider a contracted graph $G \in \mathcal{G}_{\mathrm{red}}(f)$. If G is disconnected then the statement follows by considering each connected component independently, so let us assume that G is connected. This implies that there exists $p \in [n]$ such that b_p^+ and b_p^- belong to different parts of the above non-crossing partition. Call these parts A_ε and B_ε so that $b_p^+ \in A_\varepsilon$ and $b_p^- \in B_\varepsilon$, and let $A, B \subset [n]$ be the corresponding connected components of $G_f^{\times}$.

Recall from Proposition 4.2 that every interior edge of G is labeled by $\{p', q'\}$ where p', q' belong to the same connected component of $G_f^{\times}$. Let v be the white interior vertex connected to b_p. Then the (boundary) edge $\{v, b_p\} \in E(G)$ is labeled by $\{p, q'\}$ where $q' = f(p) \in A$ while $p \in B$. Label the edges incident to v by $e_1, e_2, \ldots, e_d$ in clockwise order, starting with $e_1 := \{v, b_p\}$. The strand labeled q' passes through e_1 and e_2, thus either e_2 is a boundary edge or some strand labeled by $q_2 \in A$ (cf. Proposition 4.2) passes through e_2 and e_3, etc. Since the strand passing through e_d and e_1 is labeled by $p \in B$, at some point we must encounter a boundary edge $e_j = \{v, b_q\}$ for some $q \in A$ such that $f(q) \notin A$. See Figure 14.

Observe that each of the cyclic intervals $P := \{q+1, \ldots, p\}$ and $Q := \{p+1, \ldots, q\}$ (indices taken modulo n) is a union of connected components of $G_f^{\times}$. Let $g := f|_P$ and $h := f|_Q$ be the corresponding restrictions of f. We would like to establish a homeomorphism $\mathrm{Crit}_f^{>0} \xrightarrow{\sim} \mathrm{Crit}_g^{>0} \times \mathrm{Crit}_h^{>0}$.

Let G_P be the connected component of b_p in the graph obtained from G by removing the edges $e_2, \ldots, e_j$ defined above. Similarly, let G_Q be the connected component of b_q in the

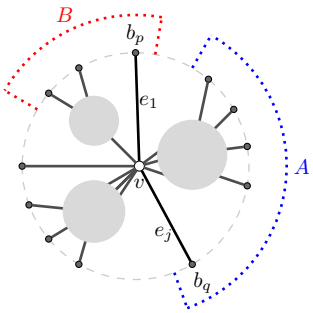

FIGURE 14. The graph G from the proof of Proposition 4.10.

graph obtained from G by removing the edges $e_{j+1}, \dots, e_1$. Abusing notation, we preserve the original boundary labeling of G_P and G_Q by $(b_{q+1}, \dots, b_p)$ and $(b_{p+1}, \dots, b_q)$, respectively.

Let $\boldsymbol{\theta} \in \mathbb{R}^n$. Clearly $\boldsymbol{\theta}$ is f-admissible if and only if the restrictions $\boldsymbol{\theta}|_P$ and $\boldsymbol{\theta}|_Q$ are g-admissible and h-admissible, respectively. Given such $\boldsymbol{\theta}$, let $X := \mathrm{Meas}_f(\boldsymbol{\theta})$, $X_P := \mathrm{Meas}_g(\mathrm{wt}_{\boldsymbol{\theta}|_P})$ and $X_Q := \mathrm{Meas}_h(\mathrm{wt}_{\boldsymbol{\theta}|_Q})$. Our goal is to understand the relationship between X and (X_P, X_Q).

Let k_P, n_P, k_Q, n_Q be such that $g \in \mathcal{B}(k_P, n_P)$ and $h \in \mathcal{B}(k_Q, n_Q)$, thus $k_P + k_Q = k + 1$. Any almost perfect matching of G contains a unique edge incident to v. By considering the possible options for this edge, we arrive at the following formulas. For two sets $L \subset P \setminus \{p\}$ and $R \subset Q \setminus \{q\}$, we have

(4.4)
$$\Delta_{L\cup R\cup p}(X) = \Delta_{L\cup R\cup q}(X) = \Delta_{L\cup p}(X_P) \cdot \Delta_{R\cup q}(X_Q), \quad \text{if } |L| = k_P - 1 \text{ and } |R| = k_Q - 1;$$

(4.5)
$$\Delta_{L\cup R}(X) = \Delta_L(X_P) \cdot \Delta_{R\cup q}(X_Q), \quad \text{if } |L| = k_P \text{ and } |R| = k_Q - 1;$$

(4.6)
$$\Delta_{L\cup R}(X) = \Delta_{L\cup p}(X_P) \cdot \Delta_R(X_Q), \quad \text{if } |L| = k_P - 1 \text{ and } |R| = k_Q.$$

Here we abbreviate $R \cup p := R \cup \{p\}$, etc. Each nonzero minor of X, X_P, and X_Q appears in these formulas. We claim that X and (X_P, X_Q) determine each other uniquely via (4.4)–(4.6). First, clearly knowing the minors of (X_P, X_Q) allows one to reconstruct the minors of X. Conversely, suppose that the minors of X are known and we need to recover the minors of, say, X_P. Since the minors are defined up to multiplication by a common scalar, we only need to find the ratios $\Delta_M(X_P)/\Delta_N(X_P)$. If $p \notin M, N$ then by (4.5), we get $\Delta_M(X_P)/\Delta_N(X_P) = \Delta_{M\cup R}(X_P)/\Delta_{N\cup R}(X_P)$ for any set R such that $\Delta_{R\cup q}(X_Q) \neq 0$. (Such a set R exists since otherwise p and q must be loops of f.) If $M = L \cup p$ but $p \notin N$ then by (4.4)–(4.5), $\Delta_{L\cup p}(X_P)/\Delta_N(X_P) = \Delta_{L\cup R\cup p}(X)/\Delta_{N\cup R}(X)$ for any R such that $\Delta_{R\cup q}(X_Q) \neq 0$. The case $p \in M$ and $p \notin N$ is handled similarly. Finally, in the case $M = L \cup p$ and $N = L' \cup p$, by (4.4) and (4.6) we have $\Delta_{L\cup p}(X_P)/\Delta_{L'\cup p}(X_P) = \Delta_{L\cup R}(X)/\Delta_{L'\cup R}(X)$ for any $R \subset Q$ such that $\Delta_R(X_Q) \neq 0$. We have established the desired homeomorphism $\mathrm{Crit}_f^{>0} \xrightarrow{\sim} \mathrm{Crit}_g^{>0} \times \mathrm{Crit}_h^{>0}$. The result follows by induction. □

We finish by clarifying the relationship[6] between our notion of connectedness for reduced strand diagrams and the standard notion of a *connected positroid* [OPS15, ARW16]. Given $f \in \mathcal{B}(k, n)$, let $G_f^{\mathcal{M}}$ be the undirected graph with vertex set $[n]$ and edge set consisting of all pairs $\{p, q\} \in \binom{[n]}{2}$ such that the line segments $[b_s, b_p]$ and $[b_t, b_q]$ (where $\bar{f}(s) = p$ and

[6]We thank Lauren Williams for comments motivating the below results.

$\bar{f}(t) = q$) have nonempty intersection. Then the *positroid* $\mathcal{M}_f$ is connected if and only if $G_f^{\mathcal{M}}$ is connected; see [ARW16, Corollary 7.9]. The connected components of $G_f^{\mathcal{M}}$ form a non-crossing partition of $[n]$ denoted $\Pi(G_f^{\mathcal{M}})$. Similarly, if f is loopless, we denote by $\Pi(G_f^{\times})$ the non-crossing partition of $[n]$ into the connected components of $G_f^{\times}$.

Proposition 4.11. *Let $f \in \mathcal{B}(k,n)$ be loopless.*

(i) *The reduced strand diagram of f is connected if and only if the positroids $\mathcal{M}_f$ and $\mathcal{M}_{f^\downarrow}$ are both connected.*
(ii) *The non-crossing partition $\Pi(G_f^{\times})$ is the common refinement of $\Pi(G_f^{\mathcal{M}})$ and $\Pi(G_{f^\downarrow}^{\mathcal{M}})$.*

Proof. Let $p, q \in [n]$ and denote $s := \bar{f}^{-1}(p)$, $t := \bar{f}^{-1}(q)$. Observe that p, q belong to different connected components of $G_f^{\times}$ if and only if there exists a chord $\alpha \to \beta$ (for two points α, β on the circle not equal to any of b_j, b_j^+, b_j^- for $j \in [n]$) which separates b_p^+ and b_q^+ and does not intersect any of the strands in the reduced strand diagram of $G_f^{\times}$.

As in the proof of Proposition 4.10, we denote $[n]_\varepsilon := \{b_1^+, b_1^-, b_2^+, b_2^-, \ldots, b_n^+, b_n^-\}$. The chord $\alpha \to \beta$ separates $[n]_\varepsilon$ into two subsets of even size. Let $x \in [n]_\varepsilon$ be the closest point to α in the clockwise direction. If $x = b_j^-$ for some $j \in [n]$ then the chord $\alpha \to \beta$ does not intersect any line segment $[b_r, b_{\bar{f}(r)}]$ for $r \in [n]$, and thus p, q belong to different connected components of $G_f^{\mathcal{M}}$.

Assume now that $x = b_j^+$ for some $j \in [n]$. Consider the dual reduced strand diagram of $f^\downarrow$. It coincides with the reduced strand diagram of f up to a simple relabeling of boundary vertices; see Section 8.4 for further details. In particular, it follows that p, q belong to different connected components of $G_{f^\downarrow}^{\mathcal{M}}$.

Conversely, it is clear that if p, q belong to different connected components of either $G_f^{\mathcal{M}}$ or $G_{f^\downarrow}^{\mathcal{M}}$ then they belong to different connected components of $G_f^{\times}$. □

5. Critical varieties

In this section, we study Zariski closures of critical cells as discussed in Section 1.4. In particular, we show that the boundary measurement map Meas_f is well defined and gives rise to *open critical varieties* Crit_f° whose definition depends on the *Laurent phenomenon* (Theorem 5.6). We study the real points of Crit_f° in Section 5.3. An important tool we rely on is the *twist map* of [MuSp17], reviewed in Section 5.4. Throughout, we assume that $f \in \mathcal{B}(k,n)$ is loopless.

5.1. **Open critical varieties.** To a sequence $\tilde{\boldsymbol{\theta}} : \mathbb{Z} \to \mathbb{R}$ we associate a sequence $\tilde{\mathbf{t}} : \mathbb{Z} \to \mathbb{C}^*$ of complex numbers defined by

$$\tilde{t}_q := \exp(i\tilde{\theta}_q) \quad \text{for all } q \in \mathbb{Z}. \tag{5.1}$$

If $\tilde{\boldsymbol{\theta}}$ satisfies (3.1) then we have $\tilde{t}_{q+n} = -\tilde{t}_q$ for all $q \in \mathbb{Z}$. Similarly to (3.1), we identify sequences $\tilde{\mathbf{t}} : \mathbb{Z} \to \mathbb{C}^*$ satisfying this condition with tuples $\mathbf{t} \in (\mathbb{C}^*)^n$.

Recall from Definition 1.12 that $\mathbf{t} = (t_1, t_2, \ldots, t_n) \in (\mathbb{C}^*)^n$ is *f-admissible* if $t_p \neq \pm t_q$ for all pairs p, q that from an f-crossing.

As in Section 4.1, we choose representatives $p_1, p_2, \ldots, p_{c_f} \in [n]$, one from each connected component of $G_f^{\times}$, and set

$$\Theta_f^\circ := \{\mathbf{t} = (t_1, t_2, \ldots, t_n) \in (\mathbb{C}^*)^n \mid \mathbf{t} \text{ is } f\text{-admissible and } t_{p_1} = t_{p_2} = \cdots = t_{p_{c_f}} = 1\}. \tag{5.2}$$

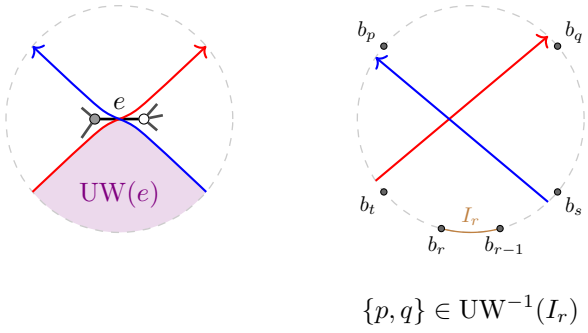

FIGURE 15. The upstream wedge.

Recall also that to each graph $G \in \mathcal{G}_{\mathrm{red}}(f)$ and each $\mathbf{t} \in (\mathbb{C}^*)^n$ we assign a weight function $\mathrm{wt}_{\mathbf{t}} : E(G) \to \mathbb{C}$ given by (1.4). As Example 1.13 demonstrates, the complex algebraic analog of Proposition 4.2 no longer holds, thus we have to be more careful in defining Meas_f.

We denote $\mathrm{Meas}_G(\mathrm{wt}_{\mathbf{t}}) := (\Delta_I(G, \mathrm{wt}_{\mathbf{t}}))_{I \in \binom{[n]}{k}}$. If the entries of $\mathrm{Meas}_G(\mathrm{wt}_{\mathbf{t}})$ are not all zero then we say that Meas_G *is well defined at* $\mathbf{t}$ and view the result as an element of the complex Grassmannian $\mathrm{Gr}(k,n)$. The following result is proved in Section 5.5.

Proposition 5.1. *There exists a unique regular map* $\mathrm{Meas}_f : \Theta_f^\circ \to \Pi_f^\circ$ *satisfying*

$$\mathrm{Meas}_f(\mathbf{t}) = \mathrm{Meas}_G(\mathrm{wt}_{\mathbf{t}}) \quad \textit{inside } \mathrm{Gr}(k,n)$$

for all $G \in \mathcal{G}_{\mathrm{red}}(f)$ *and all* $\mathbf{t} \in \Theta_f^\circ$ *such that* Meas_G *is well defined at* $\mathbf{t}$.

By Definition 1.14, the *open critical variety* $\mathrm{Crit}_f^\circ \subset \Pi_f^\circ$ is the image of the map Meas_f:

$$\mathrm{Crit}_f^\circ := \mathrm{Meas}_f(\Theta_f^\circ).$$

Even though we use the terms *open* and *variety*, it is an open problem to describe Crit_f° as an open subvariety of Crit_f, even in the case $f = f_{k,n}$.

Problem 5.2.

(1) Show that the variety Crit_f is irreducible of dimension d_f and describe Crit_f by polynomial equations.
(2) Show that Crit_f° is an open subvariety of Crit_f and describe its complement by polynomial equations.
(3) Describe $\mathrm{Crit}_f^{>0} \subset \Pi_f^{>0}$ by polynomial equations and inequalities.

See (2.4)–(2.6) for the analogous results for positroid varieties. We caution that in general, $\mathrm{Crit}_f^{>0} \subsetneq \mathrm{Crit}_f^\circ \cap \mathrm{Gr}_{\geqslant 0}(k,n)$, unlike in the case of positroid varieties. For example, $\mathrm{Crit}_{2,3}^{>0}$ consists of all points of $\mathrm{Gr}_{>0}(2,3)$ whose Plücker coordinates satisfy the triangle inequalities.

Remark 5.3. Fix a coloopless $f \in \mathcal{B}(k,n)$. We say that $\mathbf{t} \in (\mathbb{C}^*)^n$ is *dual* f*-admissible* if $t_p \neq \pm t_q$ whenever p, q form a dual f-crossing. Similarly to what we did above, one can introduce the *dual boundary measurement map* $\widehat{\mathrm{Meas}} : \widehat{\Theta}_f^\circ \to \widehat{\mathrm{Crit}}_f^\circ$ whose image is the *dual open critical variety* $\widehat{\mathrm{Crit}}_f^\circ$, and whose restrictions to appropriate open subsets of $\widehat{\Theta}_f^\circ$ coincide with $\widehat{\mathrm{Meas}}_G$ for $G \in \mathcal{G}_{\mathrm{red}}(f)$.

5.2. **The Laurent phenomenon.** Let $\mathcal{I}_f = (I_1, I_2, \ldots, I_n)$ be the Grassmann necklace of f defined in Section 2.4. For $r \in [n]$, we label by I_r the arc connecting $b^+_{(r-1)}$ to b^-_r. Choose $1 \leqslant p < q \leqslant n$ such that the arrows $b^+_s \to b^-_p$ and $b^+_t \to b^-_q$ form an f-crossing. Following the terminology of [MuSp17], we say that I_r belongs to the *upstream wedge of* $\{p, q\}$ if the arc labeled I_r is contained in the arc connecting b^+_s to b^+_t that does not contain b^-_p, b^-_q; see Figure 15(right). We let $\mathrm{UW}^{-1}(I_r)$ denote the set of all pairs $\{p, q\}$ such that I_r belongs to the upstream wedge of $\{p, q\}$.

Our first goal is to give a product formula for the boundary measurements associated with the Grassmann necklace, which is a simple consequence of the results of Muller–Speyer [MuSp17].

Proposition 5.4. *Let $G \in \mathcal{G}_{\mathrm{red}}(f)$ and suppose that Meas_G is well defined at $\mathbf{t} \in \Theta^\circ_f$. Then, after a multiplication by a common scalar, we have*

$$\Delta_{I_r}(G, \mathrm{wt}_{\mathbf{t}}) = \prod_{p<q:\ \{p,q\} \in \mathrm{UW}^{-1}(I_r)} [\![t_q, t_p]\!] \quad \text{for all } r \in [n]. \tag{5.3}$$

See Section 5.5 for a proof. Observe that the right hand side of (5.3) is a Laurent polynomial in $\mathbf{t}$ (homogeneous of degree 0) that does not depend on the choice of G. Moreover, all $\Delta_{I_r}(G, \mathrm{wt}_{\mathbf{t}})$ are nonzero precisely when $\mathbf{t}$ is f-admissible.

Example 5.5. Consider the case $f = f_{2,4}$ from Figure 1. The Grassmann necklace is

$$I_1 = \{1, 2\}, \quad I_2 = \{2, 3\}, \quad I_3 = \{3, 4\}, \quad I_4 = \{1, 4\}.$$

From the reduced strand diagram on the right in Figure 2(b), we find $\mathrm{UW}^{-1}(I_1) = \{\{2, 3\}\}$, $\mathrm{UW}^{-1}(I_2) = \{\{3, 4\}\}$, $\mathrm{UW}^{-1}(I_3) = \{\{1, 4\}\}$, and $\mathrm{UW}^{-1}(I_4) = \{\{1, 2\}\}$. Thus (5.3) agrees with the values computed in Figure 1(d), after canceling out the term (24).

According to Proposition 5.4, the entries of Meas_G may be rescaled so that (5.3) holds. We refer to this rescaling as the *canonical gauge-fix* of Meas_G.

Theorem 5.6 (Laurent phenomenon)**.** *Let $G \in \mathcal{G}_{\mathrm{red}}(f)$ and suppose that Meas_G is well defined at $\mathbf{t} \in \Theta^\circ_f$. Then the entries $\Delta_I(G, \mathrm{wt}_{\mathbf{t}})$ of the canonical gauge-fix of Meas_G are Laurent polynomials in $\mathbf{t}$.*

See Section 5.5 for a proof. By (2.4), we see that the map Meas_G may be extended to a map

$$\mathrm{Meas}_f : \Theta^\circ_f \to \Pi^\circ_f.$$

Moreover, $\mathrm{Meas}_G(\mathrm{wt}_{\mathbf{t}}) \notin \Pi^\circ_f$ when $\mathbf{t} \in \mathbb{C}^*$ is not f-admissible. This again confirms that reduced strand diagrams give the "correct" notion of f-admissibility, even though a priori it may appear that a more restrictive notion is required (cf. Example 1.13).

Example 5.7. Unlike in the case of open positroid varieties, the map $\mathrm{Meas}_f : \Theta^\circ_f \to \mathrm{Crit}^\circ_f$ is in general *not* injective. For example, consider two tuples

$$\mathbf{t} := (1, \exp(i\pi/4), \exp(i\pi/2), \exp(3i\pi/4)), \quad \mathbf{t}' := (1, \exp(3i\pi/4), \exp(-i\pi/2), \exp(i\pi/4)).$$

Then for $f = f_{3,4}$ (cf. Figure 3(c)), we find that $\mathbf{t}, \mathbf{t}' \in \Theta^\circ_f$ and $\mathrm{Meas}_f(\mathbf{t}) = \mathrm{Meas}_f(\mathbf{t}')$, since both $\mathrm{Meas}_f(\mathbf{t})$ and $\mathrm{Meas}_f(\mathbf{t}')$ give rise to the cyclically symmetric point $X_0^{(3,4)} \in \mathrm{Gr}_{\geqslant 0}(3, 4)$ (all of whose Plücker coordinates are equal). Note that if $\boldsymbol{\theta}$ and $\boldsymbol{\theta}'$ are related respectively to $\mathbf{t}$ and $\mathbf{t}'$ via (5.1) then $\boldsymbol{\theta} \in \Theta^{>0}_f$ but $\boldsymbol{\theta}' \notin \Theta^{>0}_f$, so this example does not contradict Theorem 4.4.

Limited computational evidence suggests that even a stronger form of the Laurent phenomenon may hold for critical varieties. It was shown in [GL19] that the coordinate ring $\mathbb{C}[\Pi_f^\circ]$ admits a cluster algebra structure, and thus we have a family of regular functions on Π_f° called *cluster variables*.

Conjecture 5.8 (Strong Laurent phenomenon)**.** All cluster variables in $\mathbb{C}[\Pi_f^\circ]$, when restricted to Crit_f°, become Laurent polynomials in $\mathbf{t}$, assuming the canonical gauge-fix (5.3).

5.3. **The real part of a critical variety.** Recall that the set $\mathrm{Gr}_\mathbb{R}(k,n)$ of real points of the complex Grassmannian consists of all $X \in \mathrm{Gr}(k,n)$ such that the ratio of any two nonzero Plücker coordinates belongs to $\mathbb{R}$. The problem of determining the set $\mathrm{Crit}_f^\circ(\mathbb{R})$ of real points of Crit_f° turns out to be quite non-trivial, and we solve it only partially even in the case of the top cell. Recall from Section 1.8 that $f^\downarrow \in \mathcal{B}(k-1,n)$ is defined by $f^\downarrow(p) := f(p-1)$ for all $p \in \mathbb{Z}$. We let $i\mathbb{R} \subset \mathbb{C}$ be the set of purely imaginary complex numbers. Denote

$$\Theta_f^\mathbb{R} = \{\mathbf{t} \in \Theta_f^\circ \mid |t_p| = 1 \text{ for all } p \in [n]\} \\ \cup \{\mathbf{t} \in \Theta_f^\circ \mid t_p \in \mathbb{R} \cup i\mathbb{R} \text{ and } t_p/t_{\bar{f}^\downarrow(p)} \in \mathbb{R} \text{ for all } p \in [n]\}.$$

Thus if $\mathbf{t} \in \Theta_f^\mathbb{R}$ then the points $v_p := t_p^2$, $p \in [n]$, all belong to the same *generalized circle*, that is, either a circle or a line. (Moreover, the circle is required to have its center at 0 while the line is required to pass through 0.)

Lemma 5.9. *Assume that $G_f^\times$ is connected. Then for $\mathbf{t} \in \Theta_f^\circ$, we have*

$$\mathbf{t} \in \Theta_f^\mathbb{R} \quad \Longrightarrow \quad \mathrm{Meas}_f(\mathbf{t}) \in \mathrm{Crit}_f^\circ(\mathbb{R}). \tag{5.4}$$

Proof. Assume first that $\mathbf{t}$ is generic and let $G \in \mathcal{G}_{\mathrm{red}}(f)$. If $|t_p| = 1$ for all $p \in [n]$ then $\mathrm{wt}_\mathbf{t}$ is gauge-equivalent to $\mathrm{wt}_{\boldsymbol{\theta}}$, where $\boldsymbol{\theta} = (\theta_1, \theta_2, \ldots, \theta_n) \in \mathbb{R}^n$ is any tuple related to $\mathbf{t}$ by (5.1). Indeed, we have $\sin(\theta_q - \theta_p) = \frac{1}{2i}[\![t_q, t_p]\!]$, and thus $\mathrm{wt}_{\boldsymbol{\theta}}$ is obtained from $\mathrm{wt}_\mathbf{t}$ by rescaling all edges incident to each interior black vertex of G by $\frac{1}{2i}$. If $t_p \in \mathbb{R}$ for all $p \in [n]$ then the edge weights $\mathrm{wt}_\mathbf{t}(e)$ are already real numbers. In either case, we see that $\mathrm{Meas}_G(\mathrm{wt}_\mathbf{t}) \in \mathrm{Gr}_\mathbb{R}(k,n)$.

Let us now consider the case where $t_p \in \mathbb{R} \cup i\mathbb{R}$ for all $p \in [n]$. Since the entries of $\mathbf{t}$ are nonzero, we have a map $\epsilon : [n] \to \{1, i\}$ such that $\epsilon(p) = 1$ if $t_p \in \mathbb{R}$ and $\epsilon(p) = i$ if $t_p \in i\mathbb{R}$. For each edge $e \in E(G)$ labeled by $\{p, q\}$, we have $\mathrm{wt}_\mathbf{t}(e) \in \mathbb{R}$ if $\epsilon(p) = \epsilon(q)$ and $\mathrm{wt}_\mathbf{t}(e) \in i\mathbb{R}$ otherwise. Consider an interior face F of G. Each strand of G passes through an even number of edges of F, and therefore $\mathrm{wt}_\mathbf{t}(e) \in i\mathbb{R}$ for an even number of edges of F. Thus the alternating product (2.7) is real for each interior face F. Suppose now that F is a boundary face of G. Since $G_f^\times$ was assumed to be connected, let b_p and b_{p+1} be the two boundary vertices of G belonging to F. Again, we see that each strand of G passes through an even number of edges of F except for the two strands labeled by $f(p)$ and $p+1$. Therefore the alternating product (2.7) is real if and only if $\epsilon(f(p)) = \epsilon(p+1)$ for all $p \in [n]$, where the indices are taken modulo n. This is equivalent to having $\epsilon(f^\downarrow(p)) = \epsilon(p)$ for all $p \in [n]$. Thus all alternating products (2.7) are real, which implies that $\mathrm{wt}_\mathbf{t}$ is gauge-equivalent to a real edge weight function.

We have shown the result for generic $\mathbf{t} \in \Theta_f^\mathbb{R}$. The general case follows by continuity. □

The converse to (5.4) is false in general, even for the top cell. For instance, if $f = f_{2,4}$ then $\mathrm{Meas}_f(\mathbf{t}) \in \mathrm{Crit}_f^\circ(\mathbb{R})$ when $\mathbf{t} \in \Theta_f^\circ$ satisfies $t_1 = t_3$ and $t_2 = t_4$; see Example 1.13. However, we expect the converse to hold in the *generic* case.

Conjecture 5.10. Let $f \in \mathcal{B}(k,n)$ be loopless and assume that $G_f^\times$ is connected. Then for all generic $\mathbf{t} \in \Theta_f^\circ$, we have

$$\mathbf{t} \in \Theta_f^{\mathbb{R}} \quad \Longleftrightarrow \quad \mathrm{Meas}_f(\mathbf{t}) \in \mathrm{Crit}_f^\circ(\mathbb{R}).$$

In Section 9, we prove this in the following special case (cf. Notation 2.2).

Theorem 5.11. *Let $2 \leqslant k \leqslant n-2$ and $f = f_{k,n}$. Then for any generic $\mathbf{t} \in (\mathbb{C}^*)^n$, we have*

$$\mathbf{t} \in \Theta_{k,n}^{\mathbb{R}} \quad \Longleftrightarrow \quad \mathrm{Meas}_{k,n}(\mathbf{t}) \in \mathrm{Crit}_{k,n}^\circ(\mathbb{R}). \tag{5.5}$$

When $k = 1$ or $k = n$, $f_{k,n}$ is not connected (and the problem is trivial). When $k = n-1$, $f_{k,n}$ is connected but our methods do not extend to this case.

5.4. **The twist map.** We review the twist map introduced by Muller–Speyer [MuSp17] generalizing the earlier results of Marsh–Scott [MaSc16]. Our goal is to express the *twisted minors* of $\mathrm{Meas}_f(\mathbf{t})$ in terms of $\mathbf{t}$; see Proposition 5.12.

We will use the *left twist* automorphism $\overleftarrow{\tau} : \Pi_f^\circ \xrightarrow{\sim} \Pi_f^\circ$. Suppose that an element $A \in \Pi_f^\circ$ is the row span of a matrix with columns $A_1, A_2, \ldots, A_n$. Extend this to a sequence $(A_q)_{q\in\mathbb{Z}}$ via (2.1). Then $\overleftarrow{\tau}(A) \in \Pi_f^\circ$ has columns $(\overleftarrow{\tau}(A)_q)_{q\in\mathbb{Z}}$ defined by

$$\langle \overleftarrow{\tau}(A)_q, A_q\rangle = 1 \quad \text{and} \quad \langle \overleftarrow{\tau}(A)_q, A_p\rangle = 0 \quad \text{for all } p,q \in \mathbb{Z} \text{ such that } p < q < f(p). \tag{5.6}$$

Here $\langle\cdot,\cdot\rangle$ denotes the standard inner product on $\mathbb{C}^k$. The set $\tilde{I}'_q := \{p \in \mathbb{Z} \mid p \leqslant q < f(p)\}$ is an element of the *reverse Grassmann necklace* of f. Similarly to the set $\tilde{I}_q$ defined in (2.3), it has size k, and the corresponding columns $(A_p)_{p\in\tilde{I}'_q}$ form a basis of $\mathbb{C}^k$. Since $f \in \mathcal{B}(k,n)$ is assumed to be loopless, we have $q \in \tilde{I}'_q$ and the column A_q is nonzero. Thus (5.6) yields a well-defined vector $\overleftarrow{\tau}(A)_q$.

Recall that we have introduced a directed graph $\vec{G}_f^\times$ in Section 4.2 (see Figure 9(c)) with edge set

$$E(\vec{G}_f^\times) = \{(p,q) \in [n]\times[n] \mid p \neq q \text{ form a positive } f\text{-crossing}\}. \tag{5.7}$$

Following [Pos06], we consider *misalignments* of f. Let $p,q,s,t \in [n]$, be such that $p \neq q$, $s = \bar{f}^{-1}(p)$, and $t = \bar{f}^{-1}(q)$. We write $\{p,q\} \in \mathrm{Mis}_f^{\downarrow\downarrow}$ if the points $b_s^+, b_p^-, b_t^+, b_q^-$ are ordered clockwise. Similarly, we write $\{p,q\} \in \mathrm{Mis}_f^{\uparrow\uparrow}$ if the points $b_s^+, b_p^-, b_t^+, b_q^-$ are ordered counterclockwise. Our definition is slightly different from that of [Pos06] in that in our case the 2-element sets $\{s,t\}$ and $\{p,q\}$ are not necessarily disjoint. See Figure 5(c,d).

For convenience, denote

$$[\![t_p, t_q]\!]_+ = [\![t_q, t_p]\!]_+ := [\![t_q, t_p]\!] \quad \text{for } 1 \leqslant p < q \leqslant n.$$

Note that we have $[\![t_p, t_q]\!] = -[\![t_q, t_p]\!]$ but $[\![t_p, t_q]\!]_+ = [\![t_q, t_p]\!]_+$.

Recall from Section 2.2 that the faces of a reduced graph G are labeled by k-element sets. We are ready to give a formula for the corresponding Plücker coordinates of $\overleftarrow{\tau}(\mathrm{Meas}_f(\mathbf{t}))$.

Proposition 5.12. *Let $G \in \mathcal{G}_{\mathrm{red}}(f)$ and assume that Meas_G is well defined at $\mathbf{t} \in \Theta_f^\circ$. Then after a multiplication by a common scalar, we have*

$$\Delta_I(\overleftarrow{\tau}(\mathrm{Meas}_G(\mathrm{wt}_{\mathbf{t}}))) = \Big(\prod_{\substack{\{p,q\}\in\mathrm{Mis}_f^{\downarrow\downarrow}:\\ p,q\in I}} [\![t_q,t_p]\!]_+\Big)\cdot\Big(\prod_{\substack{\{p,q\}\in\mathrm{Mis}_f^{\uparrow\uparrow}:\\ p,q\notin I}} [\![t_q,t_p]\!]_+\Big)\cdot\Big(\prod_{\substack{(p,q)\in E(\vec{G}_f^\times):\\ p\in I, q\notin I}} [\![t_q,t_p]\!]_+\Big)^{-1} \tag{5.8}$$

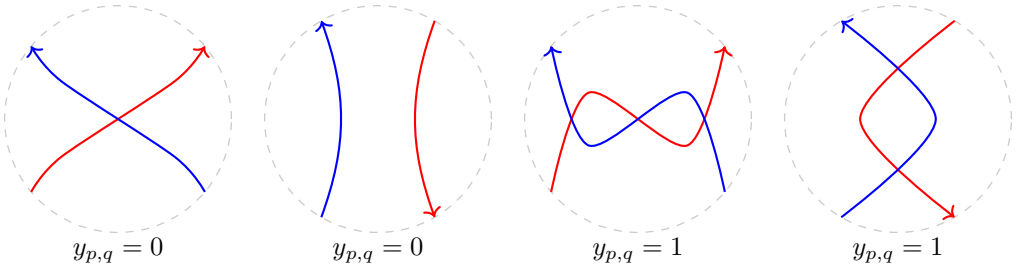

FIGURE 16. The integer $y_{p,q}(G)$ defined in (5.9).

for all face labels I of G.

(Again, observe that the right hand side depends only on f and I but not on G.)

Proof. According to [MuSp17, Theorem 7.1], $\Delta_I \circ \overleftarrow{\tau} \circ \mathrm{Meas}_G(\mathrm{wt}_{\mathbf{t}})$ is a monomial in the edge weights $\mathrm{wt}_{\mathbf{t}}$. Specifically, it is the product of $\mathrm{wt}_{\mathbf{t}}(e)^{-1}$ over all edges e such that the face of G labeled by I belongs to the *upstream wedge* of e; see [MuSp17, Figure 4] and Figure 15(left). The set of such edges forms an almost perfect matching denoted $\overleftarrow{M}(F)$, where F is the face of G labeled by I. Consider two strands terminating at b_p and b_q. In general, they may intersect several times, giving rise to several interior edges e labeled by $\{p,q\}$. The corresponding edge weights are all equal to $\mathrm{wt}_{\mathbf{t}}(e) = [\![t_q, t_p]\!]_+$. Let $x_{p,q}(G)$ denote the number of edges labeled by $\{p,q\}$. Observe that $x_{p,q}(G)$ is odd if p,q form an f-crossing and is even otherwise. Let

$$y_{p,q}(G) := \begin{cases} \frac{1}{2}(x_{p,q}(G)-1), & \text{if } p,q \text{ form an } f\text{-crossing}, \\ \frac{1}{2}x_{p,q}(G), & \text{otherwise;} \end{cases} \tag{5.9}$$

see Figure 16. Consider the product

$$R_G(\mathbf{t}) := \prod_{1\leqslant p<q\leqslant n} ([\![t_q, t_p]\!])^{y_{p,q}(G)}. \tag{5.10}$$

It is then straightforward to see that the product of $\mathrm{wt}_{\mathbf{t}}(e)^{-1}$ over all $e \in \overleftarrow{M}(f)$ is equal to the right hand side of (5.8) divided by $R_G(\mathbf{t})$. □

5.5. **Proofs.** First, we use the twist map to deduce the formula for Grassmann necklace minors.

Proof of Proposition 5.4. As explained in the proof of [MuSp17, Proposition 6.6], we have

$$\Delta_{I_r}(A) = \frac{1}{\Delta_{I_r}(\overleftarrow{\tau}(A))} \quad \text{for all } r \in [n].$$

The result follows from Proposition 5.12. □

Next, we focus on the Laurent phenomenon (Theorem 5.6). For that, we will need several straightforward lemmas.

Lemma 5.13. *Let $\boldsymbol{\theta}$ be an f-admissible tuple, and suppose that $\boldsymbol{\theta}$ and $\mathbf{t}$ are related by* (5.1). *Then for any $G \in \mathcal{G}_{\mathrm{red}}(f)$, $\mathbf{t}$ is f-admissible,* Meas_G *is well defined at $\mathbf{t}$, and* $\mathrm{Meas}_G(\mathrm{wt}_{\boldsymbol{\theta}}) = \mathrm{Meas}_G(\mathrm{wt}_{\mathbf{t}})$ *inside* $\mathrm{Gr}(k,n)$.

Proof. The f-admissibility claim is obvious. Next, observe that $\mathrm{wt}_{\boldsymbol{\theta}}$ and $\mathrm{wt}_{\mathbf{t}}$ are gauge-equivalent; cf. the proof of Lemma 5.9. This implies the remaining statements. □

It is known that when all edge weights $\mathrm{wt}_{\boldsymbol{\theta}}(e)$ are positive reals, $\mathrm{Meas}_G(\mathrm{wt}_{\boldsymbol{\theta}})$ gives rise to a point in $\Pi_f^{>0}$. In particular, $\Delta_I(G, \mathrm{wt}_{\boldsymbol{\theta}})$ is zero for $I \notin \mathcal{M}_f$ and positive for $I \in \mathcal{M}_f$; see (2.6). In what follows, we treat $\mathbf{t} = (t_1, t_2, \ldots, t_n)$ as a collection of algebraically independent variables. To avoid confusion, we denote $Z_{I,G}(\mathrm{wt}_{\mathbf{t}}) := \Delta_I(G, \mathrm{wt}_{\mathbf{t}})$ and treat $\mathbf{Z}_G := (Z_{I,G}(\mathrm{wt}_{\mathbf{t}}))_{I \in \binom{[n]}{k}}$ as a collection of rational functions in $\mathbf{t}$ defined by (1.1). We do *not* consider the entries of $\mathbf{Z}_G$ modulo rescaling since we need to explicitly talk about the entries being Laurent polynomials.

Corollary 5.14. *For a graph $G \in \mathcal{G}_{\mathrm{red}}(f)$, $Z_{I,G}(\mathrm{wt}_{\mathbf{t}})$ is zero for $I \notin \mathcal{M}_f$. For $I \in \mathcal{M}_f$, $Z_{I,G}(\mathrm{wt}_{\mathbf{t}})$ is a nonzero Laurent polynomial in $\mathbf{t}$.*

Proof. The fact that $Z_{I,G}(\mathrm{wt}_{\mathbf{t}})$ is zero for $I \notin \mathcal{M}_f$ follows since the edge weights $\mathrm{wt}_{\boldsymbol{\theta}}$ are all positive, so $\Delta_I(G, \mathrm{wt}_{\boldsymbol{\theta}}) = 0$ implies that G has no almost perfect matchings with boundary I. If $I \in \mathcal{M}_f$ then $\Delta_I(G, \mathrm{wt}_{\boldsymbol{\theta}}) > 0$, and by Lemma 5.13, it is a specialization of $Z_{I,G}(\mathrm{wt}_{\mathbf{t}})$, hence $Z_{I,G}(\mathrm{wt}_{\mathbf{t}}) \neq 0$ as a rational function in $\mathbf{t}$. Finally, $Z_{I,G}(\mathrm{wt}_{\mathbf{t}})$ is a Laurent polynomial in $\mathbf{t}$ since it is a polynomial in the edge weights $\mathrm{wt}_{\mathbf{t}}(e)$, each of which is a Laurent polynomial in $\mathbf{t}$. □

Next we prove the complex algebraic analog of the square move invariance of Meas_f.

Lemma 5.15. *Suppose that reduced graphs G and G' are related by a square move. Then $\mathbf{Z}_G(\mathrm{wt}_{\mathbf{t}})$ and $\mathbf{Z}_{G'}(\mathrm{wt}'_{\mathbf{t}})$ agree up to multiplication by a common factor, where $\mathrm{wt}_{\mathbf{t}}$ and $\mathrm{wt}'_{\mathbf{t}}$ are defined by* (1.4) *on the edges of G and G', respectively.*

Proof. The result follows from the algebraic identity

$$[\![t_1, t_2]\!] \cdot [\![t_3, t_4]\!] + [\![t_1, t_4]\!] \cdot [\![t_2, t_3]\!] = [\![t_1, t_3]\!] \cdot [\![t_2, t_4]\!] \quad \text{for all } t_1, t_2, t_3, t_4 \in \mathbb{C}^*. \tag{5.11}$$

□

Proof of Proposition 5.1 and Theorem 5.6. Let $G \in \mathcal{G}_{\mathrm{red}}(f)$. By [MuSp17, Proposition 5.13], for each $r \in [n]$, G contains a unique almost perfect matching with boundary I_r, and this almost perfect matching coincides with $\overleftarrow{M}(F_r)$ from the proof of Proposition 5.12. Here F_r is the boundary face of G labeled by I_r. In particular, $Z_{I,G}(\mathrm{wt}_{\mathbf{t}})$ is the product of weights of edges in $\overleftarrow{M}(F_r)$. For $I \in \binom{[n]}{k}$, define

$$Y_I(\mathbf{t}) := \frac{Z_{I,G}(\mathrm{wt}_{\mathbf{t}})}{R_G(\mathbf{t})}, \tag{5.12}$$

where $R_G(\mathbf{t})$ is defined in (5.10). We see that $Y_{I_r}(\mathbf{t})$ is equal to the product on the right hand side of (5.3), thus the tuple $(Y_I(\mathbf{t}))_{I \in \binom{[n]}{k}}$ is canonically gauge-fixed. By Corollary 5.14, $Y_I(\mathbf{t})$ is nonzero (as a rational function in $\mathbf{t}$) precisely when $I \in \mathcal{M}_f$. By Lemma 5.15, $Y_I(\mathbf{t})$ depends only on f and I and not on G.

Fix $I \in \mathcal{M}_f$. We need to show that $Y_I(\mathbf{t})$ is a Laurent polynomial in $\mathbf{t}$. The denominator $R_G(\mathbf{t})$ on the right hand side of (5.12) is a product of linear factors since $[\![t_q, t_p]\!] = \frac{1}{t_p t_q}(t_q - t_p)(t_q + t_p)$. Thus up to a monomial, the denominator of $Y_I(\mathbf{t})$ is the product of some linear factors that divides $R_G(\mathbf{t})$ for any G.

Fix $1 \leqslant p < q \leqslant n$. By (5.10), it suffices to show that there exists a graph $G \in \mathcal{G}_{\mathrm{red}}(f)$ such that the integer $y_{p,q}(G)$ defined in (5.9) is zero. The problem is trivial when either p or q is a coloop. Next, assume that we have either $\bar{f}(p) \neq q$ or $\bar{f}(q) \neq p$. Then one can check using the description (1.5) of the Grassmann necklace of f that there exists an index $r \in [n]$ such that either $p, q \in I_r$ or $p, q \notin I_r$. After cyclically shifting (as in Section 3.1), we may

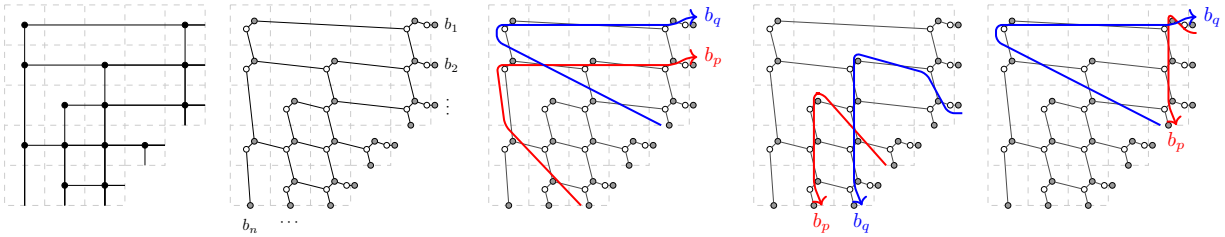

(a) Le-diagram Γ (b) graph $G(\Gamma)$ (c) $p, q \in I_1$ (d) $p, q \notin I_1$ (e) $\bar{f}(p) = q$ and $\bar{f}(q) = p$

FIGURE 17. A Le-diagram Γ and the associated planar bipartite graph $G(\Gamma)$ from the proof of Proposition 5.1 and Theorem 5.6.

assume that $r = 1$. Let Γ be the *Le-diagram* of f (see Figure 17(a)); we refer to [Pos06, Section 20] for background on Le-diagrams. Let $G(\Gamma)$ be the corresponding planar bipartite graph (shown in Figure 17(b)) and let G be the contracted version of $G(\Gamma)$. It is clear that in both cases $p, q \in I_1$ and $p, q \notin I_1$, the strands terminating at b_p and b_q intersect at most once; see Figure 17(c,d). Finally, consider the case $\bar{f}(p) = q, \bar{f}(q) = p$. After applying the cyclic symmetry, we may assume that $p = 1$, and then taking G to be the Le-diagram graph again, we see that the strands terminating at b_p and b_q do not intersect; see Figure 17(e). (Recall that G is contracted unlike $G(\Gamma)$ so the double crossing in Figure 17(e) appears in $G(\Gamma)$ but not in G.) This implies that $y_{p,q}(G) = 0$, and thus the denominator of $Y_I(\mathbf{t})$ is not divisible by $[\![t_q, t_p]\!]$ for any $1 \leqslant p < q \leqslant n$, so $Y_I(\mathbf{t})$ is a Laurent polynomial in $\mathbf{t}$.

Now we can finally introduce the map $\mathrm{Meas}_f : \Theta_f^\circ \to \Pi_f^\circ$ in Proposition 5.1 whose image is the open critical variety Crit_f°. Namely, we set $\mathrm{Meas}_f(\mathbf{t}) := (Y_I(\mathbf{t}))_{I \in \binom{[n]}{k}}$; cf. (5.12). We have already shown above that this map satisfies all of the required properties. □

6. The boundary measurement formula

In this section, we prove the formula stated in Theorem 1.17 and extend it to non-generic tuples $\boldsymbol{\theta} \in \Theta_f^{>0}$, as well as to complex tuples $\mathbf{t} \in \Theta_f^\circ$. The proofs are adapted from the analogous arguments developed in [Gal20]. Throughout, we assume that $f \in \mathcal{B}(k, n)$ is loopless.

6.1. **Nondegenerate boundary measurements.** We start by recasting the formula (1.6) for $\boldsymbol{\gamma}_{f,\boldsymbol{\theta}}(t)$ using the affine notation introduced in Section 3.1. Recall from (2.3) that to each $r \in \mathbb{Z}$ we assign a k-element subset $\tilde{I}_r \subset \mathbb{Z}$ whose reduction modulo n gives an element I_r of the Grassmann necklace of f. Since f is loopless, $\tilde{I}_r$ contains r and we set $\tilde{J}_r := \tilde{I}_r \setminus \{r\}$. For $r \in [n]$, the reduction of $\tilde{J}_r$ modulo n is the set J_r introduced in (1.5). The affine version of (1.6) then reads

$$\tilde{\gamma}_r(t) = \prod_{p \in \tilde{J}_r} \sin(t - \tilde{\theta}_p) \qquad \text{for } r \in \mathbb{Z}. \tag{6.1}$$

Here $(\tilde{\gamma}_r(t))_{r \in \mathbb{Z}}$ is the unique sequence of functions of t satisfying $\tilde{\gamma}_r(t) = \gamma_r(t)$ for $r \in [n]$ and $\tilde{\gamma}_{r+n}(t) = (-1)^{k-1}\tilde{\gamma}_r(t)$ for all $r \in \mathbb{Z}$. The latter condition follows from the analogous condition (3.1) on $\tilde{\boldsymbol{\theta}}$. In particular, the sign $(-1)^{k-1}$ is compatible with the cyclic symmetry of $\mathrm{Gr}_{\geqslant 0}(k, n)$ in Section 3.1. As we see, the sign ϵ_r appears in (1.6) but disappears in (6.1).

Recall from Figure 5(d) that for $1 \leqslant p \neq q \leqslant n$, we write $\{p,q\} \in \mathrm{Mis}_f^{\downuparrows}$ if the points $b_s^+, b_p^-, b_t^+, b_q^-$ are ordered counterclockwise, where $s := \bar{f}^{-1}(p)$ and $t := \bar{f}^{-1}(q)$.

Definition 6.1. We say that $\boldsymbol{\theta} \in \Theta_f^{>0}$ is *f-nondegenerate* if we have $\theta_p \not\equiv \theta_q$ modulo π for all $\{p,q\} \in \mathrm{Mis}_f^{\downuparrows}$. Similarly, $\mathbf{t} \in \Theta_f^{\circ}$ is *f-nondegenerate* if $t_p \neq \pm t_q$ for all $\{p,q\} \in \mathrm{Mis}_f^{\downuparrows}$.

Recall that Theorem 1.17 was stated for the case when $\boldsymbol{\theta}$ is *generic* (and f-admissible); every such tuple is also f-nondegenerate.

Next, let us generalize the curve $\boldsymbol{\gamma}_{f,\boldsymbol{\theta}}(t)$ to the complex algebraic setting. Write

$$\tilde{\gamma}_r^{\mathbb{C}}(t) := \frac{1}{(2i)^{k-1}} \prod_{p \in \tilde{J}_r} [\![t, \tilde{t}_p]\!] \quad \text{for } r \in \mathbb{Z}. \tag{6.2}$$

We again have $\tilde{\gamma}_{r+n}^{\mathbb{C}}(t) = (-1)^{k-1}\tilde{\gamma}_r^{\mathbb{C}}(t)$ for $r \in \mathbb{Z}$; cf. Section 5.1. For $r \in [n]$, let $\gamma_r^{\mathbb{C}}(t) := \tilde{\gamma}_r^{\mathbb{C}}(t)$ and introduce a map $\boldsymbol{\gamma}_{f,\mathbf{t}}^{\mathbb{C}} : \mathbb{C}^* \to \mathbb{C}^n$ given by $\boldsymbol{\gamma}_{f,\mathbf{t}}^{\mathbb{C}}(t) = (\gamma_1^{\mathbb{C}}(t), \ldots, \gamma_n^{\mathbb{C}}(t))$. Thus $\boldsymbol{\gamma}_{f,\mathbf{t}}^{\mathbb{C}}(t)$ specializes to $\boldsymbol{\gamma}_{f,\boldsymbol{\theta}}(t)$ when $\mathbf{t}$ and $\boldsymbol{\theta}$ are related by (5.1).

Theorem 6.2. *Suppose that $\mathbf{t} \in \Theta_f^{\circ}$ is f-nondegenerate. Then $\mathrm{Span}_{\mathbb{C}}(\boldsymbol{\gamma}_{f,\mathbf{t}}^{\mathbb{C}})$ has dimension k and we have*

$$\mathrm{Meas}_f(\mathbf{t}) = \mathrm{Span}_{\mathbb{C}}(\boldsymbol{\gamma}_{f,\mathbf{t}}^{\mathbb{C}}) \quad \textit{inside } \mathrm{Gr}(k,n).$$

Corollary 6.3. *Suppose that $\boldsymbol{\theta} \in \Theta_f^{>0}$ is f-nondegenerate. Then $\mathrm{Span}_{\mathbb{R}}(\boldsymbol{\gamma}_{f,\boldsymbol{\theta}})$ has dimension k and we have*

$$\mathrm{Meas}_f(\boldsymbol{\theta}) = \mathrm{Span}_{\mathbb{R}}(\boldsymbol{\gamma}_{f,\boldsymbol{\theta}}) \quad \textit{inside } \mathrm{Gr}_{\geqslant 0}(k,n).$$

As explained above, this result generalizes Theorem 1.17 from generic to f-nondegenerate tuples $\boldsymbol{\theta} \in \Theta_f^{>0}$.

We also mention a boundary measurement formula for dual critical varieties. Fix a coolopless $f \in \mathcal{B}(k,n)$ and recall the notation from Remark 5.3. We write $\{p,q\} \in \widehat{\mathrm{Mis}}_f^{\downuparrows}$ if the points $b_s^-, b_p^+, b_t^-, b_q^+$ are ordered counterclockwise for $s := \bar{f}^{-1}(p)$ and $t := \bar{f}^{-1}(q)$. We say that $\mathbf{t} \in \widehat{\Theta}_f^{\circ}$ is *dual f-nondegenerate* if $t_p \neq \pm t_q$ whenever $\{p,q\} \in \widehat{\mathrm{Mis}}_f^{\downuparrows}$. Let $\widehat{\boldsymbol{\gamma}}_{f,\mathbf{t}}^{\mathbb{C}}(t) = (\widehat{\gamma}_1^{\mathbb{C}}(t), \widehat{\gamma}_2^{\mathbb{C}}(t), \ldots, \widehat{\gamma}_n^{\mathbb{C}}(t))$ be given by

$$\widehat{\gamma}_r^{\mathbb{C}}(t) := [\![\tilde{t}_{f(r)}, \tilde{t}_r]\!] \cdot \gamma_r^{\mathbb{C}}(t) \quad \text{for } r \in [n], \tag{6.3}$$

where $\gamma_r^{\mathbb{C}}(t)$ is defined by (6.2). Note that when $r \in [n]$ is a loop, we have $\widehat{\gamma}_r^{\mathbb{C}}(t) = 0$ since $[\![\tilde{t}_{f(r)}, \tilde{t}_r]\!] = 0$. The proof of the following result is completely analogous to the proof of Theorem 6.2 given below.

Theorem 6.4. *Let $f \in \mathcal{B}(k,n)$ be coolopless and $\mathbf{t} \in \widehat{\Theta}_f^{\circ}$ be dual f-nondegenerate. Then*

$$\widehat{\mathrm{Meas}}_f(\mathbf{t}) = \mathrm{Span}_{\mathbb{C}}(\widehat{\boldsymbol{\gamma}}_{f,\mathbf{t}}^{\mathbb{C}}) \quad \textit{inside } \mathrm{Gr}(k,n).$$

Example 6.5. Consider the case $f = f_{1,4}$. Even though $\mathrm{Crit}_f^{>0}$ is a single point, $\widehat{\mathrm{Crit}}_f^{>0}$ is not a single point since the four boundary edges of the corresponding reduced graph G have weights $[\![t_2,t_1]\!], [\![t_3,t_2]\!], [\![t_4,t_3]\!], [\![t_4,t_1]\!]$. Therefore $\mathrm{Meas}_f(\mathbf{t}) \in \mathrm{Gr}(1,4)$ is given by the point $\widehat{\mathrm{Meas}}_f(\mathbf{t}) = ([\![t_2,t_1]\!] : [\![t_3,t_2]\!] : [\![t_4,t_3]\!] : [\![t_4,t_1]\!])$. For each $r \in [n]$, we have $J_r = \emptyset$, thus $\gamma_r^{\mathbb{C}}(t) = 1$. But because we have the extra term in (6.3), we find that $\widehat{\boldsymbol{\gamma}}_{f,\mathbf{t}}^{\mathbb{C}}$ depends on $\mathbf{t}$ (but not on t):

$$\widehat{\boldsymbol{\gamma}}_{f,\mathbf{t}}^{\mathbb{C}}(t) = ([\![t_2,t_1]\!], [\![t_3,t_2]\!], [\![t_4,t_3]\!], [\![\tilde{t}_5,t_4]\!]).$$

We see that $\mathrm{Span}_{\mathbb{C}}(\widehat{\boldsymbol{\gamma}}^{\mathbb{C}}_{f,\mathbf{t}})$ agrees with $\widehat{\mathrm{Meas}}_f(\mathbf{t})$ since $[\![\tilde{t}_5, t_4]\!] = -[\![t_1, t_4]\!] = [\![t_4, t_1]\!]$.

Remark 6.6. It follows by combining Proposition 3.4 with Theorems 6.2 and 6.4 that the curves $\boldsymbol{\gamma}_{f,\tilde{\boldsymbol{\theta}}}$ and $\widehat{\boldsymbol{\gamma}}_{\hat{f},\tilde{\boldsymbol{\theta}}\circ f}$ span orthogonal subspaces of $\mathbb{R}^n$. We do not have a direct explanation for this phenomenon, even for $f = f_{k,n}$.

Proof of Theorem 6.2. Recall that $f \in \mathcal{B}(k,n)$ is assumed to be loopless. Suppose that $f(r) = r+n$ for some coloop $r \in [n]$. Then $r \notin J_r$ but $r \in J_q$ for all $q \in [n] \setminus \{r\}$. Moreover, since $\mathbf{t}$ is f-nondegenerate, we see that $t_r \neq \pm t_p$ for all $p \in J_r$. Thus $\boldsymbol{\gamma}^{\mathbb{C}}_{f,\mathbf{t}}(t_r) \in \mathbb{C}^n$ has a single nonzero coordinate in position r. Let $f' \in \mathcal{B}(k-1,n-1)$ be obtained from f by removing the coloop at r, and let $\mathbf{t}'$ be obtained from $\mathbf{t}$ by omitting t_r. Clearly f' is loopless and $\mathbf{t}'$ is f'-nondegenerate. The entries of $\boldsymbol{\gamma}^{\mathbb{C}}_{f',\mathbf{t}'}$ are obtained from the corresponding entries $\gamma^{\mathbb{C}}_q(t)$ of $\boldsymbol{\gamma}^{\mathbb{C}}_{f,\mathbf{t}}$ (for $q \neq r$) by dividing by $\frac{1}{2i}[\![t, t_r]\!]$. It follows that if the statement of Theorem 6.2 is true for f' then it is true for f.

We proceed by induction using the bridge removal procedure from Section 2.3. For the base case $k = n = 1$, the statement is clear. Let $f \in \mathcal{B}(k,n)$ be loopless. We have shown above that we may assume that f is also coloopless. As explained in Section 2.3, there exists some index $r \in [n]$ such that f has a bridge at r, thus $r < r+1 \leqslant f(r) < f(r+1) \leqslant r+n$. Let $f' := s_r f \in \mathcal{B}(k,n)$ and consider a graph $G \in \mathcal{G}_{\mathrm{red}}(f)$ that contains a bridge at b_r, b_{r+1} as shown in Figure 7(left). It may happen that f' is not loopless when $f(r) = r+1$, thus we first consider this case.

Assume that $f(r) = r+1$. Then $r+1$ does not appear in J_q for any $q \in [n]$ and we have $\tilde{\gamma}^{\mathbb{C}}_r(t) = \tilde{\gamma}^{\mathbb{C}}_{r+1}(t)$ for all $t \in \mathbb{C}^*$. The r-th and $(r+1)$-th columns of $\mathrm{Meas}_f(\mathbf{t})$ also agree; see Section 4.4. Let $f'' \in \mathcal{B}(k,n-1)$ be obtained from f' by removing the loop at r. We see that if the boundary measurement formula holds for f'' then it holds for f.

Assume now that $f(r) > r+1$. Let $a = f(r)$ and $b = f(r+1)$. Since both $\mathrm{Meas}_f(\mathbf{t})$ and $\boldsymbol{\gamma}^{\mathbb{C}}_{f,\mathbf{t}}$ are compatible with the cyclic shift from Section 3.1, we may assume that $1 \leqslant r < r+1 < a < b \leqslant n$. Then it is easy to check using [Lam16, Lemma 7.6] and Figure 7 that $\mathrm{Meas}_{f'}(\mathbf{t}) = \mathrm{Meas}_f(\mathbf{t}) \cdot g$, where $g = x_r(-[\![t_b, t_a]\!]/[\![t_b, t_{r+1}]\!]) \cdot d_{r+1}([\![t_b, t_{r+1}]\!]/[\![t_a, t_{r+1}]\!])$ and the matrices $x_j(t), d_j(t) \in \mathrm{GL}_n(\mathbb{C})$ differ from the identity matrix as follows: $x_j(t)$ contains a single nonzero off-diagonal entry equal to t in row j and column $j+1$ while $d_j(t)$ is a diagonal matrix whose (j,j)-th entry is equal to t and all other diagonal entries of $d_j(t)$ are equal to 1. The 2×2 block of g in rows and columns $r, r+1$ is given by

$$g|_{\{r,r+1\}\times\{r,r+1\}} = \begin{pmatrix} 1 & -[\![t_b, t_a]\!]/[\![t_a, t_{r+1}]\!] \\ 0 & [\![t_b, t_{r+1}]\!]/[\![t_a, t_{r+1}]\!] \end{pmatrix}.$$

We claim that $\boldsymbol{\gamma}^{\mathbb{C}}_{f',\mathbf{t}}(t) = \boldsymbol{\gamma}^{\mathbb{C}}_{f,\mathbf{t}}(t) \cdot g$ for all $t \in \mathbb{C}^*$. Denote the coordinates of $\boldsymbol{\gamma}^{\mathbb{C}}_{f',\mathbf{t}}(t)$ by $\gamma^{\mathbb{C}}_{f',q}(t)$ for $q \in [n]$, and let J'_q be the set associated to q by (1.5) using the strand diagram of f'. First, observe that $\gamma^{\mathbb{C}}_{f',q}(t) = \gamma^{\mathbb{C}}_q(t)$ for $q \neq r+1$. The $(r+1)$-th coordinates differ since $J'_{r+1} = J_{r+1} \setminus \{a\} \sqcup \{b\}$. Thus $\gamma^{\mathbb{C}}_{r+1}(t) = P(t) \cdot [\![t, t_a]\!]$ while $\gamma^{\mathbb{C}}_{f',r+1}(t) = P(t) \cdot [\![t, t_b]\!]$ for some rational function $P(t)$. Note also that $\gamma^{\mathbb{C}}_r(t) = \gamma^{\mathbb{C}}_{f',r}(t) = P(t) \cdot [\![t, t_{r+1}]\!]$. A direct computation yields

$$\begin{pmatrix} [\![t, t_{r+1}]\!] & [\![t, t_a]\!] \end{pmatrix} \cdot \begin{pmatrix} 1 & -[\![t_b, t_a]\!]/[\![t_a, t_{r+1}]\!] \\ 0 & [\![t_b, t_{r+1}]\!]/[\![t_a, t_{r+1}]\!] \end{pmatrix} = \begin{pmatrix} [\![t, t_{r+1}]\!] & [\![t, t_b]\!] \end{pmatrix}.$$

This implies the desired identity $\boldsymbol{\gamma}^{\mathbb{C}}_{f',\mathbf{t}}(t) = \boldsymbol{\gamma}^{\mathbb{C}}_{f,\mathbf{t}}(t) \cdot g$. Thus if the boundary measurement formula holds for f' then it holds for f, which finishes the induction step. $\square$

6.2. **Choosing a basis.** Even though Theorem 6.2 describes $\mathrm{Meas}_f(\mathbf{t})$ as an element of $\mathrm{Gr}(k,n)$, it is convenient to specify an explicit $k \times n$ matrix representative for such a space. We discuss two ways of describing such representatives: taking k distinct points on the curve $\boldsymbol{\gamma}_{f,\boldsymbol{\theta}}(t)$ and taking the basis of its Fourier coefficients. The proofs translate verbatim from [Gal20, Section 3].

Proposition 6.7.

(i) *Assume that $\boldsymbol{\theta} \in \Theta_f^{>0}$ is f-nondegenerate. Then for any $0 \leqslant s_1 < s_2 < \cdots < s_k < \pi$, the vectors $\boldsymbol{\gamma}_{f,\boldsymbol{\theta}}(s_1), \boldsymbol{\gamma}_{f,\boldsymbol{\theta}}(s_2), \ldots, \boldsymbol{\gamma}_{f,\boldsymbol{\theta}}(s_k)$ form a basis of $\mathrm{Span}_{\mathbb{R}}(\boldsymbol{\gamma}_{f,\boldsymbol{\theta}})$.*

(ii) *Assume that $\mathbf{t} \in \Theta_f^{\circ}$ is f-nondegenerate. Then for any generic tuple $(s_1, s_2, \ldots, s_k) \in (\mathbb{C}^*)^k$, the vectors $\boldsymbol{\gamma}^{\mathbb{C}}_{f,\mathbf{t}}(s_1), \boldsymbol{\gamma}^{\mathbb{C}}_{f,\mathbf{t}}(s_2), \ldots, \boldsymbol{\gamma}^{\mathbb{C}}_{f,\mathbf{t}}(s_k)$ form a basis of $\mathrm{Span}_{\mathbb{C}}(\boldsymbol{\gamma}^{\mathbb{C}}_{f,\mathbf{t}})$.*

Proof. By Theorem 6.2, the spaces $\mathrm{Span}_{\mathbb{R}}(\boldsymbol{\gamma}_{f,\boldsymbol{\theta}})$ and $\mathrm{Span}_{\mathbb{C}}(\boldsymbol{\gamma}^{\mathbb{C}}_{f,\mathbf{t}})$ are k-dimensional. It suffices to show that the given vectors span these subspaces. This can be shown by multiplying on the left by an appropriate Vandermonde-type matrix; see [Gal20, Lemma 3.2] for details. □

To describe the Fourier basis, observe that the coordinates of $\boldsymbol{\gamma}^{\mathbb{C}}_{f,\mathbf{t}}(t)$ are Laurent polynomials in t:

$$\gamma^{\mathbb{C}}_r(t) = \frac{1}{(2i)^{k-1}} \sum_{p=1}^{k} (-1)^{k-p} c_{p,r} t^{2p-k-1}.$$

Here $c_{p,r}$ is the $(r-1)$-th elementary symmetric polynomial in the variables $(t_q^2)_{q \in J_r}$ divided by $\prod_{q \in J_r} t_q$; see [Gal20, Equation (3.2)].

Let $F_{f,\mathbf{t}} = (c_{p,r})_{p \in [k], r \in [n]}$ be the corresponding $k \times n$ *Fourier coefficient matrix*.[7] The next result also follows by combining the proof of [Gal20, Lemma 3.2] with Theorem 6.2.

Proposition 6.8. *Assume that $\mathbf{t} \in \Theta_f^{\circ}$ is f-nondegenerate. Then the rows of $F_{f,\mathbf{t}}$ form a $\mathbb{C}$-basis of $\mathrm{Span}_{\mathbb{C}}(\boldsymbol{\gamma}^{\mathbb{C}}_{f,\mathbf{t}})$.* □

6.3. **Degenerate boundary measurements.** The boundary measurement formula in Theorem 6.2 holds when $\mathbf{t} \in \Theta_f^{\circ}$ is f-nondegenerate. If $\mathbf{t} \in \Theta_f^{\circ}$ is f-degenerate (that is, not f-nondegenerate) then it is not hard to see that the span of $\boldsymbol{\gamma}^{\mathbb{C}}_{f,\mathbf{t}}(t)$ has dimension strictly less than k. Nevertheless, $\mathrm{Meas}_f(\mathbf{t}) \in \mathrm{Gr}(k,n)$ is still defined for all $\mathbf{t} \in \Theta_f^{\circ}$. In order to extend the boundary measurement formula to all of Θ_f°, we adapt the constructions from [Gal20, Section 6].

First, we introduce a slight modification of $\boldsymbol{\gamma}^{\mathbb{C}}_{f,\mathbf{t}}(t)$. Let

$$\tilde{\Gamma}_r(t) := \frac{1}{(2i)^{k-1}} \prod_{p \in \tilde{J}_r} \left(\frac{t}{\tilde{t}_p} - \tilde{t}_p \right) \quad \text{for } r \in \mathbb{Z}. \tag{6.4}$$

Thus (6.4) differs from (6.2) in that the terms on the right hand side are of the form $\left(t/\tilde{t}_p - \tilde{t}_p\right)$ rather than $[\![t, \tilde{t}_p]\!] = (t/\tilde{t}_p - \tilde{t}_p/t)$. We let $\Gamma_r(t) := \tilde{\Gamma}_r(t)$ for $r \in [n]$ and $\boldsymbol{\Gamma}_{f,\mathbf{t}}(t) = (\Gamma_1(t), \Gamma_2(t), \ldots, \Gamma_n(t))$. Unlike for $\boldsymbol{\gamma}^{\mathbb{C}}_{f,\mathbf{t}}(t)$, the coordinates of $\boldsymbol{\Gamma}_{f,\mathbf{t}}(t)$ are genuine polynomials in t.

For $q \in [n]$, let $\mathrm{supp}_f(q) := \{r \in [n] \mid q \notin J_r\}$ and $v_q := t_q^2$. Thus $\Gamma_r(v_q) = 0$ for $r \notin \mathrm{supp}_f(q)$. For $x \in \mathbb{C}^n$ and $S \subset [n]$, let $x|_S \in \mathbb{C}^n$ be the vector obtained from x by

[7] The name is explained by the fact that if $\boldsymbol{\theta}$ and $\mathbf{t}$ are related by (5.1) then up to a simple transformation, the rows of $F_{f,\mathbf{t}}$ yield the Fourier coefficients of $\boldsymbol{\gamma}_{f,\boldsymbol{\theta}}(t)$, viewed as a 2π-periodic function of t.

sending the coordinates x_r to zero for $r \notin S$. For $m \geqslant 0$, denote by $\mathbf{\Gamma}_{f,\mathbf{t}}^{(m)}(t)$ the m-fold derivative of $\mathbf{\Gamma}_{f,\mathbf{t}}(t)$. Finally, for $r \in [n]$, let $m_r := \#\{q \in J_r \mid v_q = v_r\}$ be the degree with which $(t - v_r)$ divides $\Gamma_r(t)$. Denote

$$u_{f,\mathbf{t}}^{(r)} := \mathbf{\Gamma}_{f,\mathbf{t}}^{(m_r)}(v_r)|_{\mathrm{supp}_f(r)} \quad \text{for } r \in [n].$$

Thus $u_{f,\mathbf{t}}^{(r)} \in \mathbb{C}^n$ is obtained by (i) differentiating $\mathbf{\Gamma}_{f,\mathbf{t}}(t)$ m_r times, (ii) substituting $t = v_r$, and (iii) sending all coordinates not in $\mathrm{supp}_f(r)$ to 0.

Theorem 6.9. *Let $f \in \mathcal{B}(k,n)$ be loopless and $\mathbf{t} \in \Theta_f^\circ$. Then for each $r \in [n]$, the vectors*

$$\{u_{f,\mathbf{t}}^{(p)} \mid p \in I_r\} \tag{6.5}$$

form a basis of $\mathrm{Meas}_f(\mathbf{t})$.

Proof. The proof is obtained by modifying the details of [Gal20, Proof of Theorem 6.1] in a straightforward fashion. □

7. Applications

We explain the results on electrical networks from Section 1.6 in more detail. Along the way, we compare them to their Ising model counterparts obtained in [Gal20].

7.1. **Embeddings into** $\mathrm{Gr}_{\geqslant 0}(k,n)$**.** Let $\mathbb{T}$ be a rhombus tiling of a polygonal region R as in Section 1.6. Let $G_{\mathbb{T}}$ be the corresponding isoradial graph with boundary vertices $B_1, B_2, \ldots, B_N$. Let $v_1, v_2, \ldots, v_{2n} \in \mathbb{C}$ be the unit vectors traversing the sides of R in clockwise order. They are labeled so that B_p is incident to v_{2p-1} and v_{2p} for each $p \in [N]$. This data gives rise to a fixed-point-free involution $\tau_R : [2N] \to [2N]$ (we refer to such involutions as *pairings*; see e.g. Figure 18(a)) defined as follows. Choose $p \in [2N]$ and consider the (unique) rhombus of $\mathbb{T}$ containing the side of R labeled by v_p. Let $v_p^{(1)}$ be the opposite side of this rhombus. Next, $v_p^{(1)}$ is contained in a unique other rhombus of $\mathbb{T}$, so we let $v_p^{(2)}$ denote the opposite side of that rhombus, etc. This way, we create a family of parallel line segments $v_p, v_p^{(1)}, v_p^{(2)}, \ldots$ which terminates at some boundary line segment labeled by v_q for $q \in [2N]$. We then set $\tau_R(p) := q$. It is easy to see that we therefore must have $q \neq p$ and $\tau_R(q) = p$, thus τ_R is indeed a fixed-point-free involution. See [Gal20, Figure 2(c)] for an example.

Following [Lam18], we associate a bounded affine permutation $f_R^{\mathrm{elec}} = f_{\tau_R}^{\mathrm{elec}} \in \mathcal{B}(N+1, 2N)$ to R. It is the unique loopless bounded affine permutation such that for each $p \in [2N]$, we have $\bar{f}_R^{\mathrm{elec}}(p) \equiv \tau_R(p+1)$ modulo $n := 2N$ (where $p+1$ is taken modulo n). See Figure 18(b).

Recall from Section 1.6 that the graph $G_{\mathbb{T}}$ is viewed as an electrical network whose $N \times N$ response matrix is denoted $\Lambda_{\mathrm{elec}}^R$. We describe Lam's embedding ϕ^{elec} of the space of $N \times N$ electrical response matrices into $\mathrm{Gr}_{\geqslant 0}(N+1, 2N)$. Let $[n]_{\mathrm{odd}} := \{1, 3, \ldots, 2N-1\}$. Then $\phi^{\mathrm{elec}}(\Lambda_{\mathrm{elec}}^R)$ is the unique element $X \in \mathrm{Gr}(N+1, 2N)$ such that

$$\Delta_{[n]_{\mathrm{odd}} \cup \{2p\}}(X) = 1 \quad \text{and} \quad \Delta_{[n]_{\mathrm{odd}} \setminus \{2q-1\} \cup \{2p-2, 2p\}}(X) = \Lambda_{p,q}^R \quad \text{for all } p \neq q \in [N]. \tag{7.1}$$

Here the index $2p-2$ is taken modulo n. The element $\phi^{\mathrm{elec}}(\Lambda_{\mathrm{elec}}^R)$ turns out to belong to $\mathrm{Gr}_{\geqslant 0}(N+1, 2N)$. Moreover, it belongs to $\Pi_{f_R^{\mathrm{elec}}}^{>0}$.

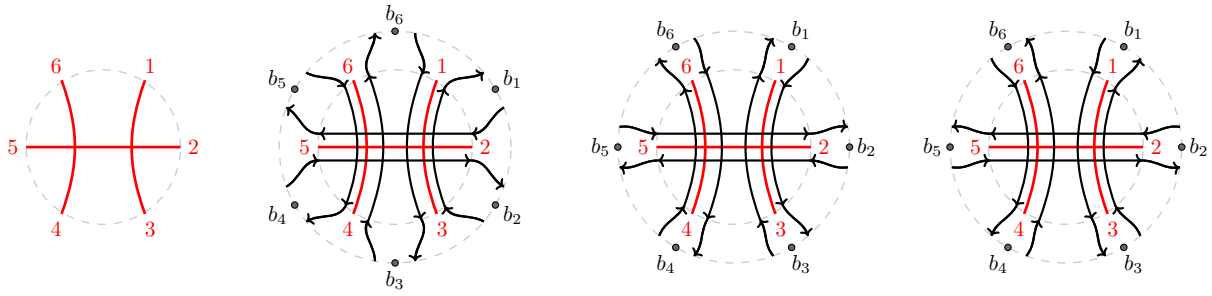

(a) pairing τ_R (b) $f_R^{\text{elec}}(p) \equiv \tau_R(p+1) \pmod n$ (c) $f_R^{\text{Ising}}(p) \equiv \tau_R(p) \pmod n$ (d) dual reduced strand diagram for f_R^{Ising}

FIGURE 18. Converting a pairing τ_R into bounded affine permutations f_R^{elec} and f_R^{Ising}.

Remark 7.1. The above embedding into $\mathrm{Gr}_{\geqslant 0}(N+1, 2N)$ is obtained from Lam's embedding into $\mathrm{Gr}_{\geqslant 0}(N-1, 2N)$ by composing it with the map $\mathrm{alt}^{\perp}$ from Section 3.2. The description (7.1) is deduced by combining [Lam18, Proposition 2.4] with the description of the embedding in terms of *concordant sets* given in [Lam18, Section 5.2].

The *Ising model* is a probability distribution on the space $\{\pm 1\}^{V(G)}$ of *spin configurations* on the vertices of a weighted graph G. Given two vertices $u, v \in V(G)$, one can consider their *spin correlation*, denoted $\langle \sigma_u \sigma_v \rangle$. It is a real number between -1 and 1. The *critical Ising model* [Bax86, Bax78] is obtained in the case where $G = G_{\mathbb{T}}$ is the graph described above, but it has a different choice of edge weights. Consider the *boundary correlations* $\langle \sigma_p \sigma_q \rangle_{\mathbb{T}} := \langle \sigma_{B_p} \sigma_{B_q} \rangle_{G_{\mathbb{T}}}$ forming an $N \times N$ *boundary correlation matrix* $M_{\text{Ising}}^{\mathbb{T}} := (\langle \sigma_p \sigma_q \rangle_{\mathbb{T}})_{p,q \in [N]}$. As in the case of electrical networks, the matrix $M_{\text{Ising}}^{\mathbb{T}}$ is invariant under star-triangle moves and therefore depends only on the region R. We denote $M_{\text{Ising}}^{R} := M_{\text{Ising}}^{\mathbb{T}}$.

Let $f_{\tau_R}^{\text{Ising}} = f_R^{\text{Ising}} \in \mathcal{B}(N, 2N)$ be the unique bounded affine permutation such that for each $p \in [2N]$, we have $f_R^{\text{Ising}}(p) \equiv \tau_R(p)$ modulo n; see Figure 18(c). In [GP20], we associated an element $\phi^{\text{Ising}}(M_{\text{Ising}}^R) \in \mathrm{Gr}_{\geqslant 0}(N, 2N)$ to any boundary correlation matrix. It belongs to the positroid cell $\Pi_{f_R^{\text{Ising}}}^{>0}$.

7.2. **Pairings.** Let $\tau : [n] \to [n]$ be a pairing. We say that $\{p, q\}$ is a *τ-pair* if $\tau(p) = q$, and we identify τ with the corresponding set $\{\{p_1, \tau(p_1)\}, \{p_2, \tau(p_2)\}, \ldots, \{p_N, \tau(p_N)\}\}$ of τ-pairs. We say that two τ-pairs $\{p, q\} \neq \{p', q'\}$ *form a τ-crossing* if the points p, p', q, q' are cyclically ordered (either clockwise or counterclockwise). We let $\mathrm{xing}(\tau)$ denote the number of τ-crossings. Similarly to (4.1), we introduce an undirected graph $G_\tau^{\times}$ with vertex set $[n]$ and two indices $p, p' \in [n]$ forming an edge whenever the corresponding τ-pairs $\{p, \tau(p)\}$ and $\{p', \tau(p')\}$ form a τ-crossing. We say that τ is *connected* if $G_\tau^{\times}$ is connected.

Consider n points $d_1, d_2, \ldots, d_n$ on a circle in clockwise order. A *τ-pseudoline arrangement* $\mathcal{A}$ is a collection of N embedded unoriented paths in a disk, each connecting d_p to $d_{\tau(p)}$ for some $p \in [n]$, such that no two paths intersect more than once and no three paths intersect at a single point. Each rhombus tiling $\mathbb{T}$ of a polygonal region R is planar dual to a τ_R-pseudoline arrangement $\mathcal{A}_{\mathbb{T}}$: the pseudoline connecting d_p to $d_{\tau_R(p)}$ is obtained by connecting the midpoints of the above line segments $v_p, v_p^{(1)}, v_p^{(2)}, \ldots$; see [Gal20, Figure 2(c)].

We say that a tuple $\boldsymbol{\theta} = (\theta_1, \theta_2, \ldots, \theta_n) \in \mathbb{R}^n$ is *τ-isotropic* if

$$\theta_q = \theta_p + \pi/2 \quad \text{for all } \tau\text{-pairs } \{p, q\} \text{ with } 1 \leqslant p < q \leqslant n. \tag{7.2}$$

Extending $\boldsymbol{\theta}$ to $\tilde{\boldsymbol{\theta}} : \mathbb{Z} \to \mathbb{R}$ via (3.1), the above condition becomes

$$\tilde{\theta}_q = \tilde{\theta}_p + \pi/2 \quad \text{for all } p < q \in \mathbb{Z} \text{ such that } f_R^{\mathrm{Ising}}(p) = q.$$

We say that a tuple $\boldsymbol{\theta} \in \mathbb{R}^n$ is *τ-admissible* if it is τ-isotropic and satisfies

$$\theta_p < \theta_{p'} < \theta_q < \theta_{q'}$$

for all $1 \leqslant p < p' < q < q' \leqslant n$ such that the τ-pairs $\{p, q\}$ and $\{p', q'\}$ form a τ-crossing. One easily observes that given a rhombus tiling $\mathbb{T}$ of R, one can choose a τ-admissible tuple $\boldsymbol{\theta}$ such that $v_p = \exp(-2i\theta_p)$ for all $p \in [n]$.

We may now view the region R as a pair $(\tau_R, \boldsymbol{\theta})$ where $\boldsymbol{\theta}$ is τ_R-admissible. Recall that for any rhombus tiling $\mathbb{T}$ of R, the response matrix $\Lambda_{\mathrm{elec}}^{\mathbb{T}} = \Lambda_{\mathrm{elec}}^R$ of the associated electrical network $G_{\mathbb{T}}$ depends only on R. More generally, it is possible to associate an electrical network $G_{(\mathcal{A},\boldsymbol{\theta})}$ to an arbitrary pair $(\mathcal{A}, \boldsymbol{\theta})$ consisting of a τ-pseudoline arrangement $\mathcal{A}$ and a τ-admissible tuple $\boldsymbol{\theta}$; see [Gal20, Section 2]. The resulting response matrix $\Lambda_{\mathrm{elec}}^{(\mathcal{A},\boldsymbol{\theta})}$ again depends only on $(\tau, \boldsymbol{\theta})$ and is denoted $\Lambda_{\mathrm{elec}}^{(\tau,\boldsymbol{\theta})}$. For a pair $(\tau, \boldsymbol{\theta})$ where $\boldsymbol{\theta}$ is τ-admissible, we denote $R := (\tau, \boldsymbol{\theta})$ and refer to R as a *generalized region* (called a *valid region* in [Gal20]).

7.3. **Back to critical cells.** Given a pairing $\tau : [n] \to [n]$, we have defined the bounded affine permutations $f_\tau^{\mathrm{elec}} \in \mathcal{B}(N+1, 2N)$, $f_\tau^{\mathrm{Ising}} \in \mathcal{B}(N, 2N)$, τ-pseudoline arrangements $\mathcal{A}$, and τ-admissible tuples $\boldsymbol{\theta}$. In this section, we discuss the relationship between these notions and the notions introduced above in the context of critical varieties, such as reduced strand diagrams and f-admissible tuples $\boldsymbol{\theta}$.

Let $\mathcal{A}$ be a τ-pseudoline arrangement. Recall that the endpoints of pseudolines in $\mathcal{A}$ are labeled $d_1, d_2, \ldots, d_n$. For each $p \in [n]$, place a point d_p^- (resp., d_p^+) slightly before (resp., after) d_p in clockwise order. Let $D_{\mathcal{A}}$ be a reduced strand diagram whose (directed) strands connect $d_p^- \to d_q^+$ whenever $\tau(p) = q$.

Relabeling the boundary points of $D_{\mathcal{A}}$ by $b_p^- := d_p^-$ and $b_p^+ := d_p^+$ for all $p \in [n]$, $D_{\mathcal{A}}$ becomes a dual reduced strand diagram of f_τ^{Ising}; see Figure 18(d). However, we may also relabel the boundary points in a different way: setting $b_p^- := d_p^+$ and $b_p^+ := d_{p+1}^-$ for all $p \in [n]$ gives rise to a reduced strand diagram of f_τ^{elec} as in Figure 18(b). See Section 8 for a detailed discussion of this "shift by 1" correspondence. For now, observe that this identification of strand diagrams allows one to relate the notions of τ-admissible, f_τ^{elec}-admissible, and f_τ^{Ising}-admissible tuples $\boldsymbol{\theta}$.

Proposition 7.2. *Let $\tau : [n] \to [n]$ be a pairing and $\boldsymbol{\theta} \in \mathbb{R}^n$. The following are equivalent:*

- *$\boldsymbol{\theta}$ is τ-admissible;*
- *$\boldsymbol{\theta}$ is τ-isotropic and f_τ^{elec}-admissible;*
- *$\boldsymbol{\theta}$ is τ-isotropic and f_τ^{Ising}-admissible.* □

We are ready to prove a generalization of Theorem 1.20.

Theorem 7.3. *Let $R := (\tau, \boldsymbol{\theta})$ be a generalized region. Then we have*

$$\phi^{\mathrm{elec}}(\Lambda_{\mathrm{elec}}^R) = \mathrm{Meas}_{f_\tau^{\mathrm{elec}}}(\boldsymbol{\theta}) \quad \textit{and} \quad \phi^{\mathrm{Ising}}(M_{\mathrm{Ising}}^R) = \mathrm{Meas}_{f_\tau^{\mathrm{Ising}}}(\boldsymbol{\theta}).$$

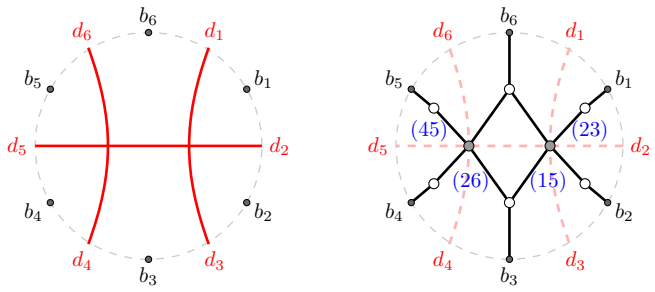

FIGURE 19. Converting a pairing τ_R into a weighted graph $G^{\mathrm{elec}} \in \mathcal{G}_{\mathrm{red}}(f_R^{\mathrm{elec}})$.

Proof. As we mentioned in Section 1.6, both results follow from the well-known fact that the critical dimer model specializes to critical electrical networks and the critical Ising model. In both cases, one transforms the weighted graph $G_{\mathbb{T}}$ into a weighted reduced planar bipartite graph $(G^{\mathrm{elec}}, \mathrm{wt}_{\boldsymbol{\theta}}^{\mathrm{elec}})$ (resp., $(G^{\mathrm{Ising}}, \mathrm{wt}_{\boldsymbol{\theta}}^{\mathrm{Ising}})$) with strand permutation f_τ^{elec} (resp., f_τ^{Ising}) satisfying $\mathrm{Meas}_{G^{\mathrm{elec}}}(\mathrm{wt}_{\boldsymbol{\theta}}^{\mathrm{elec}}) = \phi^{\mathrm{elec}}(\Lambda_{\mathrm{elec}}^R)$ (resp., $\mathrm{Meas}_{G^{\mathrm{Ising}}}(\mathrm{wt}_{\boldsymbol{\theta}}^{\mathrm{Ising}}) = \phi^{\mathrm{Ising}}(M_{\mathrm{Ising}}^R)$).

To define G^{elec}, we recall from [Lam18] the *generalized Temperley trick* of [KPW00]. Place $4n$ points

$$b_1^- = d_1^+, b_1, b_1^+ = d_2^-, d_2, b_2^- = d_2^+, b_2, \ldots, b_n, b_n^+ = d_1^-$$

on the circle in clockwise order. For each $p \in [n]$, connect d_p to $d_{\tau(p)}$ by a pseudoline as in Figure 19(left). We get a τ-pseudoline arrangement $\mathcal{A}$. Place a black interior vertex on every crossing of two pseudolines and a white interior vertex in every face of $\mathcal{A}$. Here by a *face* we mean a connected component of the complement of $\mathcal{A}$ in the disk. These are the black and white interior vertices of the graph G^{elec}, which also has n black boundary vertices $b_1, b_2, \ldots, b_n$. Each interior black vertex v of G^{elec} is an intersection point of two pseudolines and therefore is adjacent to four faces of $\mathcal{A}$. Connect v to the corresponding four white interior vertices of G^{elec}. In addition, observe that each boundary vertex b_p is adjacent to a single face of $\mathcal{A}$, so we connect b_p by an edge to the corresponding white vertex of G^{elec}. We have described the vertices and the edges of G^{elec}. To describe $\mathrm{wt}_{\boldsymbol{\theta}}^{\mathrm{elec}}$, color the faces of $\mathcal{A}$ black and white in a bipartite way so that for each $r \in [n]$, the face containing b_r is colored black if and only if r is odd. Then for each interior edge e of G^{elec}, we set $\mathrm{wt}_{\boldsymbol{\theta}}^{\mathrm{elec}}(e) := 1$ if e is contained in a white face of $\mathcal{A}$ and $\mathrm{wt}_{\boldsymbol{\theta}}^{\mathrm{elec}}(e) := \sin(\theta_q - \theta_p)$ if e is labeled by $\{p, q\}$ (as in Section 1.2) for $1 \leqslant p < q \leqslant n$ and is contained in a black face of $\mathcal{A}$. See Figure 19(right). Consider a black interior vertex v of G^{elec} corresponding to an intersection of two pseudolines connecting τ-pairs $\{p, q\}$ and $\{p', q'\}$ with $1 \leqslant p < p' < q < q' \leqslant n$. Then v has degree 4 in G^{elec} and is incident to edges of weights either $(1, \sin(\theta_{q'} - \theta_q), 1, \sin(\theta_{p'} - \theta_p))$ or $(1, \sin(\theta_{q'} - \theta_p), 1, \sin(\theta_q - \theta_{p'}))$ in clockwise order. Since $\boldsymbol{\theta}$ is τ-admissible, we have $\sin(\theta_{q'} - \theta_q) = \sin(\theta_{p'} - \theta_p)$ and $\sin(\theta_{q'} - \theta_p) = \sin(\theta_q - \theta_{p'})$. Therefore these edge weights coincide with (the dual version of) the edge weights in [Lam18, Section 5.1]. On the other hand, we clearly have $\mathrm{wt}_{\boldsymbol{\theta}}^{\mathrm{elec}}(e) = \mathrm{wt}_{\boldsymbol{\theta}}(e)$ for all edges e of G^{elec}. We have shown the result for electrical networks.

Similarly, for the Ising model, the edge weights $\mathrm{wt}_{\boldsymbol{\theta}}^{\mathrm{Ising}}$ of the graph G^{Ising} studied in [Dub11, GP20] are easily seen to coincide with $\mathrm{wt}_{\boldsymbol{\theta}}$. We refer to [GP20, Gal20] for further details. □

7.4. **Cyclically symmetric case.** Recall from Section 1.7 that for each $k \leqslant n$, there exists a unique point $X_0^{(k,n)} \in \mathrm{Gr}_{\geqslant 0}(k, n)$ that is invariant under the cyclic shift: $S(X_0^{(k,n)}) = X_0^{(k,n)}$.

In other words, the point $X_0^{(k,n)}$ is characterized by the property that its Plücker coordinates are all positive and satisfy $\Delta_I(X_0^{(k,n)}) = \Delta_{\sigma I}(X_0^{(k,n)})$ for all $I \in \binom{[n]}{k}$. Recall also that we set $\boldsymbol{\theta}^{\mathrm{reg}} = (\theta_1, \theta_2, \ldots, \theta_n)$ to be given by $\theta_r := \frac{r\pi}{n}$ for all $r \in [n]$.

Proposition 7.4. *For all $k \in [n]$, we have*

$$\mathrm{Meas}_{k,n}(\boldsymbol{\theta}^{\mathrm{reg}}) = X_0^{(k,n)}.$$

Proof. Choose a graph $G \in \mathcal{G}_{\mathrm{red}}(f_{k,n})$, then $\mathrm{Meas}_{k,n}(\boldsymbol{\theta}^{\mathrm{reg}}) = \mathrm{Meas}_G(\mathrm{wt}_{\boldsymbol{\theta}^{\mathrm{reg}}})$. Now let G' be obtained from G by cyclically relabeling the boundary vertices. Since $G' \in \mathcal{G}_{\mathrm{red}}(f_{k,n})$, it follows that $S(\mathrm{Meas}_{k,n}(\boldsymbol{\theta}^{\mathrm{reg}})) = \mathrm{Meas}_{k,n}(\boldsymbol{\theta}^{\mathrm{reg}})$. Since $\mathrm{Meas}_{k,n}(\boldsymbol{\theta}^{\mathrm{reg}}) \in \mathrm{Gr}_{\geqslant 0}(k,n)$, the result follows. □

The above observation can be applied to deduce new simple formulas for electrical networks and the Ising model.

Recall that the boundary correlations $\langle \sigma_p \sigma_q \rangle_{\mathbb{T}}$ of the critical Ising model do not depend on the choice of a rhombus tiling $\mathbb{T}$ of a region R and may thus be denoted by $\langle \sigma_p \sigma_q \rangle_R$. Let R_N be a regular $2N$-gon.

Theorem 7.5 ([Gal20, Theorem 1.1])**.** *For $1 \leqslant p, q \leqslant N$ and $d := |p-q|$, we have*

$$\langle \sigma_p \sigma_q \rangle_{R_N} = \frac{2}{N} \left(\frac{1}{\sin\left((2d-1)\pi/2N\right)} - \frac{1}{\sin\left((2d-3)\pi/2N\right)} + \cdots \pm \frac{1}{\sin\left(\pi/2N\right)} \right) \mp 1.$$

Below we prove the analog of this result for electrical networks.

Theorem 7.6. *For $1 \leqslant p, q \leqslant N$ and $d := |p-q|$, we have*

$$\Lambda_{p,q}^{R_N} = \frac{\sin(\pi/N)}{N \cdot \sin((2d-1)\pi/2N) \cdot \sin((2d+1)\pi/2N)}. \tag{7.3}$$

Proof. We sketch the argument; the details may be found in [Gal20, Section 5.2]. Rather than working with dual version of Lam's embedding, we will work with the original embedding $\mathrm{alt}^{\perp} \circ \phi^{\mathrm{elec}}$ of the space of $N \times N$ response matrices into $\mathrm{Gr}_{\geqslant 0}(N-1, 2N)$. It sends a response matrix $\Lambda_{\mathrm{elec}}^R$ to the unique element $X \in \mathrm{Gr}(N-1, 2N)$ whose Plücker coordinates satisfy

$$\Delta_{[n]_{\mathrm{even}} \setminus \{2p\}}(X) = 1 \quad \text{and} \quad \Delta_{[n]_{\mathrm{even}} \setminus \{2p-2, 2p\} \cup \{2q-1\}}(X) = \Lambda_{p,q}^R \quad \text{for all } p \neq q \in [N]. \tag{7.4}$$

This description is obtained from (7.1) by applying (3.5). In fact, we also have

$$\Delta_{[n]_{\mathrm{even}} \setminus \{2p-2, 2p\} \cup \{2p-1\}}(X) = -\Lambda_{p,p}^R \quad \text{for all } p \in [N]. \tag{7.5}$$

Our goal is to determine $\Lambda_{p,q}^{R_N}$, where R_N is a regular $2N$-gon. By Proposition 7.4 and Theorem 7.3, we see that $\phi^{\mathrm{elec}}(\Lambda_{\mathrm{elec}}^{R_N}) = X_0^{(N+1,2N)}$ and thus $\mathrm{alt}^{\perp} \circ \phi^{\mathrm{elec}}(\Lambda_{\mathrm{elec}}^{R_N}) = X_0^{(N-1,2N)}$. Let $\zeta := \exp(i\pi/2N)$ and

$$z_p := \zeta^{-N+2p} \quad \text{for } p \in [N-1].$$

Then $X := X_0^{(N-1,2N)}$ is the row span of an $(N-1) \times 2N$ Vandermonde matrix

$$A := \begin{pmatrix} 1 & z_1 & z_1^2 & \ldots & z_1^{2N-1} \\ 1 & z_2 & z_2^2 & \ldots & z_2^{2N-1} \\ \vdots & \vdots & \vdots & \ddots & \vdots \\ 1 & z_{N-1} & z_{N-1}^2 & \ldots & z_{N-1}^{2N-1} \end{pmatrix}.$$

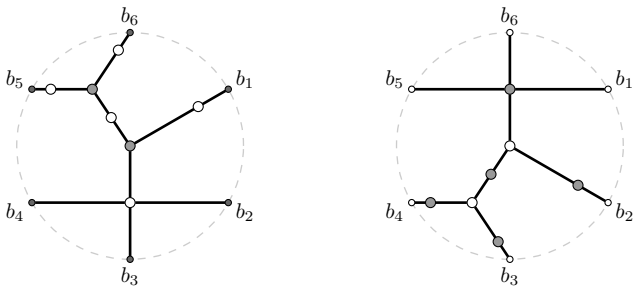

$G \in \mathcal{G}^{\blacktriangleright}_{\mathrm{red}}(f)$ $\qquad$ $G \in \mathcal{G}^{\triangleright}_{\mathrm{red}}(f)$

FIGURE 20. A black-trivalent and a white-trivalent graph.

Let K be a $2N \times (N-1)$ matrix such that $K_{p,q} = 1$ if $p = 2q$ and $K_{p,q} = 0$ otherwise. Thus AK is the submatrix of A with columns $2, 4, \ldots, 2N-2$, and by (7.4), we see that AK is invertible. Moreover, AK is very close to a discrete Fourier transform matrix (which is unitary), so the inverse of AK is easy to compute. We will only be interested in the last row of $(AK)^{-1}$, which is given by

$$((AK)^{-1})_{N-1,p} = (-1)^N \frac{z_p(1+z_p^2)}{N} \quad \text{for all } p \in [N-1]. \tag{7.6}$$

Let us now consider the matrix $M := (AK)^{-1}A$ and denote its entries by $M = (m_{p,q})$. The submatrix of M with columns $2, 4, \ldots, 2N-2$ is the identity matrix. It follows from (7.4)–(7.5) that

$$\Lambda^{R_N}_{p,1} = (-1)^p m_{N-1,2N-2p+1} \quad \text{for all } p \in [N]. \tag{7.7}$$

By (7.6), we have

$$m_{N-1,q} = \frac{(-1)^N}{N} \sum_{p=1}^{N-1} z_p^{q+1}(1+z_p^2) \quad \text{for all } q \in [2N].$$

Summing the two geometric progressions and applying (7.7), we obtain the formula (7.3) for $\Lambda^{R_N}_{p,1}$ for all $p \in [N]$. The formula for arbitrary $\Lambda^{R_N}_{p,q}$ then follows from the compatibility of all constructions with the cyclic symmetry of $\mathrm{Gr}_{\geqslant 0}(N-1, 2N)$. □

8. Shift by 1

Recall from Section 1.8 that for a loopless bounded affine permutation $f \in \mathcal{B}(k,n)$, we let $f^{\downarrow} \in \mathcal{B}(k-1,n)$ be defined by $f^{\downarrow}(p) := f(p-1)$ for all $p \in \mathbb{Z}$. The goal of this section is to relate $\mathrm{Crit}^{>0}_f$ to $\widehat{\mathrm{Crit}}^{>0}_{f^{\downarrow}}$ and $\Pi^{>0}_f$ to $\Pi^{>0}_{f^{\downarrow}}$.

8.1. **Shift for reduced graphs.** The following two classes of reduced graphs were introduced (for the case $f = f_{k,n}$) in [GPW19, Section 7.7].

Definition 8.1. A reduced graph is called *black-trivalent* if it has black boundary and all of its interior black vertices are trivalent. Similarly, a reduced graph is called *white-trivalent* if it has white boundary and all of its interior white vertices are trivalent.

See Figure 20 for an example.

Remark 8.2. Unlike [GPW19], we continue to require all reduced graphs to be bipartite. Thus our white-trivalent graphs are obtained from the *black-partite* graphs of [GPW19, Definition 7.14] by placing a degree 2 black vertex in the middle of each edge connecting two trivalent white vertices.

Denote

$$\mathcal{G}^{\blacktriangleright}_{\mathrm{red}}(f) := \{G \in \mathcal{G}_{\mathrm{red}}(f) \mid G \text{ is black-trivalent}\},$$
$$\mathcal{G}^{\triangleright}_{\mathrm{red}}(f) := \{G \in \mathcal{G}_{\mathrm{red}}(f) \mid G \text{ is white-trivalent}\}.$$

Recall from Section 2.2 that we label the faces of a reduced graph G by k-element sets. The following result generalizes [GPW19, Proposition 7.15].

Proposition 8.3. *Let $f \in \mathcal{B}(k,n)$ be loopless. Then there is a bijection*

$$\mathcal{G}^{\blacktriangleright}_{\mathrm{red}}(f) \to \mathcal{G}^{\triangleright}_{\mathrm{red}}(f^{\downarrow}), \quad G \mapsto G^{\downarrow},$$

characterized by the following property: for any trivalent black vertex of G with adjacent faces labeled by Sab, Sac, Sbc, the graph $G^{\downarrow}$ contains a trivalent white vertex with adjacent faces labeled Sa, Sb, Sc.

Here we abbreviate $Sab := S \sqcup \{a,b\}$, etc. See Figure 21 for an example.

Remark 8.4. The bijection $G \mapsto G^{\downarrow}$ was independently considered in [PSBW21, Section 8.2], where it is described using the planar dual of G.

Proof. We assume familiarity with the results of [OPS15, Gal18]. Let us denote by $\mathcal{F}(G) \subset \binom{[n]}{k}$ the collection of face labels of G. We say that two sets $S, T \subset [n]$ (not necessarily of the same size) are *chord separated* if there do not exist indices $1 \leqslant a < b < c < d \leqslant n$ such that $a, c \in S \setminus T$ and $b, d \in T \setminus S$ or vice versa. By the results of [OPS15], the collection $\mathcal{F}(G)$ is chord separated and there exists $G_{k,n} \in \mathcal{G}_{\mathrm{red}}(f_{k,n})$ such that $\mathcal{F}(G) \subset \mathcal{F}(G_{k,n})$. The planar dual of G is a certain polygonal complex called a *plabic tiling* and denoted $\Sigma_k(G)$. Each face of $\Sigma_k(G)$ is a convex polygon whose vertices are labeled by the elements of $\mathcal{F}(G)$. Whenever G has a degree 2 white vertex, $\Sigma_k(G)$ contains a degenerate white 2-gon of width zero as in Figure 21. Since G is black-trivalent, each black face of $\Sigma_k(G)$ is triangulated (with diagonals replaced with zero-width 2-gons). The plabic tiling $\Sigma_k(G)$ is a subcomplex of a larger plabic tiling $\Sigma_k(G_{k,n})$. Specifically, $\Sigma_k(G)$ consists of all faces of $\Sigma_k(G_{k,n})$ which lie inside a polygonal curve passing through the Grassmann necklace of f; see [OPS15, Proposition 9.8].[8] We call this curve the *Grassmann necklace curve of f*.

We triangulate the remaining black and white faces of $\Sigma_k(G)$, after which it becomes a *triangulated plabic tiling* in the language of [Gal18]. By [Gal18, Remark 1.5], any triangulated plabic tiling appears as a horizontal section Σ_k by the plane $z = k$ of some fine zonotopal tiling Σ of a cyclic polytope in $\mathbb{R}^3$. Let Σ_{k-1} be the horizontal section of Σ by the plane $z = k-1$. Then its planar dual is a graph $G_{k-1,n} \in \mathcal{G}_{\mathrm{red}}(f_{k-1,n})$. Moreover, the face labels of $G_{k-1,n}$ contain the Grassmann necklace of $f^{\downarrow}$, which consists of the sets $(J_2, J_3, \ldots, J_n, J_1)$ where $J_p = I_p \setminus p = I_p \cap I_{p+1}$ as above and $(I_1, I_2, \ldots, I_n) = \mathcal{I}_f$ is the Grassmann necklace of f. The reason this is true is that by construction, $\Sigma_k(G)$ contains an edge connecting I_p to I_{p+1} for all $p \in [n]$ (indices taken modulo n). When $I_p \neq I_{p+1}$, Σ contains a 2-dimensional

[8] In order to invoke [OPS15, Proposition 9.8], one needs to assume that the Grassmann necklace of f is connected. However, even when it is not connected, the Grassmann necklace curve may be deformed slightly into a simple closed curve surrounding $\Sigma_k(G)$; see the discussion around [BW20, Definition 4.4].

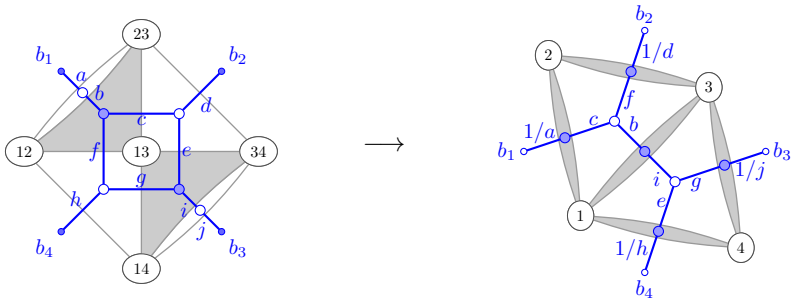

FIGURE 21. The bijection $(G, \mathrm{wt}) \mapsto (G^\downarrow, \mathrm{wt}^\downarrow)$, where $G \in \mathcal{G}^{\triangleright}_{\mathrm{red}}(f)$ and $G^\downarrow \in \mathcal{G}^{\triangleright}_{\mathrm{red}}(f^\downarrow)$ for $f = f_{2,4}$. See Proposition 8.3 and (8.1). The triangulated plabic tilings $\Sigma_k(G)$ and $\Sigma_{k-1}(G^\downarrow)$ are shown in grey.

face with vertices labeled $J_p, I_p, I_{p+1}, I_p \cup I_{p+1}$. When $J_p \neq J_{p+1}$, Σ contains a 2-dimensional face with vertices labeled $J_p \cap J_{p+1}, J_p, J_{p+1}, I_{p+1}$. It follows that Σ contains a 2-dimensional subcomplex C whose intersection with the plane $z = k$ is the Grassmann necklace curve of f and whose intersection with the plane $z = k-1$ is the Grassmann necklace curve of $f^\downarrow$. Let $G^\downarrow$ be the planar dual of the subcomplex $\Sigma_{k-1}(G^\downarrow)$ of Σ_{k-1} contained inside the Grassmann necklace curve of $f^\downarrow$.

Consider a black trivalent vertex of G with adjacent faces labeled by Sab, Sac, Sbc. Then $\Sigma_k(G)$ contains a black triangle with vertices labeled Sab, Sac, Sbc, thus Σ_{k-1} contains a white triangle with vertices labeled Sa, Sb, Sc. Moreover, Σ contains a cube with vertices labeled $S, Sa, Sb, Sc, Sab, Sac, Sbc, Sabc$. Since the triangle Sab, Sac, Sbc lies inside the Grassmann necklace curve of $f^\downarrow$, and since the cube cannot intersect C transversally, we see that the triangle Sa, Sb, Sc lies inside the Grassmann necklace curve of $f^\downarrow$. Thus $\mathcal{F}(G^\downarrow)$ is a chord separated collection all of whose elements belong to $\mathcal{M}_{f^\downarrow}$. Using Euler's formula, one can check that it is in fact maximal by size; cf. the proof of [Gal18, Lemma 4.2]. By the results of [OPS15], $G^\downarrow$ must belong to $\mathcal{G}_{\mathrm{red}}(f^\downarrow)$. It remains to note that by construction, the white faces of the plabic tiling $\Sigma_{k-1}(G^\downarrow)$ are triangulated, and therefore $G^\downarrow \in \mathcal{G}^{\triangleright}_{\mathrm{red}}(f^\downarrow)$. □

8.2. **Shift for positroid cells.** We extend the above bijection $G \mapsto G^\downarrow$ to a bijection $(G, \mathrm{wt}) \mapsto (G^\downarrow, \mathrm{wt}^\downarrow)$ on weighted reduced graphs. Let $G \in \mathcal{G}^{\triangleright}_{\mathrm{red}}(f)$ and $G^\downarrow \in \mathcal{G}^{\triangleright}_{\mathrm{red}}(f^\downarrow)$ be as above. Denote $E := E(G)$ and $E^\downarrow := E(G^\downarrow)$. Choose a weight function $\mathrm{wt} : E(G) \to \mathbb{R}_{>0}$. Consider an interior edge $e \in E$. Exactly one of its endpoints is a black trivalent vertex $v \in V(G)$. Assume that the faces adjacent to v are labeled by Sab, Sac, Sbc, with the faces adjacent to e being labeled by Sab and Sac. Then the edge e is labeled by $\{b, c\}$. Let $v^\downarrow \in V(G^\downarrow)$ be the trivalent white vertex corresponding to v as in Proposition 8.3. The faces adjacent to $v^\downarrow$ are labeled by Sa, Sb, Sc, and we let $e^\downarrow \in E^\downarrow$ be the edge adjacent to the faces labeled Sb and Sc. In particular, the edge $e^\downarrow$ is also labeled by $\{b, c\}$. We set $\mathrm{wt}^\downarrow(e^\downarrow) := \mathrm{wt}(e)$. It remains to extend this construction to the boundary edges. Let e_p be the boundary edge of G adjacent to b_p for $p \in [n]$. Let $e_p^\downarrow \in E^\downarrow$ be the edge adjacent to b_p in $G^\downarrow$. We set $\mathrm{wt}^\downarrow(e_p^\downarrow) := \frac{1}{\mathrm{wt}(e_p)}$. We have described the bijection $(G, \mathrm{wt}) \mapsto (G^\downarrow, \mathrm{wt}^\downarrow)$, and along the way we have also constructed a bijection $E \to E^\downarrow$ sending $e \mapsto e^\downarrow$. See Figure 21 for an example.

Recall from Section 2.4 that the boundary measurement map yields a homeomorphism $\mathrm{Meas}_G : \mathbb{R}_{>0}^E/\operatorname{Gauge} \xrightarrow{\sim} \Pi_f^{>0}$. Instead of considering gauge transformations at all vertices of G, let us denote by $\mathbb{R}_{>0}^E/\operatorname{Gauge}^{\blacktriangleright}$ the space of positive edge weight functions on G modulo gauge transformations at trivalent black vertices. Similarly, $\mathbb{R}_{>0}^{E^\downarrow}/\operatorname{Gauge}^{\triangleright}$ is defined as the space of positive edge weight functions on $G^\downarrow$ modulo gauge transformations at trivalent white vertices. For a black trivalent vertex v of G, gauge transformations of (G, wt) at v correspond to gauge transformations of $(G^\downarrow, \mathrm{wt}^\downarrow)$ at $v^\downarrow$. We obtain a natural homeomorphism

$$\mathbb{R}_{>0}^E/\operatorname{Gauge}^{\blacktriangleright} \xrightarrow{\sim} \mathbb{R}_{>0}^{E^\downarrow}/\operatorname{Gauge}^{\triangleright}, \quad \mathrm{wt} \mapsto \mathrm{wt}^\downarrow. \tag{8.1}$$

We will see later (Figure 23) that any two graphs $G_1, G_2 \in \mathcal{G}_{\mathrm{red}}^{\blacktriangleright}(f)$ are related by certain kinds of *moves*, and that these moves preserve the space $\mathbb{R}_{>0}^E/\operatorname{Gauge}^{\blacktriangleright}$ and commute with the shift map (8.1). As a result, we will show (Remark 8.8) that both sides of (8.1) depend only on f and not on the choice of G. We thus denote

$$\Pi_{f,f^\downarrow}^{>0} := \mathbb{R}_{>0}^E/\operatorname{Gauge}^{\blacktriangleright} \cong \mathbb{R}_{>0}^{E^\downarrow}/\operatorname{Gauge}^{\triangleright},$$

keeping in mind that until Remark 8.8 is shown, this space also depends on the choice of G.

Recall that Meas_G yields a homeomorphism $\mathbb{R}_{>0}^E/\operatorname{Gauge} \xrightarrow{\sim} \Pi_f^{>0}$, while $\mathrm{Meas}_{G^\downarrow}$ yields a homeomorphism $\mathbb{R}_{>0}^{E^\downarrow}/\operatorname{Gauge} \xrightarrow{\sim} \Pi_{f^\downarrow}^{>0}$. For the next result, we consider Meas_G and $\mathrm{Meas}_{G^\downarrow}$ to be defined on $\mathbb{R}_{>0}^E/\operatorname{Gauge}^{\blacktriangleright}$ and $\mathbb{R}_{>0}^{E^\downarrow}/\operatorname{Gauge}^{\triangleright}$, respectively.

Proposition 8.5. *For any loopless $f \in \mathcal{B}(k,n)$ and $G \in \mathcal{G}_{\mathrm{red}}^{\blacktriangleright}(f)$, we have a homeomorphism*

$$(\mathrm{Meas}_G, \mathrm{Meas}_{G^\downarrow}) : \Pi_{f,f^\downarrow}^{>0} \xrightarrow{\sim} \Pi_f^{>0} \times \Pi_{f^\downarrow}^{>0}. \tag{8.2}$$

Proof. Consider the group $\mathbb{R}_{>0}^{V_\circ(G)}$ of gauge transformations at white interior vertices of G. Thus two elements $\mathrm{wt}_1, \mathrm{wt}_2 \in \mathbb{R}_{>0}^E/\operatorname{Gauge}^{\blacktriangleright}$ satisfy $\mathrm{Meas}_G(\mathrm{wt}_1) = \mathrm{Meas}_G(\mathrm{wt}_2)$ if and only if they are related by the action of $\mathbb{R}_{>0}^{V_\circ(G)}$. Rescaling all edge weights by the same constant clearly yields the same element of $\mathbb{R}_{>0}^E/\operatorname{Gauge}^{\blacktriangleright}$, and the quotient group $\mathbb{R}_{>0}^{V_\circ(G)}/\mathbb{R}_{>0}$ acts simply transitively on the preimage of any point under the surjective map $\mathrm{Meas}_G : \mathbb{R}_{>0}^E/\operatorname{Gauge}^{\blacktriangleright} \to \Pi_f^{>0}$.

Let us now transfer this action via (8.1) into the action of $\mathbb{R}_{>0}^{V_\circ(G)}$ on $\mathbb{R}_{>0}^{E^\downarrow}/\operatorname{Gauge}^{\triangleright}$. It follows from the proof of Proposition 8.3 that the white vertices of G are in bijection with the faces of $G^\downarrow$. Namely, for a white vertex $w \in V_\circ(G)$ of G, let $S_1, S_2, \ldots, S_m$ be the labels of the faces adjacent to w, then $S_1 \cap S_2 \cap \cdots \cap S_m$ is a face label $\lambda(F) \in \mathcal{F}(G^\downarrow)$ of some face F of $G^\downarrow$. See also the proof of [Gal18, Lemma 4.2]. Suppose that $\mathrm{wt}_1, \mathrm{wt}_2 \in \mathbb{R}_{>0}^E/\operatorname{Gauge}^{\blacktriangleright}$ are related via a gauge transformation at w:

$$\mathrm{wt}_2(e) := \begin{cases} t\,\mathrm{wt}_1(e), & \text{if } e \text{ is incident to } w; \\ \mathrm{wt}_1(e), & \text{otherwise} \end{cases}$$

for some $t \in \mathbb{R}_{>0}$. Let $X_1 := \mathrm{Meas}_{G^\downarrow}(\mathrm{wt}_1^\downarrow)$ and $X_2 := \mathrm{Meas}_{G^\downarrow}(\mathrm{wt}_2^\downarrow)$. We claim that the twisted minors (cf. Section 5.4) of X_1 and X_2 are related as follows: for each $I \in \mathcal{F}(G^\downarrow)$, we have

$$\Delta_I(\overline{\tau}(X_2)) = \begin{cases} t\Delta_I(\overline{\tau}(X_1)), & \text{if } I = \lambda(F), \\ \Delta_I(\overline{\tau}(X_1)), & \text{otherwise.} \end{cases} \tag{8.3}$$

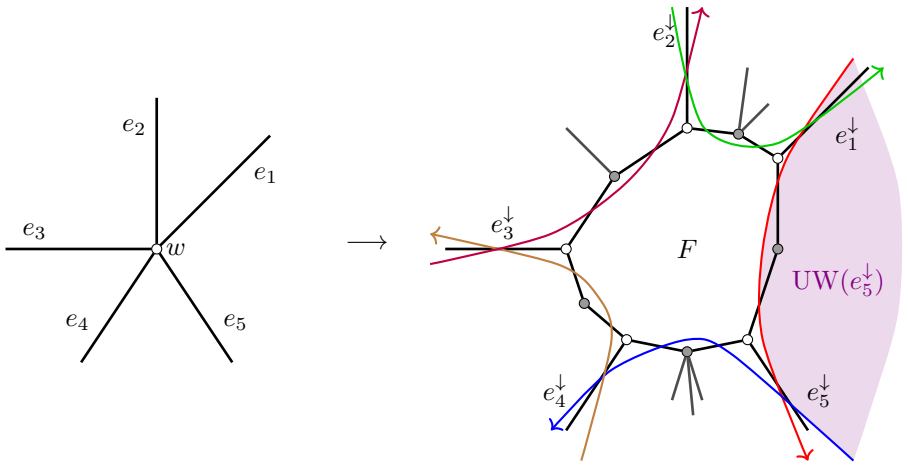

FIGURE 22. A white vertex w of G corresponding to a face F of $G^\downarrow$. The upstream wedges of $e_1^\downarrow, e_2^\downarrow, e_3^\downarrow, e_4^\downarrow, e_5^\downarrow$ cover all faces of $G^\downarrow$ except for F.

To prove (8.3), suppose that w is incident to $e_1, e_2, \dots, e_r \in E$ and let $e_1^\downarrow, e_2^\downarrow, \dots, e_r^\downarrow \in E^\downarrow$ be the corresponding edges of $G^\downarrow$. First, assume that none of $e_1, e_2, \dots, e_r$ are boundary edges. It is then easy to check that

$$\overleftarrow{M}(F) \cap \{e_1^\downarrow, e_2^\downarrow, \dots, e_r^\downarrow\} = \emptyset \quad \text{and} \quad |\overleftarrow{M}(F') \cap \{e_1^\downarrow, e_2^\downarrow, \dots, e_r^\downarrow\}| = 1 \tag{8.4}$$

for each face $F' \neq F$ of $G^\downarrow$. Indeed, the tails of any two intersecting strands cannot intersect in a reduced graph, thus the upstream wedges of $e_1^\downarrow, e_2^\downarrow, \dots, e_r^\downarrow$ partition the set of faces of $G^\downarrow$ not equal to F; see Figure 22.

Assume now that we have a partition $\{e_1^\downarrow, e_2^\downarrow, \dots, e_r^\downarrow\} = A \sqcup B$ where A consists of interior edges and B consists of boundary edges. Then (8.4) no longer holds, but instead we have

$$(\overleftarrow{M}(F) \cap A) \triangle B = \emptyset \quad \text{and} \quad |(\overleftarrow{M}(F') \cap A) \triangle B| = 1$$

for all $F' \neq F$, where $\triangle$ denotes symmetric difference. (By definition, the *upstream wedge* of a boundary edge e adjacent to b_p consists of all faces to the right of the strand terminating at b_p.) Since the weights of boundary edges are inverted in the definition of $\mathrm{wt}^\downarrow$, and since the twisted minor $\Delta_I(\overline{\tau}(X_2))$ for $I := \lambda(F')$ equals the product of the edge weights $\mathrm{wt}_2^\downarrow(e)$ over $e \in \overleftarrow{M}(F')$, (8.3) follows.

We have shown that the $\mathbb{R}_{>0}^{V_\circ(G)}$-action on $\mathbb{R}_{>0}^E/\operatorname{Gauge}$ translates into the action of the group $\mathbb{R}_{>0}^{\mathcal{F}(G^\downarrow)}$ on $\Pi_{f^\downarrow}^{>0}$ by rescaling the twisted minors associated to the face labels of $G^\downarrow$. Rescaling all edges by the same constant transforms into rescaling all twisted minors by the same constant, and thus the $\mathbb{R}_{>0}^{V_\circ(G)}/\mathbb{R}_{>0}$-action on $\mathbb{R}_{>0}^E/\operatorname{Gauge}$ translates into the $\mathbb{R}_{>0}^{\mathcal{F}(G^\downarrow)}/\mathbb{R}_{>0}$-action on $\Pi_{f^\downarrow}^{>0}$. The latter action is well known [MuSp17] to be simply transitive.

Let us go back to studying the map $(\mathrm{Meas}_G, \mathrm{Meas}_{G^\downarrow})$ in (8.2). First, observe that this map is bijective. Indeed, $\mathbb{R}_{>0}^{\mathcal{F}(G^\downarrow)}/\mathbb{R}_{>0}$ acts simply transitively on the preimages of points under Meas_G while at the same time it acts simply transitively on the image of $\mathrm{Meas}_{G^\downarrow}$, since it is identified under (8.1) with the action of $\mathbb{R}_{>0}^{\mathcal{F}(G^\downarrow)}/\mathbb{R}_{>0}$ on the twisted minors. Second, the map is clearly continuous, and since $\Pi_{f,f^\downarrow}^{>0}$ and $\Pi_f^{>0} \times \Pi_{f^\downarrow}^{>0}$ are both homeomorphic to open balls

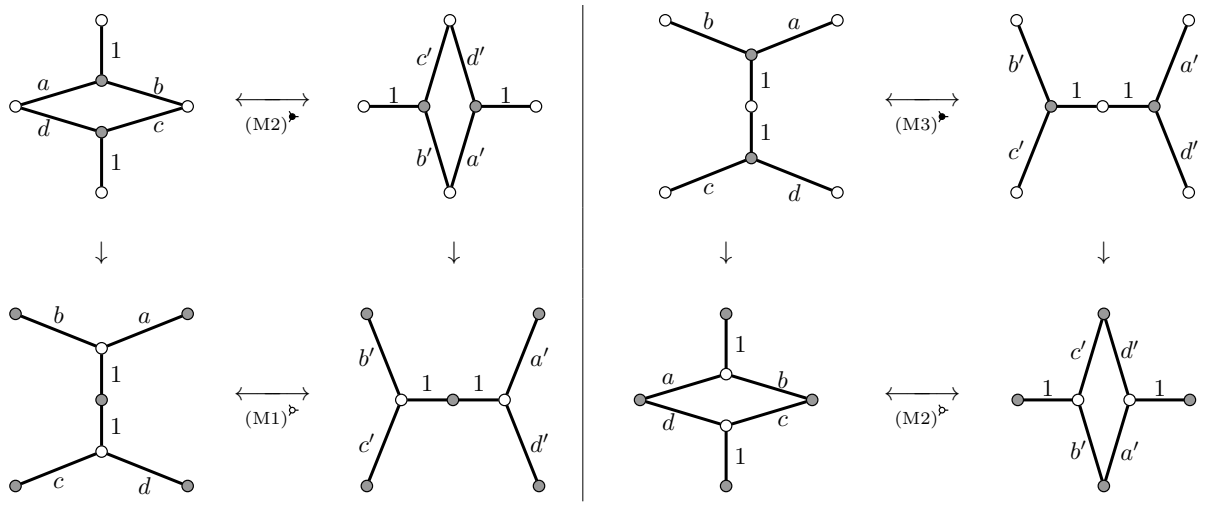

FIGURE 23. The moves for white- and black-trivalent graphs. The vertical maps are given by $(G, \mathrm{wt}) \mapsto (G^{\downarrow}, \mathrm{wt}^{\downarrow})$. Here $a' := \frac{a}{ac+bd}$, etc. as in Figure 6.

of the same dimension, the map $(\mathrm{Meas}_G, \mathrm{Meas}_{G^{\downarrow}})$ is a homeomorphism by the invariance of domain theorem. □

Example 8.6. Let $f = f_{2,4}$, thus $f^{\downarrow} = f_{1,4}$ as in Figure 21. The boundary measurements of $X := \mathrm{Meas}_{G^{\downarrow}}(\mathrm{wt}^{\downarrow})$ computed from Figure 21(right) are given by

$$\Delta_1(X) = \frac{ci}{djh}, \quad \Delta_2(X) = \frac{fi}{ajh}, \quad \Delta_3(X) = \frac{bg}{adh}, \quad \Delta_4(X) = \frac{be}{adj}.$$

(Recall that since the boundary vertices of the graph in Figure 21(right) are white, the boundary of an almost perfect matching $\mathcal{A}$ consists of the boundary vertices *not* used in $\mathcal{A}$.) By the definition of the twist map, the Plücker coordinates of $\overleftarrow{\tau}(X)$ are just the inverses of the Plücker coordinates of X: we have $\Delta_1(\overleftarrow{\tau}(X)) = \frac{djh}{ci}$, $\Delta_2(\overleftarrow{\tau}(X)) = \frac{ajh}{fi}$, etc. The graph G in Figure 21(left) has four white vertices, which are in bijection with the four faces of the graph $G^{\downarrow}$ in Figure 21(right). We see that applying a gauge transformation to all edges incident to a given white vertex of G corresponds to rescaling $\Delta_I(\overleftarrow{\tau}(X))$ by the same constant (where $I \in \binom{[4]}{1}$ labels the corresponding face) while leaving the other Plücker coordinates of $\overleftarrow{\tau}(X)$ unchanged. For example, multiplying a and b by t corresponds to dividing $\Delta_2(X)$ by t and preserving $\Delta_1(X), \Delta_3(X), \Delta_4(X)$. This corresponds to multiplying $\Delta_2(\overleftarrow{\tau}(X))$ by t. Similarly, multiplying each of f, g, h by t corresponds to multiplying $\Delta_1(\overleftarrow{\tau}(X))$ by t. This agrees with (8.3).

8.3. **Moves.** Next, we introduce moves for weighted white- and black-trivalent graphs, as shown in Figure 23. Here we have used the allowed gauge transformations at black (resp., white) trivalent vertices to make the weights of certain edges to be equal to 1. It follows from the results of [Pos06] that for any $G_1, G_2 \in \mathcal{G}^{\blacktriangleright}_{\mathrm{red}}(f)$, G_1 and G_2 are connected by moves[9] $(\mathrm{M2})^{\blacktriangleright}$ and $(\mathrm{M3})^{\blacktriangleright}$, and $G_1^{\downarrow}$ and $G_2^{\downarrow}$ are connected by moves $(\mathrm{M1})^{\triangleright}$ and $(\mathrm{M2})^{\triangleright}$. Moreover, we

[9]The names (M1), (M2), (M3) for the moves in Figure 23 are taken from [Gal18]: these moves are obtained from a single transformation of 3-dimensional zonotopal tilings by taking horizontal sections by planes $z = k$ for $k = 1, 2, 3$, respectively; see [Gal18, Figure 8].

see from Figure 23 that the shift map (8.1) transforms $(\mathrm{M3})^{\blacktriangleright}$ into $(\mathrm{M2})^{\triangleright}$ and $(\mathrm{M2})^{\blacktriangleright}$ into $(\mathrm{M1})^{\triangleright}$. We therefore obtain the following consequence of Proposition 8.5.

Corollary 8.7. *Let $f \in \mathcal{B}(k,n)$ be loopless, and suppose that $G_1, G_2 \in \mathcal{G}^{\blacktriangleright}_{\mathrm{red}}(f)$ are related by either $(\mathrm{M2})^{\blacktriangleright}$ or $(\mathrm{M3})^{\blacktriangleright}$. Then we have commutative diagrams*

$$\begin{array}{ccc} \mathbb{R}^{E(G_1)}_{>0}/\operatorname{Gauge}^{\blacktriangleright} & \xrightarrow[(\mathrm{M2})^{\blacktriangleright}]{\sim} & \mathbb{R}^{E(G_2)}_{>0}/\operatorname{Gauge}^{\blacktriangleright} \\ \sim\downarrow & & \downarrow\sim \\ \Pi_f^{>0}\times\Pi_{f^\downarrow}^{>0} & \xrightarrow[\mathrm{id}]{\sim} & \Pi_f^{>0}\times\Pi_{f^\downarrow}^{>0} \\ \sim\uparrow & & \uparrow\sim \\ \mathbb{R}^{E(G_1^\downarrow)}_{>0}/\operatorname{Gauge}^{\blacktriangleright} & \xrightarrow[(\mathrm{M1})^{\blacktriangleright}]{\sim} & \mathbb{R}^{E(G_2^\downarrow)}_{>0}/\operatorname{Gauge}^{\blacktriangleright}, \end{array} \qquad \textit{resp.,} \qquad \begin{array}{ccc} \mathbb{R}^{E(G_1)}_{>0}/\operatorname{Gauge}^{\blacktriangleright} & \xrightarrow[(\mathrm{M3})^{\blacktriangleright}]{\sim} & \mathbb{R}^{E(G_2)}_{>0}/\operatorname{Gauge}^{\blacktriangleright} \\ \sim\downarrow & & \downarrow\sim \\ \Pi_f^{>0}\times\Pi_{f^\downarrow}^{>0} & \xrightarrow[\mathrm{id}]{\sim} & \Pi_f^{>0}\times\Pi_{f^\downarrow}^{>0} \\ \sim\uparrow & & \uparrow\sim \\ \mathbb{R}^{E(G_1^\downarrow)}_{>0}/\operatorname{Gauge}^{\blacktriangleright} & \xrightarrow[(\mathrm{M2})^{\blacktriangleright}]{\sim} & \mathbb{R}^{E(G_2^\downarrow)}_{>0}/\operatorname{Gauge}^{\blacktriangleright}, \end{array}$$

where all vertical maps are given by (8.2).

Remark 8.8. It follows that if a sequence of moves relates $G \in \mathcal{G}^{\blacktriangleright}_{\mathrm{red}}(f)$ to itself, the induced map $\mathbb{R}^{E(G)}_{>0}/\operatorname{Gauge}^{\blacktriangleright} \xrightarrow{\sim} \mathbb{R}^{E(G)}_{>0}/\operatorname{Gauge}^{\blacktriangleright}$ must be the identity map since after applying the homeomorphism (8.2), we get the identity map $\Pi_f^{>0}\times\Pi_{f^\downarrow}^{>0} \xrightarrow{\sim} \Pi_f^{>0}\times\Pi_{f^\downarrow}^{>0}$ by Corollary 8.7. This confirms that the space $\Pi_{f,f^\downarrow}^{>0}$ depends canonically only on f and not on the choice of $G \in \mathcal{G}^{\blacktriangleright}_{\mathrm{red}}(f)$.

8.4. **Shift for critical varieties.** Even though the above constructions follow naturally from the geometry of zonotopal tilings, we discovered them in relation to critical varieties, as we now explain. Let $f \in \mathcal{B}(k,n)$ be loopless. Observe first that $\boldsymbol{\theta} \in \mathbb{R}^n$ is f-admissible if and only if it is $f^\downarrow$-admissible, since the reduced strand diagram of f coincides with the dual reduced strand diagram of $f^\downarrow$; compare e.g. Figure 18(b) and Figure 18(d). Thus we have a homeomorphism $\Theta_f^{>0} \xrightarrow{\sim} \widehat{\Theta}_{f^\downarrow}^{>0}$ given by the identity map $\boldsymbol{\theta} \mapsto \boldsymbol{\theta}$.

Proposition 8.9. *For each loopless $f \in \mathcal{B}(k,n)$, we have the commutative diagram in Figure 24(a). Moreover, if the injectivity conjecture (Conjecture 4.3) holds for f, we have the commutative diagram in Figure 24(b), where the dashed arrow is the composition of the three homeomorphisms in the square on the left hand side.*

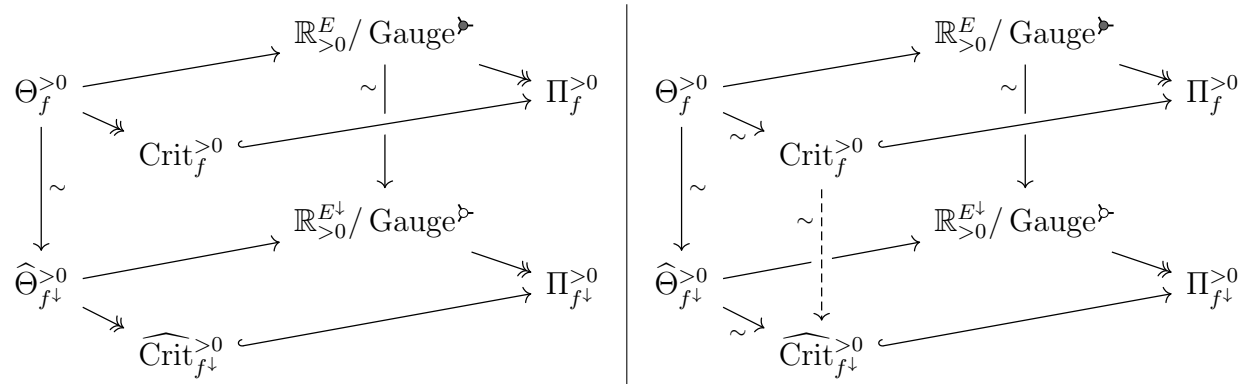

(a) arbitrary loopless $f \in \mathcal{B}(k,n)$ *(b) assuming the injectivity conjecture for f*

FIGURE 24. The shift map for critical varieties.

Note that $\Pi_f^{>0} \ncong \Pi_{f^\downarrow}^{>0}$ since these spaces usually have different dimension. Instead, they have the same *codimension* $\ell(f) = \ell(f^\downarrow)$ inside $\mathrm{Gr}(k,n)$, resp., $\mathrm{Gr}(k-1,n)$.

Remark 8.10. By Theorem 4.4, the dashed arrow in Figure 24(b) yields a homeomorphism

$$\mathrm{Crit}_{k,n}^{>0} \xrightarrow{\sim} \widehat{\mathrm{Crit}}_{k-1,n}^{>0}$$

for each $1 \leqslant k \leqslant n$.

Proof of Proposition 8.9. First, let us explain the maps in Figure 24. The map $\Theta_f^{>0} \xrightarrow{\sim} \widehat{\Theta}_{f^\downarrow}^{>0}$ is the identity, and $\Theta_f^{>0} \to \mathrm{Crit}_f^{>0}$ and $\widehat{\Theta}_{f^\downarrow}^{>0} \to \widehat{\mathrm{Crit}}_{f^\downarrow}^{>0}$ are given by Meas_f and $\widehat{\mathrm{Meas}}_{f^\downarrow}$, respectively. The maps $\mathrm{Crit}_f^{>0} \hookrightarrow \Pi_f^{>0}$ and $\widehat{\mathrm{Crit}}_f^{>0} \hookrightarrow \Pi_{f^\downarrow}^{>0}$ are inclusions of subsets, while $\Theta_f^{>0} \to \mathbb{R}_{>0}^E/\operatorname{Gauge}^\blacktriangleright$ and $\widehat{\Theta}_{f^\downarrow}^{>0} \to \mathbb{R}_{>0}^{E^\downarrow}/\operatorname{Gauge}^\triangleright$ are given by $\boldsymbol{\theta} \mapsto \mathrm{wt}_{\boldsymbol{\theta}}$, resp., $\boldsymbol{\theta} \mapsto \widehat{\mathrm{wt}}_{\boldsymbol{\theta}}$. We have already explained the dashed arrow in Figure 24(b), and the remaining map $\mathbb{R}_{>0}^E/\operatorname{Gauge}^\blacktriangleright \xrightarrow{\sim} \mathbb{R}_{>0}^{E^\downarrow}/\operatorname{Gauge}^\triangleright$ is given by (8.1).

The commutativity of the top and bottom squares is obvious. The commutativity of

$$\begin{array}{ccc} \Theta_f^{>0} & \longrightarrow & \mathbb{R}_{>0}^E/\operatorname{Gauge}^\blacktriangleright \\ \sim\downarrow & & \sim\downarrow \\ \widehat{\Theta}_f^{>0} & \longrightarrow & \mathbb{R}_{>0}^{E^\downarrow}/\operatorname{Gauge}^\triangleright \end{array}$$

follows from the observation in Section 8.2 that whenever an interior edge $e \in E$ is labeled by $\{p,q\}$, the edge $e^\downarrow \in E^\downarrow$ is also interior and labeled by $\{p,q\}$. The left square in Figure 24(b) commutes by construction. □

Question 8.11. Which of the above results extend to the complex algebraic setting (with Π_f° replacing $\Pi_f^{>0}$ and Crit_f° replacing $\mathrm{Crit}_f^{>0}$)?

9. Proofs of the results for the top cell

Our goal is to prove the injectivity conjecture (Theorem 4.4) and the description (Theorem 5.11) of the real points of an open critical variety in the case $f = f_{k,n}$. We start by stating several auxiliary lemmas.

Lemma 9.1. *Let $(t_1,t_2,t_3) \in (\mathbb{C}^*)^3$ be a generic triple.*

(i) *If $\frac{[\![t_2,t_1]\!]}{[\![t_3,t_1]\!]}, \frac{[\![t_3,t_2]\!]}{[\![t_3,t_1]\!]} \in \mathbb{R}$ then either $|t_1| = |t_2| = |t_3|$ or $\frac{t_1}{t_2}, \frac{t_2}{t_3} \in \mathbb{R}$.*

(ii) *If $\frac{[\![t_2,t_1]\!]}{[\![t_3,t_1]\!]}, \frac{[\![t_3,t_2]\!]}{[\![t_3,t_1]\!]} \in i\mathbb{R}$ then $\frac{t_1}{t_2}, \frac{t_2}{t_3} \in i\mathbb{R}$.*

Proof. Since $[\![t_q,t_p]\!]$ is invariant under rescaling t_p and t_q by the same nonzero constant, we may assume that $t_2 = 1$. In this case, the resulting systems of equations on the real and imaginary parts of t_1 and t_3 may be solved explicitly, and both statements are then verified directly in a straightforward fashion. □

Lemma 9.2. *Let $(t_1,t_2,t_3,t_4) \in (\mathbb{C}^*)^4$ be a generic quadruple satisfying*

$$\frac{[\![t_2,t_1]\!]}{[\![t_3,t_2]\!]}, \frac{[\![t_3,t_2]\!]}{[\![t_4,t_3]\!]}, \frac{[\![t_4,t_3]\!]}{[\![t_4,t_1]\!]}, \frac{[\![t_4,t_1]\!]}{[\![t_2,t_1]\!]} \in \mathbb{R}.$$

Then either

$$|t_1| = |t_2| = |t_3| = |t_4|, \quad \frac{t_1}{t_2}, \frac{t_2}{t_3}, \frac{t_3}{t_4}, \frac{t_4}{t_1} \in \mathbb{R}, \quad \text{or} \quad \frac{t_1}{t_2}, \frac{t_2}{t_3}, \frac{t_3}{t_4}, \frac{t_4}{t_1} \in i\mathbb{R}. \tag{9.1}$$

Proof. Denote

$$z_1 := [\![t_2, t_1]\!], \quad z_2 := [\![t_3, t_2]\!], \quad z_3 := [\![t_4, t_3]\!], \quad z_4 := [\![t_4, t_1]\!], \quad x := [\![t_3, t_1]\!], \quad y := [\![t_4, t_2]\!].$$

Then we have relations

$$x^2 = \frac{(z_1z_3 + z_2z_4)(z_1z_4 + z_2z_3)}{z_1z_2 + z_3z_4} \quad \text{and} \quad y^2 = \frac{(z_1z_3 + z_2z_4)(z_1z_2 + z_3z_4)}{z_1z_4 + z_2z_3}.$$

Let $\epsilon \in \mathbb{C}^*$, $|\epsilon| = 1$ be such that $\epsilon z_j \in \mathbb{R}$ for $j = 1, 2, 3, 4$. Then $(\epsilon x)^2, (\epsilon y)^2 \in \mathbb{R}$, thus $\epsilon x, \epsilon y \in \mathbb{R} \cup i\mathbb{R}$. Additionally, by (5.11), we have $xy = z_1z_3 + z_2z_4$, so $\epsilon x \cdot \epsilon y \in \mathbb{R}$. Thus either $\epsilon x, \epsilon y \in \mathbb{R}$ or $\epsilon x, \epsilon y \in i\mathbb{R}$. In the former case, by Lemma 9.1(i), we get either $|t_1| = |t_2| = |t_3| = |t_4|$ or $\frac{t_1}{t_2}, \frac{t_2}{t_3}, \frac{t_3}{t_4}, \frac{t_4}{t_1} \in \mathbb{R}$. In the latter case, by Lemma 9.1(ii), we get $\frac{t_1}{t_2}, \frac{t_2}{t_3}, \frac{t_3}{t_4}, \frac{t_4}{t_1} \in i\mathbb{R}$. □

The next well-known result states that knowing the ratios of side lengths of an inscribed convex polygon is sufficient to reconstruct its angles.

Lemma 9.3. *Let $(a_1, a_2, \ldots, a_m) \in \mathbb{R}^m_{>0}$ be such that no a_p is greater than $\sum_{q \neq p} a_q$. Then there exists a unique tuple $(\theta_1, \theta_2, \ldots, \theta_m)$ such that $0 = \theta_1 < \theta_2 < \cdots < \theta_m < \pi$, and*

$$\frac{\sin(\theta_{p+1} - \theta_p)}{\sin(\theta_{q+1} - \theta_q)} = \frac{a_p}{a_q} \quad \textit{for all } p, q \in [m], \tag{9.2}$$

where we set $\theta_{m+1} := \pi$. □

Proof of Theorems 4.4 and 5.11. Let $f = f_{k,n}$. Recall that Theorem 4.4 is stated for $1 \leqslant k \leqslant n$ while Theorem 5.11 only deals with the case $2 \leqslant k \leqslant n-2$. First, Theorem 4.4 is trivial to see when $k = 1$ or $k = n$ because each of $\Theta_f^{>0}$ and $\mathrm{Crit}_f^{>0}$ consists of a single point in these cases. When $k = n-1$, $\mathrm{Meas}_f(\boldsymbol{\theta})$ records the ratios of sines on the left hand side of (9.2), and thus the injectivity conjecture in this case follows from Lemma 9.3. From now on, we restrict to the case $2 \leqslant k \leqslant n-2$ and prove Theorems 4.4 and 5.11 simultaneously. (Note in particular that each $\mathbf{t}$ corresponding to $\boldsymbol{\theta} \in \Theta_f^{>0}$ via (5.1) is automatically generic.)

By the results of [OPS15], for all quadruples $1 \leqslant a < b < c < d \leqslant n$, there exists a graph $G \in \mathcal{G}_{\mathrm{red}}(f)$ containing a square face F whose boundary edges are labeled by $\{a, b\}$, $\{b, c\}$, $\{c, d\}$, and $\{a, d\}$. Denote $v_p := t_p^2$ for $p \in [n]$ as above. Consider a *cross-ratio*

$$(v_a, v_b; v_c, v_d) := \frac{[\![t_c, t_a]\!][\![t_d, t_b]\!]}{[\![t_c, t_b]\!][\![t_d, t_a]\!]} = \frac{(v_c - v_a)(v_d - v_b)}{(v_c - v_b)(v_d - v_a)}. \tag{9.3}$$

We have $(v_a, v_b; v_c, v_d) = 1 - (v_a, v_c; v_b, v_d)$, and by [MuSp17, Corollary 5.11], $(v_a, v_c; v_b, v_d)$ may be written as a ratio of Plücker coordinates of the left twist $\overleftarrow{\tau}(\mathrm{Meas}_f(\mathbf{t}))$ corresponding to the four faces of G adjacent to F. All such Plücker coordinates are monomials in the edge weights which are nonzero since $\mathbf{t}$ is generic. In particular, $(v_a, v_b; v_c, v_d) \in \mathbb{R}$ when $\mathrm{Meas}_f(\mathbf{t}) \in \mathrm{Crit}_f^{\circ}(\mathbb{R})$, and moreover, $(v_a, v_b; v_c, v_d)$ may be reconstructed from $\mathrm{Meas}_f(\mathbf{t})$. We observe that in the setting of Theorem 5.11, all cross-ratios $(v_a, v_b; v_c, v_d)$ are real, and therefore the (pairwise distinct) points $(v_p)_{p \in [n]}$ all belong to the same circle or to the same line.

Next, we see that f has a bridge at r for all $r \in [n]$. By [Lam16, Lemma 7.6], we find that for each $p \in [n]$, $[\![t_p, t_{p-k}]\!]/[\![t_p, t_{p-1}]\!]$ may be written as a ratio of two Plücker coordinates of $\mathrm{Meas}_f(\mathbf{t})$, where the indices are taken modulo n. We thus see that

$$[\![t_p, t_{p-k}]\!]/[\![t_p, t_{p-1}]\!] \in \mathbb{R} \quad \text{for } p \in [n] \tag{9.4}$$

and $[\![t_p, t_{p-k}]\!]/[\![t_p, t_{p-1}]\!]$ may be reconstructed from $\mathrm{Meas}_f(\mathbf{t})$.

The cross-ratio $(v_a, v_b; v_c, v_d) \in \mathbb{R}$ changes predictably under permuting the indices. Substituting $\{a, b, c, d\} = \{1, 2, k, k+1\}$ or $\{a, b, c, d\} = \{1, 2, k+1, k+2\}$ into (9.3) and $p = k+1$ or $p = k+2$ into (9.4), we find

$$\frac{[\![t_2, t_1]\!]}{[\![t_k, t_2]\!]}, \frac{[\![t_k, t_2]\!]}{[\![t_{k+1}, t_k]\!]}, \frac{[\![t_{k+1}, t_k]\!]}{[\![t_{k+1}, t_1]\!]}, \frac{[\![t_{k+1}, t_1]\!]}{[\![t_2, t_1]\!]} \in \mathbb{R} \tag{9.5}$$

and that all these ratios may be reconstructed from $\mathrm{Meas}_f(\mathbf{t})$. Applying Lemma 9.2, we find that the points t_1, t_2, t_k, t_{k+1} satisfy the conditions in (9.1). Recall that we have shown above that all points $(v_p)_{p\in[n]}$ belong to either a common circle or a common line. By (9.1), if it is a circle then its center must pass through 0, and if it is a line then it must pass through the origin. In the case of the line, we note additionally that (9.1) implies $\frac{t_1}{t_k} \in \mathbb{R}$, and by cyclic symmetry, we must have $\frac{t_p}{t_{p+k-1}} \in \mathbb{R}$ for all $p \in [n]$ (taken modulo n). By the definition of Θ_f°, we have, say, $t_1 = 1$, and therefore we either have $|t_p| = 1$ for all $p \in [n]$ or $t_p \in \mathbb{R} \cup i\mathbb{R}$ for all $p \in [n]$. This finishes the proof of Theorem 5.11.

We now focus on Theorem 4.4. Recall that the ratios in (9.5) may be reconstructed from $\mathrm{Meas}_f(\mathbf{t})$. Combining this with Lemma 9.3, we can uniquely reconstruct (modulo shift) the quadruple $(\theta_1, \theta_2, \theta_k, \theta_{k+1})$ from $\mathrm{Meas}_f(\mathbf{t})$. For each $q \notin \{1, k, k+1\}$, we may plug in $\{a, b, c, d\} = \{1, q, k, k+1\}$ into (9.3) and $p = k+1$ into (9.4) to see that $[\![t_q, t_1]\!]/[\![t_q, t_k]\!]$ can be uniquely reconstructed from $\mathrm{Meas}_f(\mathbf{t})$, and therefore having already recovered θ_1 and θ_k, we can now also recover θ_q. We have shown that $\mathrm{Meas}_f : \Theta_f^{>0} \to \mathrm{Crit}_f^{>0}$ is injective (and thus bijective). It is clearly continuous and its inverse is also continuous since the map in Lemma 9.3 is continuous. Thus $\mathrm{Meas}_f : \Theta_f^{>0} \xrightarrow{\sim} \mathrm{Crit}_f^{>0}$ is a homeomorphism, and it remains to note that $\Theta_f^{>0}$ is homeomorphic to the interior of an $(n-1)$-dimensional simplex. We are done with the proof of Theorem 4.4. □

10. Further directions

In addition to the multiple conjectures mentioned in the body of the text, we list a few other questions which arise in relation to critical varieties. The general philosophy is that critical varieties should be considered as *critical parts* of positroid varieties, and thus for each existing result for positroid varieties (resp., open positroid varieties, their totally positive and totally nonnegative parts) an immediate direction is to investigate analogs of that result for critical varieties and critical cells.

10.1. **The totally nonnegative part.** Taking the closure of a positroid cell $\Pi_f^{>0}$ inside $\mathrm{Gr}_{\geqslant 0}(k, n)$ gives rise to a remarkable topological space denoted $\Pi_f^{\geqslant 0}$. For instance, it was recently shown in [GKL19] that $\Pi_f^{\geqslant 0}$ is a regular CW complex homeomorphic to a closed ball.

Definition 10.1. Let $f \in \mathcal{B}(k, n)$ be loopless. The *totally nonnegative part* $\mathrm{Crit}_f^{\geqslant 0}$ of Crit_f is defined as the closure of $\mathrm{Crit}_f^{>0}$ in the usual (Hausdorff) topology on $\mathrm{Gr}_{\geqslant 0}(k, n)$.

The topology and combinatorics of the cell structure of $\mathrm{Crit}_f^{\geqslant 0}$ is explored in a separate paper [Gal21b]. Among other things, we establish the following result.

Theorem 10.2 ([Gal21b]). *For $2 \leqslant k \leqslant n-1$, $\mathrm{Crit}_{k,n}^{\geqslant 0}$ is homeomorphic (via a stratification-preserving homeomorphism) to the hypersimplex $\Delta_{2,n}$.*

Thus, unlike $\Pi_{k,n}^{\geqslant 0}$, the space $\mathrm{Crit}_{k,n}^{\geqslant 0}$ is homeomorphic to a polytope (which does not depend on k). What happens in the case of arbitrary loopless $f \in \mathcal{B}(k,n)$ remains an open question which depends, among other things, on the injectivity conjecture (Conjecture 4.3). The properties of the associated polytopes are developed in [Gal21a]. In particular, the structure of $\mathrm{Crit}_{k,n}^{\geqslant 0}$ is intimately tied with the *cyclohedron* [BT94, Sim03], which is a natural compactification of the space $\Theta_{k,n}^{>0}$; see [Gal21b, Theorem 1.3].

10.2. **Algebraic geometry of critical varieties.** Besides the topology of $\mathrm{Crit}_f^{\geqslant 0}$, it is also interesting to study Crit_f and Crit_f° as algebraic varieties, since their positroid counterparts possess many nice properties (normal, Cohen–Macaulay, etc.); see [KLS13]. One particularly optimistic direction is to investigate the cohomology of Crit_f and Crit_f°. The analogous questions for Π_f° have recently attracted some interest [GL20].

10.3. **Peterson variety.** On the surface, critical varieties look very similar to the *Peterson variety* Pet_n, which is a certain subvariety of the flag variety introduced by D. Peterson in the 1990s; see e.g. [Kos96, Rie03]. For example, both Pet_n and $\mathrm{Crit}_{k,n}$ have dimension $n-1$. The coordinate ring of Pet_n is of great importance since it computes the quantum cohomology ring of the flag variety [Rie03]. It would be interesting to see whether there is some projection relating Pet_n to $\mathrm{Crit}_{k,n}$, and whether the coordinate ring of $\mathrm{Crit}_{k,n}$ (or, more generally, of Crit_f) also recovers some well-studied cohomology ring.

10.4. **Chow quotient.** The *torus* T consisting of diagonal $n \times n$ matrices acts on $\mathrm{Gr}(k,n)$ by right multiplication. One can consider the corresponding *Chow quotient* and study its totally nonnegative part, see e.g. the recent results of [AHLS20, LPW20]. Observe that the critical varieties and the dual critical varieties only differ by the action of T, thus the resulting quotients coincide. The cross-ratios (9.3) that we used above yield natural coordinates on the Chow quotient, thus it seems plausible that the questions we studied for critical varieties have simpler Chow quotient analogs.

10.5. **Boundary measurements for reduced strand diagrams.** Our results (especially Propositions 5.1 and 4.2) suggest that there could be a formula for Meas_f directly in terms of the reduced strand diagram of f. (For instance, it could be some "oriented strand version" of the *six-vertex model*.) An optimistic hope would be that such a formula would potentially provide a positive answer to [Gal20b, Question 7.6].

10.6. **More general edge weights.** Given a reduced graph $G \in \mathcal{G}_{\mathrm{red}}(f)$ and an edge $e \in E(G)$ labeled by $\{p,q\}$ with $1 \leqslant p < q \leqslant n$, we have set the edge weight to either $\sin(\theta_q - \theta_p)$ or to $[\![t_q, t_p]\!]$. One can consider the following more general assignment of edge weights: choose an element $\mathbf{T} \in \mathrm{Gr}(2,n)$, and then set $\mathrm{wt}_{\mathbf{T}}(e) := \Delta_{p,q}(\mathbf{T})$. This weight assignment includes the ones we have considered as special cases, and the resulting dimer model is still invariant under square moves. It appears that most of our constructions extend to this more general set up in a straightforward fashion, in particular, we have the corresponding versions of critical cells ($\mathbf{T} \in \mathrm{Gr}_{>0}(2,n)$) and (open) critical varieties, where

the condition $t_p \neq \pm t_q$ is replaced with $\Delta_{p,q}(\mathbf{T}) \neq 0$. The underlying combinatorics is still dictated by reduced strand diagrams. It would be interesting to expand this further, for instance, to extend the boundary measurement formula or the injectivity conjecture to such weights.

10.7. **Plabic tilings as isoradial embeddings.** The starting point for this work was the observation that the plabic tilings of [OPS15] may be naturally considered as special cases of isoradial embeddings of planar bipartite graphs. Thus one can study the asymptotic properties of this special family of isoradial embeddings, and potentially apply the vast literature on such embeddings to study convergence and conformal invariance questions for families of plabic tilings. For instance, an interesting question appears to be whether the results of [CLR20] apply in this case, since plabic tilings are easily seen to satisfy the *small origami* property introduced in [CLR20]. We thank Marianna Russkikh for discussions related to these questions.

References

[AHBC+16] Nima Arkani-Hamed, Jacob Bourjaily, Freddy Cachazo, Alexander Goncharov, Alexander Postnikov, and Jaroslav Trnka. *Grassmannian Geometry of Scattering Amplitudes*. Cambridge University Press, Cambridge, 2016.

[AHLS20] Nima Arkani-Hamed, Thomas Lam, and Marcus Spradlin. Positive configuration space. `arXiv:2003.03904v2`, 2020.

[AHT14] Nima Arkani-Hamed and Jaroslav Trnka. The amplituhedron. *Journal of High Energy Physics*, 2014(10):30, Oct 2014.

[ARW16] Federico Ardila, Felipe Rincón, and Lauren Williams. Positroids and non-crossing partitions. *Trans. Amer. Math. Soc.*, 368(1):337–363, 2016.

[Bax78] R. J. Baxter. Solvable eight-vertex model on an arbitrary planar lattice. *Philos. Trans. Roy. Soc. London Ser. A*, 289(1359):315–346, 1978.

[Bax86] R. J. Baxter. Free-fermion, checkerboard and **Z**-invariant lattice models in statistical mechanics. *Proc. Roy. Soc. London Ser. A*, 404(1826):1–33, 1986.

[BCFW05] Ruth Britto, Freddy Cachazo, Bo Feng, and Edward Witten. Direct proof of the tree-level scattering amplitude recursion relation in Yang-Mills theory. *Phys. Rev. Lett.*, 94(18):181602, 4, 2005.

[BT94] Raoul Bott and Clifford Taubes. On the self-linking of knots. *J. Math. Phys.*, 35(10):5247–5287, 1994.

[BW20] Alexey Balitskiy and Julian Wellman. Flip cycles in plabic graphs. *Selecta Math. (N.S.)*, 26(1):Paper No. 15, 29, 2020.

[CLR20] Dmitry Chelkak, Benoît Laslier, and Marianna Russkikh. Dimer model and holomorphic functions on t-embeddings of planar graphs. `arXiv:2001.11871v1`, 2020.

[CW11] Sylvie Corteel and Lauren K. Williams. Tableaux combinatorics for the asymmetric exclusion process and Askey-Wilson polynomials. *Duke Math. J.*, 159(3):385–415, 2011.

[Dub11] Julien Dubédat. Exact bosonization of the Ising model. `arXiv:1112.4399v1`, 2011.

[FPST17] Sergey Fomin, Pavlo Pylyavskyy, Eugenii Shustin, and Dylan Thurston. Morsifications and mutations. `arXiv:1711.10598v3`, 2017.

[FZ02] Sergey Fomin and Andrei Zelevinsky. Cluster algebras. I. Foundations. *J. Amer. Math. Soc.*, 15(2):497–529 (electronic), 2002.

[Gal18] Pavel Galashin. Plabic graphs and zonotopal tilings. *Proc. Lond. Math. Soc. (3)*, 117(4):661–681, 2018.

[Gal20] Pavel Galashin. A formula for boundary correlations of the critical Ising model. `arXiv:2010.13345v2`, 2020.

[Gal20b] Pavel Galashin. Symmetries of stochastic colored vertex models. *Ann. Probab.*, to appear. `arXiv:2003.06330v2`, 2020.

[Gal21a] Pavel Galashin. Poset associahedra. `arXiv:2110.07257v1`, 2021.

[Gal21b] Pavel Galashin. Totally nonnegative critical varieties. arXiv:2110.08548v1, 2021.
[GKL17] Pavel Galashin, Steven N. Karp, and Thomas Lam. The totally nonnegative Grassmannian is a ball. arXiv:1707.02010, 2017.
[GKL19] Pavel Galashin, Steven N. Karp, and Thomas Lam. Regularity theorem for totally nonnegative flag varieties. arXiv:1904.00527v2, 2019.
[GL18] Pavel Galashin and Thomas Lam. Parity duality for the amplituhedron. *Compos. Math.*, to appear. arXiv:1805.00600, 2018.
[GL19] Pavel Galashin and Thomas Lam. Positroid varieties and cluster algebras. arXiv:1906.03501v1, 2019.
[GL20] Pavel Galashin and Thomas Lam. Positroids, knots, and q,t-Catalan numbers. arXiv:2012.09745v2, 2020.
[GP20] Pavel Galashin and Pavlo Pylyavskyy. Ising model and the positive orthogonal Grassmannian. *Duke Math. J.*, 169(10):1877–1942, 2020.
[GPW19] Pavel Galashin, Alexander Postnikov, and Lauren Williams. Higher secondary polytopes and regular plabic graphs. arXiv:1909.05435v1, 2019.
[Kar17] Steven N. Karp. Sign variation, the Grassmannian, and total positivity. *J. Combin. Theory Ser. A*, 145:308–339, 2017.
[Kar19] Steven N. Karp. Moment curves and cyclic symmetry for positive Grassmannians. *Bull. Lond. Math. Soc.*, 51(5):900–916, 2019.
[Ken93] Richard Kenyon. Tiling a polygon with parallelograms. *Algorithmica*, 9(4):382–397, 1993.
[Ken02] R. Kenyon. The Laplacian and Dirac operators on critical planar graphs. *Invent. Math.*, 150(2):409–439, 2002.
[KLRR18] Richard Kenyon, Wai Yeung Lam, Sanjay Ramassamy, and Marianna Russkikh. Dimers and Circle patterns. arXiv:1810.05616v2, 2018.
[KLS13] Allen Knutson, Thomas Lam, and David E. Speyer. Positroid varieties: juggling and geometry. *Compos. Math.*, 149(10):1710–1752, 2013.
[Kos96] Bertram Kostant. Flag manifold quantum cohomology, the Toda lattice, and the representation with highest weight ρ. *Selecta Math. (N.S.)*, 2(1):43–91, 1996.
[KPW00] Richard W. Kenyon, James G. Propp, and David B. Wilson. Trees and matchings. *Electron. J. Combin.*, 7:Research Paper 25, 34, 2000.
[Lam16] Thomas Lam. Totally nonnegative Grassmannian and Grassmann polytopes. In *Current developments in mathematics 2014*, pages 51–152. Int. Press, Somerville, MA, 2016.
[Lam18] Thomas Lam. Electroid varieties and a compactification of the space of electrical networks. *Adv. Math.*, 338:549–600, 2018.
[LPW20] Tomasz Lukowski, Matteo Parisi, and Lauren K. Williams. The positive tropical Grassmannian, the hypersimplex, and the m=2 amplituhedron. arXiv:2002.06164v2, 2020.
[Lus94] G. Lusztig. Total positivity in reductive groups. In *Lie theory and geometry*, volume 123 of *Progr. Math.*, pages 531–568. Birkhäuser Boston, Boston, MA, 1994.
[Lus98] George Lusztig. Introduction to total positivity. In *Positivity in Lie theory: open problems*, volume 26 of *De Gruyter Exp. Math.*, pages 133–145. de Gruyter, Berlin, 1998.
[Mer01] Christian Mercat. Discrete Riemann surfaces and the Ising model. *Comm. Math. Phys.*, 218(1):177–216, 2001.
[MaSc16] R. J. Marsh and J. S. Scott. Twists of Plücker coordinates as dimer partition functions. *Comm. Math. Phys.*, 341(3):821–884, 2016.
[MuSp17] Greg Muller and David E. Speyer. The twist for positroid varieties. *Proc. Lond. Math. Soc. (3)*, 115(5):1014–1071, 2017.
[OPS15] Suho Oh, Alexander Postnikov, and David E. Speyer. Weak separation and plabic graphs. *Proc. Lond. Math. Soc. (3)*, 110(3):721–754, 2015.
[Pos06] Alexander Postnikov. Total positivity, Grassmannians, and networks. Preprint, http://math.mit.edu/~apost/papers/tpgrass.pdf, 2006.
[PSBW21] Matteo Parisi, Melissa Sherman-Bennett, and Lauren Williams. The m=2 amplituhedron and the hypersimplex: signs, clusters, triangulations, Eulerian numbers. arXiv:2104.08254v3, 2021.

[PSW09] Alexander Postnikov, David Speyer, and Lauren Williams. Matching polytopes, toric geometry, and the totally non-negative Grassmannian. *J. Algebraic Combin.*, 30(2):173–191, 2009.

[Rie03] Konstanze Rietsch. Totally positive Toeplitz matrices and quantum cohomology of partial flag varieties. *J. Amer. Math. Soc.*, 16(2):363–392, 2003.

[Sim03] Rodica Simion. A type-B associahedron. volume 30, pages 2–25. 2003. Formal power series and algebraic combinatorics (Scottsdale, AZ, 2001).

[STWZ19] Vivek Shende, David Treumann, Harold Williams, and Eric Zaslow. Cluster varieties from Legendrian knots. *Duke Math. J.*, 168(15):2801–2871, 2019.

[Tal08] Kelli Talaska. A formula for Plücker coordinates associated with a planar network. *Int. Math. Res. Not. IMRN*, Art. ID rnn081, 2008.

Department of Mathematics, University of California, Los Angeles, CA 90095, USA
Email address: galashin@math.ucla.edu